



UNIVERSITY OF  
BIRMINGHAM

**Statistical Modelling of the Transition Toughness  
Properties of Low Alloy Pressure Vessel Steels  
Volume 2: Appendices**

by

**DANIEL J. COGSWELL**

A thesis submitted to the  
**Department of Metallurgy and Materials, School of Engineering,  
The University of Birmingham**

For the degree of  
**Engineering Doctorate in Engineered Materials for High Performance  
Applications in Aerospace and Related Technologies**

Structural Materials Research Centre  
School of Engineering  
The University of Birmingham  
Birmingham  
UK  
July 2010

UNIVERSITY OF  
BIRMINGHAM

**University of Birmingham Research Archive**

**e-theses repository**

This unpublished thesis/dissertation is copyright of the author and/or third parties. The intellectual property rights of the author or third parties in respect of this work are as defined by The Copyright Designs and Patents Act 1988 or as modified by any successor legislation.

Any use made of information contained in this thesis/dissertation must be in accordance with that legislation and must be properly acknowledged. Further distribution or reproduction in any format is prohibited without the permission of the copyright holder.

# Contents

- Appendix A Fracture of Low Alloy Steel: 1<sup>st</sup> Year Report
- Appendix B Fracture of Low Alloy Steel: 2<sup>nd</sup> Year Report
- Appendix C Process Modelling of Low Alloy Steel
- Appendix D NPCT Process Modelling Phase 2 Detailed Plan
- Appendix E NPCT Toughness Strategy – Technical Justification
- Appendix F The Effects of Microstructure on the Mechanical Properties of A508-3 Heavy Section Forgings
- Appendix G Upper Transition Model Assessment



*Appendix A*

**Fracture of Low Alloy Steel: 1<sup>st</sup>  
Year Report**

UNIVERSITY OF  
BIRMINGHAM



# *FRACTURE OF LOW ALLOY STEEL*

**Daniel Cogswell**

Submitted to the  
**Department of Metallurgy and Materials, School of Engineering,  
The University of Birmingham**

For the degree of  
**Engineering Doctorate in Engineered Metals for High Performance  
Applications in Aerospace and Related Technologies**

**FIRST YEAR REPORT**

9,785 Words

**EPSRC**  
Engineering and Physical Sciences  
Research Council



**Rolls-Royce**

## Contents

Section	Page
1. Summary	1
2. Introduction	2
3. Mechanical Properties Of Low Alloy Steels	5
3.1 Uses Of Low Alloy Steels	5
3.2 Factors Affecting The Use Of Low Alloy Steels In The Nuclear Industry	7
3.3 Testing Methods	13
3.4 Failure Mechanisms	17
3.5 Current And Emergent Toughness Models	22
4. Business Context of the Project	35
5. Projects	
5.1 High $T_0$ Investigation	37
5.2 Micro-Arrest Testing	40
6. References	41
7. Appendices	
A - EngD Project Breakdown	46
B - SINTAP $K_{MAT}$ Estimation	48
C - High $T_0$ Investigation Initial Results	53
D - Micro-Arrest Equipment Set Up	56
E - EngD Conference 2004 Presentation	58
F - EngD Conference 2005 Poster	63

<b>Table</b>		<b>Page</b>
3.4.1	Ductile Failure Mechanism	18
3.4.2	Brittle Failure Mechanism	19

<b>Figure</b>		<b>Page</b>
2.	Civil Pressurised Water Reactor Schematic	4
3.2.5.1	Effect of Irradiation on Yield and Fracture Stress of Reactor Pressure Vessel Steel	12
3.2.5.2	Effect of Irradiation on the Impact Properties of Reactor Pressure Vessel Steel	12
3.2.5.3	Effect of Irradiation on the Fracture Toughness of Reactor Pressure Vessel Steel	12
3.3.1	Form of the Charpy Impact Test and V-Notch Geometry	15
3.3.2	Fracture Toughness Specimen Geometries	15
3.3.3	Simple and Advanced J-Integral Test Methods	16
3.5.1.1	Pellini Drop Weight Test Apparatus and Specimens	23
3.5.1.2	Extended EPRI Database Normalised by Nil-Ductility Temperature	23
3.5.2.1	Master Curve Probability Density Function	25
3.5.3.1	Unified Curve Probabilistic Failure Model	28
3.5.4.1	Results of the Simulakram Simulation	31



3.5.4.2	Probability of Micro Arrest Plots	32
3.5.4.3	Effect of Long Crack Front Lengths on Micro Arrest	33
4.1	Schematic Representation Of The Areas That Combine To Form A Fitness For Purpose Assessment	36

## 1. Summary

The importance of brittle fracture in structural steels cannot be under estimated and failure to properly predict this property has resulted in many well-known and catastrophic failures, commonly these failures cause loss of life. With the introduction of modern clean steel production the controlling property for brittle failure has been steadily improved in the past century, however the underlying mechanisms that cause brittle failure are still not fully understood. An assessment of the ductile and brittle failure mechanisms has been made, however these are only theoretical and no excepted model can link the microstructure of the material to a controlling property for brittle fracture.

Current debate in the field of fracture mechanics is based on modelling the probability distribution, which arises when ferritic steels are tested for brittle fracture. Current excepted methods for toughness prediction, based on both deterministic and probabilistic approaches, are overly conservative due to the uncertainty in model parameters. These are chosen to be conservative on the grounds of safety, however as the need to extend the life of ferritic components becomes increasingly important due to energy needs and financial pressures. The current approaches are outlined in the following text and the benefits that can be gained from moving to a deterministic based approach, such as the ASME code, to a probabilistic method, such as the so-called 'Master Curve' are discussed. A review of new models that may provide a solution to the conservatism inherent in current models is included, the present front runner being the Rolls-Royce developed micro arrest methodology based on the master curve concept.

A brief description of the factors that effect large ferritic components for reactor pressure vessels; time at temperature, fatigue, corrosion, etc. are briefly visited with reference to civil examples. The hardening mechanisms of irradiation damage being the most important have been described in more detail. Interest in accurately modelling irradiation damage has increased since the realisation that these mechanisms have the greatest long-term effect on the toughness of ferritic steels. The effects of irradiation are to degrade the mechanical properties of the reactor pressure vessel to a point where it is no longer safe to operate for fear of public safety.

## 2. Introduction

There has been much talk in the media recently about the need to switch to non-carbon dioxide (CO<sub>2</sub>) producing power generation. It has been reported that if there is not a change in the use of fossil fuels in the near future, then global warming may become a run-away effect. Fossil fuels are also a non-renewable resource and will eventually run out. Some predictions state that if current usage continues, the world oil supply will be used up within a century and the supply of coal and gas within 400 years. Many governments have been conducting studies on how they can change energy policies to meet agreements made at an international level, such as the Kyoto agreement, for the use of fossil fuels and pollution control. One way that targets for CO<sub>2</sub> reduction can be met is by the use of alternative sources of energy that are CO<sub>2</sub> neutral and will have no effect on global warming.<sup>[1, 2, 3]</sup>

The use of wind farms and hydroelectric power has become an attractive option recently and many governments have switched to wind turbines as the front-runner for meeting CO<sub>2</sub> targets<sup>[3, 4]</sup>. However, both wind farms and hydroelectric power have their drawbacks. Hydroelectric power requires large amounts of water to generate energy on a utility scale, in order to produce a steady supply a dam is commonly used, flooding large areas and changing the natural environmental cycle of the river downstream. Wind farms, by their nature, produce a random supply of electricity and hence cannot be used to supply base load or be relied on for peak loading of a power grid<sup>[5, 6, 7]</sup>.

The only power source currently available that can meet the short-term requirements of low CO<sub>2</sub> emissions and a steady and predictable power supply is nuclear fission. The problems associated with nuclear power generation are by no means small and the legacy of nuclear waste will be of concern for many years to come. Until nuclear fusion can be demonstrated at a utility scale to provide clean power then nuclear fission is the only option, radioactive materials are still produced in a fusion reactor. However, this is only a small part of the structure and is not a consumable in the same way that fuel rods/pellets are for fission reactors; hence, the waste is greatly reduced. A large amount of research is being conducted into low activation materials, i.e. those that have very short radiation half-life's, to reduce the legacy of radioactive waste<sup>[8, 9]</sup>.

Public perceptions of nuclear power are very low, due largely to the Chernobyl incident of 1986. It is now understood that the incident was caused by a combination of poor design and by inexperienced operators under pressure to perform a series of reactor test operations without the necessary safety procedures being taken into account. Given the concerns of the public nuclear energy policy in the UK is a contentious issue and the process of deciding to build a new reactor to actual construction takes approximately ten years <sup>[10, 11, 12]</sup>. Within this time, at least one general election will take place and recommending nuclear new-build while public opinion is so heavily against it will certainly be damaging to any governments chances of re-election, so at present nuclear power in the UK will be limited to the ageing reactors currently in operation. A similar situation exists across the world and as of 2003, there are 438 nuclear reactors producing electricity on a utility scale worldwide, there are also many reactors used for maritime power generation all utilised for military purposes<sup>[13]</sup>.

There are several different reactor designs currently in use and some new designs considered for new-build by 2010. By far the most common reactor type is the pressurised water reactor (PWR); used in both utility and marine power generation. The PWR design uses an enriched uranium oxide fuel and light water (H<sub>2</sub>O) as a moderator and coolant. Steam generation is indirect; heat is transferred from the primary coolant, which is kept liquid by maintaining a high pressure into a secondary system via a heat exchanger. The controlling factor for the safe operation of these reactors is the fitness for purpose of the main containment shield, in most cases a steel reactor pressure vessel<sup>[13, 14]</sup>. The modelling methods used to ascertain the material properties used in these assessments will be outlined in a later section of the report, as well as the factors that influence these properties.

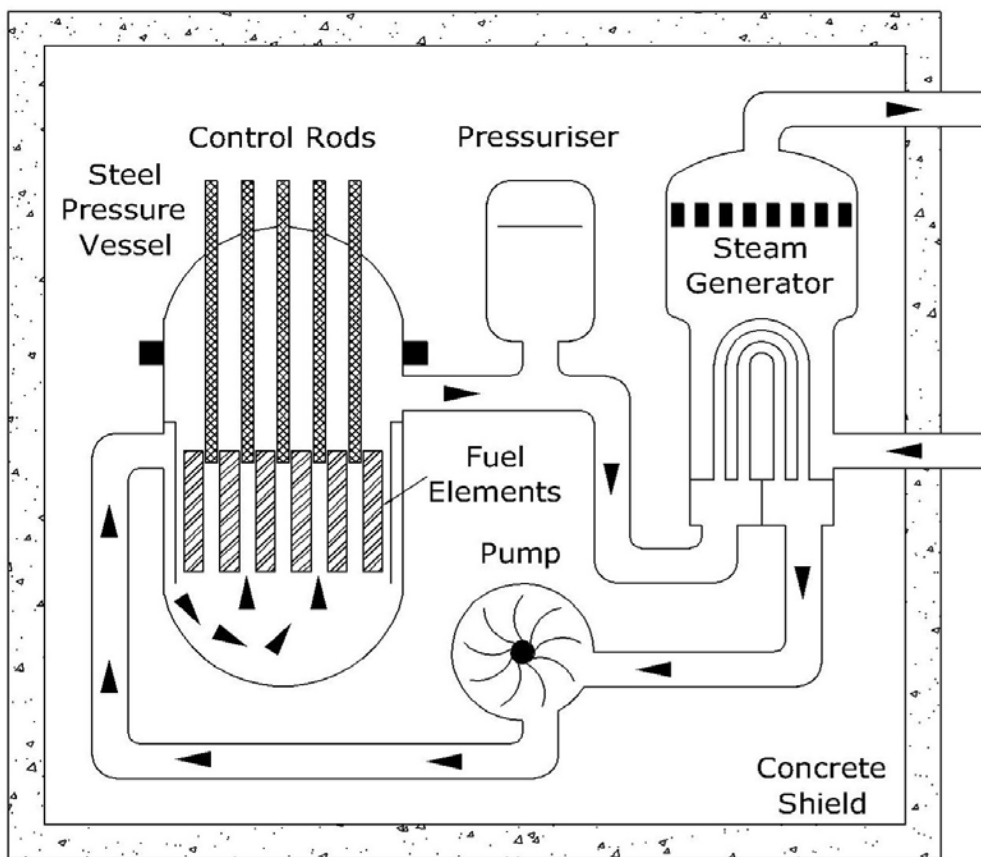


Figure 2. Civil Pressurised Water Reactor Schematic<sup>[14]</sup>

## **3. Mechanical Properties Of Low Alloy Steels**

### **3.1 Uses Of Low Alloy Steels**

Low alloy steels are used in a large variety of applications but all suffer from a similar problem. Due to the body centred cubic atomic structure of these steels a transition is observed in the toughness, most commonly described by the ductile-brittle transition temperature (DBTT) found in impact testing. Misunderstanding of the toughness properties has caused many large-scale accidents, some well reported and in others, the cause of failure has not become apparent until recently. The wide spread use of low alloy steels due to their low price and good tensile properties has lead to a variety of failures.

The sinking of the Titanic following a collision with an iceberg on its maiden voyage in 1912 was largely a mystery. Until recently only survivors statements were all that were available to piece together what happened. However, in 1985 a group using deep-sea submersibles catalogued and photographed the remains of the Titanic. It was found to be in two sections a large distance apart on the sea floor. A section of the hull plating was lifted allowing experimental work to be conducted. Charpy impact testing has been used to determine the DBTT of the material and it was concluded that at the ambient temperature of the water on that night, -1 °C, the hull plate was in the brittle region. Current belief is that striking the iceberg caused water to be taken on in vast quantities submerging the bow of the ship, this caused the stern to be lifted out of the water putting a great deal of stress on the mid point of the ship, as it was now effectively in three point bend. The ship then fractured in two starting near the top deck and several features have been observed on the wreck which corroborates the above; buckling is noted in the keel at the mid point and the fracture line above it simply runs through plate boundaries and no localised plastic deformation is seen at the rivets, implying brittle failure <sup>[15, 16]</sup>.

Many other examples exist from bridge failures to molasses containers where brittle failure has resulted in the loss of life <sup>[15]</sup>. The most demanding application for these steels also has the greatest potential for tragedy. Ferritic steel is used as the main

structural material in the construction of nuclear pressure vessels; this is a very demanding role as the pressure vessel is the first, and commonly the only form of containment for the reactor core. In normal operation the pressure stresses on the vessel are low, however during a loss of coolant accident (LOCA) large amounts of cold coolant are added creating thermal gradients across the vessel wall resulting in an increase in stress due to contraction of the inner surface. For a vessel to withstand these high stresses it must conform to a minimum toughness that is safe to operate, however the mechanical properties of the steel are degraded over time by several mechanisms.

## **3.2 Factors Affecting The Use Of Low Alloy Steels In The Nuclear Industry**

### **3.2.1 Temperature**

Long times at high temperature can change the mechanical properties of steel greatly; however, the majority of reactors operate at temperatures of  $\sim 288$  °C, negating most of these effects <sup>[13]</sup>. The problem associated with even moderate temperature operation in a pressure vessel steel (PVS) is the development of small-scale precipitates. These increase the yield stress of the material, which is known to have a detrimental effect on toughness.

### **3.2.2 Corrosion**

The resistance to corrosion of the steels used structurally in reactor construction, i.e. the pressure vessel, is relatively poor as exhibited by the discovery of a heavily corroded vessel head at the Davis-Besse PWR in Ohio, USA. A small crack in an access for a control rod drive mechanism allowed coolant to leak on to the vessel, the coolant is a mixture of light water and boric acid added to capture any stray neutrons from the reaction process. Initial reactor design dictated that any small leak of coolant would prove harmless to a reactor, as the coolant would evaporate due to the high temperatures in the vessel leaving harmless boric acid crystals. It has been shown that this is not the case and on top of the reactor vessel a strong boric acid solution can be created either by the escaping coolant or from moisture in the air, i.e. the coolant stays in liquid form.

This caused an opening approximately 15 x 18 cm to be created throughout the 15 cm thick vessel. Containment of coolant within the vessel was maintained by a stainless steel cladding layer welded to the inside of the RPV to provide corrosion resistance. It became apparent that the reactor was not functioning normally; however, a management decision was made to skip a planned shutdown in order to maximise operation, allowing the situation to worsen. The Nuclear Regulatory Commission (NRC) of the USA ordered inspections of all similar reactors following this discovery and several small-scale leaks became apparent after the discovery of



boric acid crystals found on the RPV's causing a change to inspection procedures required for licensing<sup>[17, 18, 19]</sup>.

### **3.2.3. Fatigue**

Civil reactors do not suffer greatly from fatigue due to the operational requirements of the reactor. Civil reactors supply base load, the constant demand, to a national power infrastructure, whereas other forms of power generation such as fossil fuels are used to supply peak load. Naval reactors are used in a very different manner. The reactor is used to provide propulsion for the craft and as such is continuously power cycled as the craft changes speed. This leads to a large number of fatigue cycles for the reactor over the course of its operational life giving crack growth from existing defects in the vessel. Intensive inspections are required in certain areas of the plant which are susceptible to fatigue compared to its civil counterpart.

### **3.2.4. Irradiation Embrittlement**

This is the key area of concern for RPV degradation during the operational life of the reactor; due to irradiation embrittlement changes to microstructure which would normally be seen at higher temperatures are found in the operating window of most reactor types.

- Matrix damage  
Fast neutrons released from the reaction process knock atoms out of the regular body centred cubic (BCC) structure causing vacancies or point defect clusters, the atoms knocked from position can then hit other atoms in the matrix causing further damage, this process is known as a cascade. This has the effect of locally disordering the matrix on an atomic scale, raising the yield stress,  $\sigma_y$ , and decreasing the work hardening rate. The following effects are a direct result of the increased vacancy concentration allowing substitutional diffusion of atoms in the matrix at the operating temperature of

the reactor, which is far below the temperature normally associated with thermal diffusion.<sup>[9, 20]</sup>

- Copper / Nickel precipitation

Copper initially found in scrap metal used to make the PVS and used as a coating on weld filler rods to prevent corrosion has a precipitation hardening effect on the steel. This was discovered in the late 1960's/early 1970's when the problem of irradiation embrittlement became apparent. At present, the amount of copper is strictly controlled and only found as a trace impurity. Nickel added in small quantities, ~0.75% weight for A508-3-1, to improve the strength and toughness also has a precipitation hardening effect on the PVS. Due to the small concentrations of each, no over-aging occurs and the RPV remains in a peak aged condition, this raises the  $\sigma_y$ .<sup>[21, 22, 23]</sup>

- Segregation of impurities

Impurities may migrate to the grain boundaries and cause grain boundary embrittlement, of most concern is phosphorus. This may cause a change in the failure mechanism from trans-granular cleavage to inter-granular fracture if the concentration of phosphorus at the grain boundaries is high enough to promote grain boundary embrittlement. This can dramatically lower the fracture toughness of the material. The processing routes of modern pressure vessel steels are much more restrictive than those of the past, meaning cleaner steels containing fewer impurities.<sup>[24]</sup>

A recently observed effect in Rolls-Royce data has shown the possibility of irradiation enhanced tempering (IET) were the combined effect of high temperature and irradiation result in continued tempering of the microstructure, leading to softening<sup>[25]</sup>. Irradiation embrittlement takes many years to alter the microstructure of a material but the macroscopic effects can be simulated by other means in a relatively short time. The yield stress can be increased by prestraining the material to a required amount to produce an increase as seen in the irradiated material. Extended heat treatments can be used to produce phosphorus segregation and promote inter-granular failure<sup>[26]</sup>.

### 3.2.5 Changes to the Mechanical Properties

The effects of irradiation embrittlement are to increase the yield strength and lower the fracture stress of the pressure vessel steel; this is expressed graphically in figure 3.2.5.1. The combined effect of the change on these two parameters is to decrease the fracture toughness; initially this was measured in a quantitative manner, but with only comparative use, by the use of Charpy impact testing. With increased dose it was noted that the DBTT is shifted to high values and the shape of the curve is changed by effectively knocking it over, i.e. the slope is reduced; as is the upper shelf, see figure 3.2.5.2.<sup>[27]</sup> The effect on toughness can be measured by normalising the curve using a reference temperature,  $T_{40J}$  see figure 3.2.5.3. This means that the material will be more susceptible to brittle failure as the length of time exposed to radiation is increased, by increasing the understanding of the processes involved more accurate toughness estimates can be produced allowing the operational life of reactors to be extended.

The worst case scenario for most reactor types is a pressurised thermal shock (PTS) event, here cold coolant is added in large quantities to the reactor vessel following a major loss of coolant accident (LOCA), this creates very large thermal stresses on the reactor vessel as it is cooled rapidly from operating temperature to near room temperature. A crack is assumed present at the resolution limit of the non-destructive examination (NDE) method used to assess the reactor in the beltline region of the vessel. The worst microstructural properties are used in the assessment, typically a weld closest to the core where it will receive the highest irradiation dose. The crack is assumed to have the most damaging geometry, commonly a semi-circular surface breaking crack, and the vessel is required to be safe from catastrophic failure through out the operational life of the plant.

A simple analysis shows that the operational life depends on the condition of the reactor vessel, i.e. its ability to withstand a PTS event, the variable in this case is not the stress or defect size but fluence and operating temperature, as these effect the fracture toughness of the material. Stress is known from thermodynamics calculations of the PTS event, and the defect size from the NDE resolution. Once the

fracture toughness reaches this critical value then the reactor must be shut down for fear of public safety<sup>[13, 28, 29]</sup>.

The effects of irradiation can be partly removed by annealing the reactor vessel, this has been performed on some military reactors as these tend to be smaller than their commercial counterparts but some commercial reactor vessels in the former USSR have been successfully annealed, effectively the same as building a new reactor at a reduced cost. This is possible due to the shape of the Russian reactors which were designed to pass easily under bridges when transported by train, so are long and thin compared to western reactor designs<sup>[28]</sup>.

Present methods of determining the end of life of a reactor tend to be very, if not overly, conservative, especially when the use of modern clean steels in reactor construction is now commonplace. If a better understanding of the long-term effects of irradiation on reactor pressure vessels and a better measurement of the toughness of these vessels is made then less conservatism can be used and the operational life of many reactors extended.

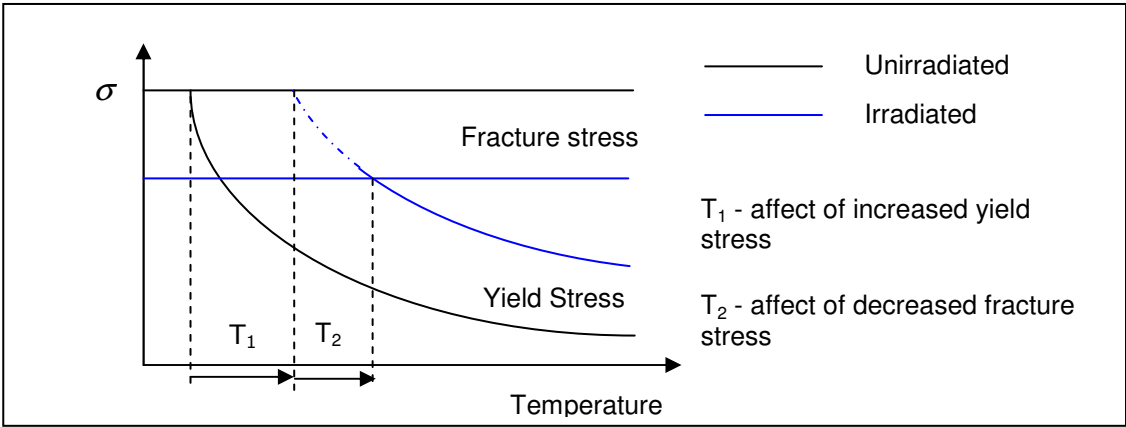


Figure 3.2.5.1 Effect of Irradiation on Yield and Fracture Stress of Reactor Pressure Vessel Steel

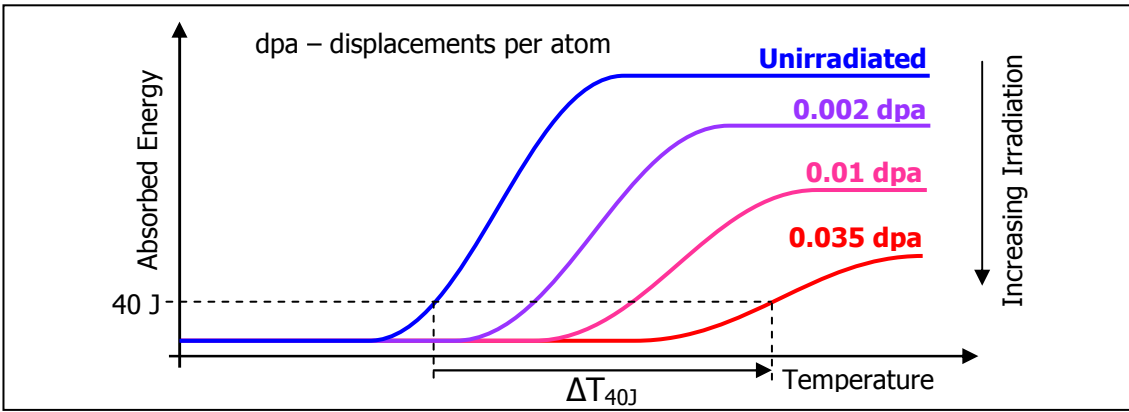


Figure 3.2.5.2 Effect of Irradiation on the Impact Properties of Reactor Pressure Vessel Steel

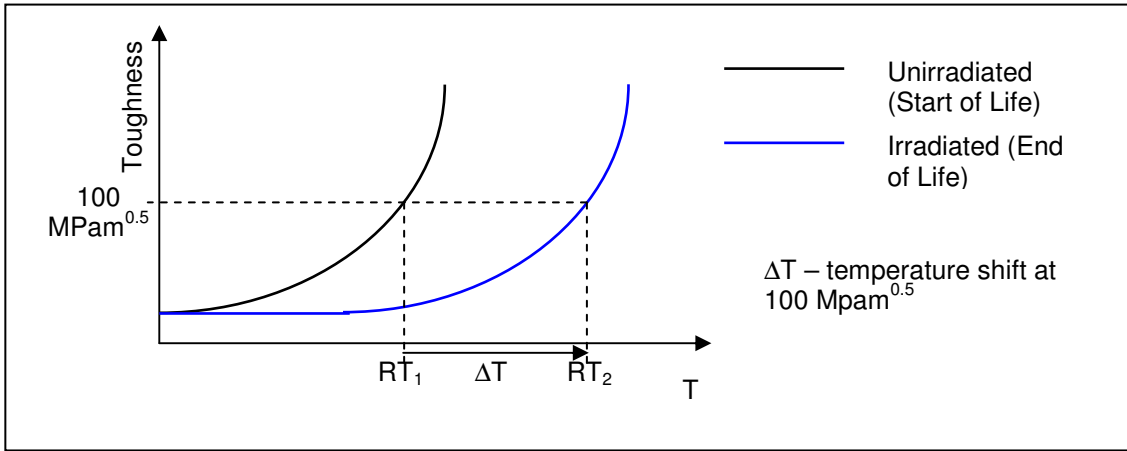


Figure 3.2.5.3 Effect of Irradiation on the Fracture Toughness of Reactor Pressure Vessel Steel

### 3.3 Testing Methods

There are three methods for testing the toughness of materials, one dynamic and two static. Dynamic testing involves impact loading of a specimen to measure the response, this is commonly done by a Charpy V-notch (CVN) impact test, see Figure 3.3.1. The loss in energy of a pendulum is used to calculate how much energy has been absorbed during fracture of a test piece. Two other measurements are commonly taken from the fractured specimen; the fracture appearance whereby the percentage area of ductile or brittle failure is measured or estimated, the second is the lateral expansion of the compression side of the test piece<sup>[30]</sup>. Both give a good quantitative representation of the materials response to loading. Although impact testing can aid in materials selection and fitness for purpose assessments it cannot give a true value to the toughness of the material, instead it is best to design by staying on the 'upper shelf', i.e. the high energy absorbing ductile region. This cannot always be accommodated and has been shown in a previous section of this report the impact properties also degrade with neutron embrittlement.

The two static methods for direct toughness measurement measure similar properties but by using different methods, one purely elastic the other allowing a small amount of plastic deformation before the onset of brittle failure. The elastic test is the much simpler of the two and requires little measurement during the test and the process of obtaining a toughness value is straightforward. A testpiece containing a deep sharp flaw is loaded till failure the final load can then be used to determine the critical value of stress intensity,  $K_{Qc}$ , that caused failure in the test piece<sup>[31, 32]</sup>. In order for the effect of loss of constraint at the free surfaces to be minimised the test piece must be of a minimum thickness empirically determined from the stress intensity factor measured in the test and the yield strength of the material:

$$B \geq 2.5 \left( \frac{K_{Qc}}{\sigma_Y} \right)^2$$

where  $B$  = specimen thickness,  $K_{Qc}$  = measured toughness and  $\sigma_Y$  = yield stress (similar material dependent constraints exist for other dimensions)

Where tough materials are measured at high temperatures, the size requirement can soon reach very large values, so finding a suitable testing machine capable of exerting the required loads becomes difficult. Some very large-scale tests have been

performed in the past to prove the high temperature toughness of RPV steels; the test pieces reached a maximum thickness of over 300 [33]. The shape of the test piece commonly takes two forms, the bend bar or the compact tension test piece. The bend bar is the simpler of the two geometries and so the test piece is easier to manufacture however, the loading of the specimen prevents simple calculation of the stress intensity and the operator must rely on established equations to determine the toughness of the material. The compact tension testpiece provides a better loading of the specimen, as the loading points remain parallel to their original position through out the test the stress intensity calculation is less complex<sup>[34, 35]</sup>.

The final form of testing uses a crack tip opening argument to calculate the amount of work that has gone into the fracture. A similar specimen to  $K_{Ic}$  determination is used but due to the different measurement procedure, much smaller specimens can be used, useful if there is limited material available. The resistance to fracture is calculated by the area under the load-displacement curve corresponding to the total amount of work done. Two methods exist for this calculation, a simple and an advanced procedure. In the simple method, the test piece is loaded until near failure and the elastic and plastic components of fracture are deduced and used to determine the J value corresponding to the energy of fracture. The advanced method takes into account the change in crack length during the experiment associated with ductile crack growth. To do this the sample is unloaded in the plastic region of the stress-strain curve to allow the compliance of the specimen to be established from which the crack length can be calculated increasing the accuracy of the J calculation<sup>[32, 36]</sup>.

By using a line-integral the energy in the vicinity of a crack tip can be calculated, the presence of plastic deformation can also be accommodated. It has been shown that the line integral can be determined if the stress and strain are known on a contour away from, but surrounding, the crack tip<sup>[37]</sup>. This type of data is readily available from finite element analysis and so fitness for purpose assessments are easier to conduct using J integral methods as the local stress of a crack tip does not have to be modelled accurately

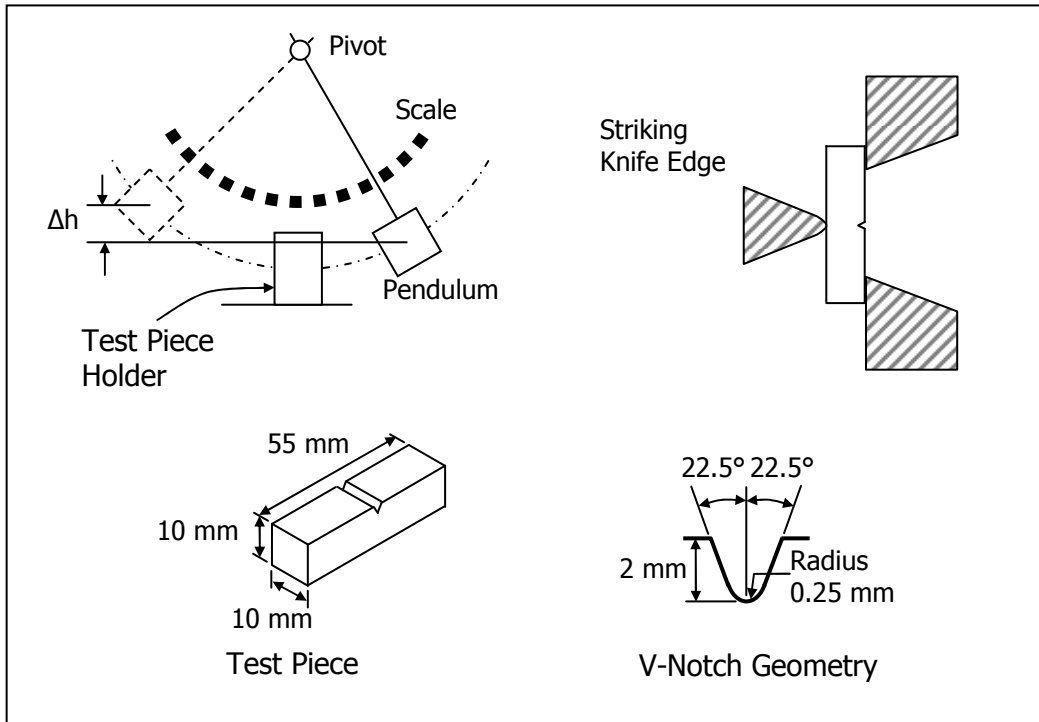


Figure 3.3.1 Form of the Charpy Impact Test and V-Notch Geometry<sup>[38]</sup>

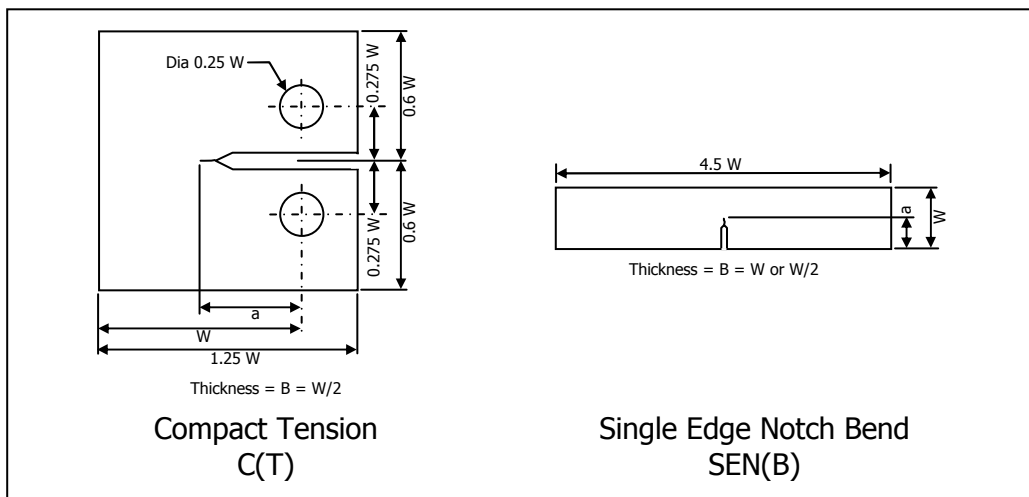


Figure 3.3.2 Fracture Toughness Specimen Geometries<sup>[31]</sup>



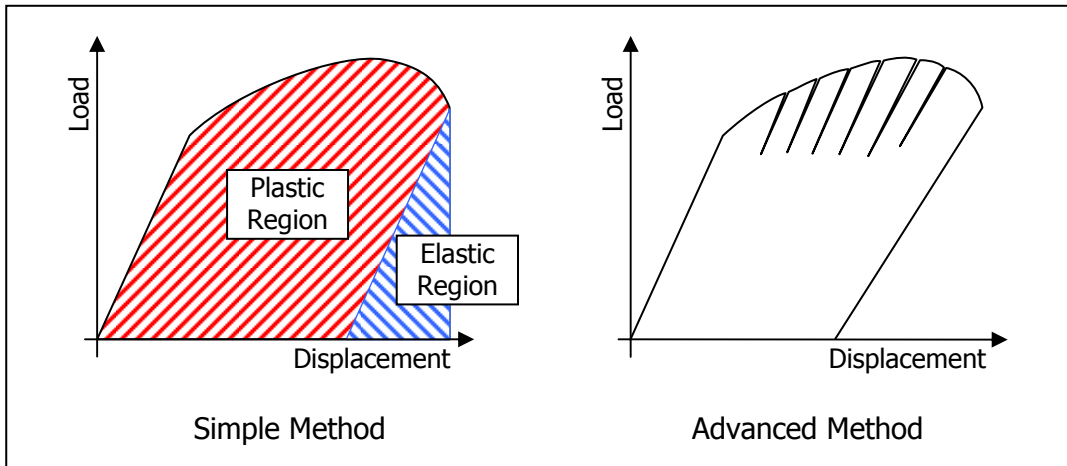


Figure 3.3.3 Simple and Advanced J-Integral Test Methods

### 3.4 Failure Mechanisms

There are six forms of failure associated with engineering structures:

1. Ductile Failure  
Permanent deformation caused by overloading
2. Brittle Failure  
Catastrophic failure
3. Deflection/Fowling  
Poor design leading to fowling of components due to deflections when loaded.
4. Fatigue  
Growth of existing cracks at low loads caused by plastic deformation at the crack tip due to cyclic loading
5. Creep  
High temperature loading causing a flow in the material
6. Buckling  
Elastic instability of slender columns

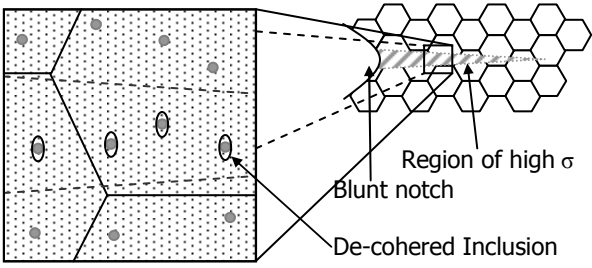
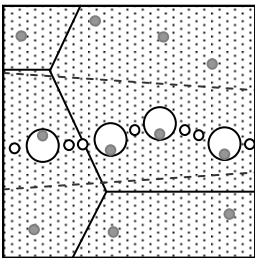
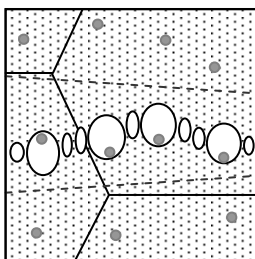
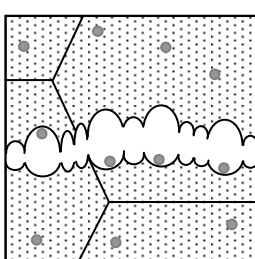
Ductile and brittle failure are the two mechanisms governed by the toughness of the material and hence, an understanding of these mechanisms is essential to the understanding of fracture of the steels used in RPV construction.

#### 3.4.1 Ductile Failure

Ductile fracture is commonly caused by poor design but is still predominantly predictable in components due to the material properties that control the resistance to plastic deformation. The controlling factor is the materials yield stress,  $\sigma_Y$ , which has very low variability at a given temperature due to the nature of dislocation movement in the material, i.e. a critical level of applied load has to be reached before the atom layers shear resulting in a permanent deformation. In engineering terms a ductile failure can be described as a slow observable process and when it does occur the component design can be changed to accommodate the problem,

such as increasing the local section thickness to reduce the local stress and prevent this exceeding  $\sigma_y$ .

In reality, the component will still be able to support the load (or after the UTS a sizeable fraction of the load) so the component may continue in service allowing time to find the problem and replace/redesign the component, but the deflections caused by this loading may prevent the component from working correctly. There are two possible ways that the component may become unfit for purpose. With small deflections where tolerances are tight, the component may start to foul others (this can also occur with elastic loading) or when large deflections are present it is more likely that plastic collapse of the component has occurred (here the zone of plasticity has grown through the net section).

①	As stress increases inclusions acting as local stress concentrators de-cohere if weakly bonded or fracture if strongly bonded to the matrix forming voids.	
②	The void sizes increase as more material deforms in a plastic manner and voids also form around the carbides showing a preferential crack path through the material.	
③	Eventually the voids will coalesce leaving only fibres supporting the load.	
④	The local stress in the fibres increases beyond the tensile strength of the material and they break causing the material to tear.	

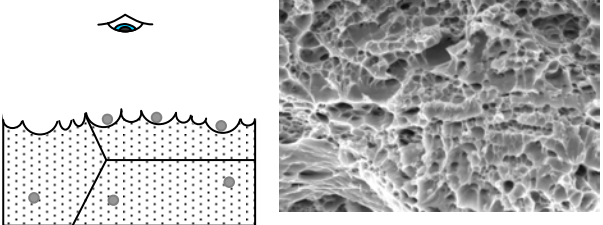
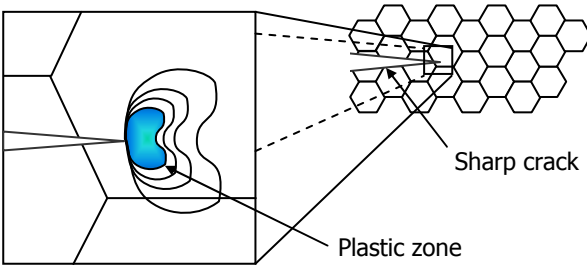
⑤	<p>As different sized weakly bonded inclusions (non-metallics, intermetallics and carbides) then the fracture surface shows two different size dimples with some inclusions left at the base.</p>	
---	---	--

Table 3.4.1 Ductile Failure Mechanism<sup>[39]</sup>

### 3.4.2 Brittle Failure

Brittle failure is catastrophic, i.e. it may happen with out warning. The material property that controls the resistance to fracture appears to have a random nature and conforms to a distribution; when loaded the user is effectively sampling from this distribution, which has very large variability, compared to  $\sigma_y$ . This random sampling can result in very low resistance to fracture and once one small packet of material fractures the rest of the component will also fail, the crack front will travel through the material at close to the speed of sound resulting in a very sudden failure. Unlike ductile failure where load is still supported by the remaining ligament, brittle failure results in complete breaking of the component, i.e., there is no remaining ligament to support any load, so when brittle failure occurs it will begin at an unpredictable point and proceed too rapidly for the load to be removed. It is therefore very difficult to design against brittle failure as commonly the trigger event is only known after a catastrophic failure has occurred, only then can the component be redesigned to reduce the potency of the initiator.

①	<p>Brittle failure requires that the local stress intensity is higher than a critical value, so a sharp crack needs to be present resulting in a plastic zone in front of the crack tip. The stress in this region is controlled by the yield stress, <math>\sigma_y</math>, of the material</p>	
---	--	--

②	<p>The stress, <math>\sigma_1</math>, in the plastic zone can be calculated by finite element analysis and normalised by <math>\sigma_y</math>. The distance from the crack tip, <math>r</math>, is normalised by crack opening displacement, <math>\delta</math>.</p>	
③	<p>Brittle failure occurs when the local stress exceeds the fracture stress of the material. Current thinking is that there is a pile up of dislocations at an inclusion or carbide causing it to fail producing a sharp crack with in the material.</p>	
④	<p>If on initial loading a suitable inclusion is not present to cause failure then the crack front will grow until the conditions for brittle failure are met. By growing in this manor the local stress intensity is also increased by having a deeper flaw. This process also leaves a ductile thumbnail on the fracture surface.</p>	
⑤	<p>Once the sharp crack is present in the material the crack can then propagate but only if there is a change in energy large enough to climb the 'hump' associated with the first few grain boundaries.</p>	
⑥	<p>Once propagation starts the crack cannot be stopped growing, as the crack front will move close to the speed of sound with in the material. The final fracture surface is faceted and is distinctive of transgranular cleavage.</p>	

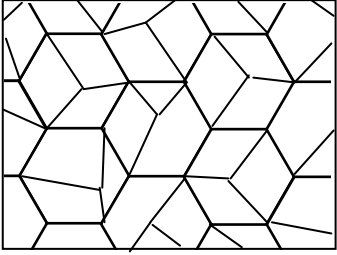
⑦	<p>Another form of brittle failure is of more concern where the grain boundaries have become embrittled by the presence of impurities, such as phosphorus, giving very low resistance to fracture. Here the grain boundaries give a preferential fracture path and the fracture surface is very distinctive.</p>	 <p>Intergranular fracture surface</p>
---	--	--

Table 3.4.2 Brittle Failure Mechanism [9, 15, 26, 37, 40-44]

## **3.5 Current and Emergent Toughness Models**

### **3.5.1 ASME Pressure Vessel Code**

At the middle of the 20<sup>th</sup> century it became apparent that toughness data were needed to prove the safety of reactor pressure vessels. The field of fracture mechanics was still in its infancy and only very limited data were available, only about 60 toughness tests had been conducted. A model was required to predict the through life properties of RPVs but first the start of life (SOL) toughness had to be known. By normalising the data using a nil-ductility reference temperature, it was possible to determine a toughness curve.

Nil ductility temperature (NDT) is established by using a Pellini drop weight test. A sharp crack is introduced into a plate of the material under investigation via a notched weld bead. The test piece is then placed bead side down and a weight is dropped on the other surface, see Figure 3.5.1.1. The weld absorbs little energy during fracture so the crack grows into the plate until it either reaches a free surface or is arrested. Failure of the test piece is considered to be when the crack reaches either of the free surfaces. The NDT is the highest temperature at which break occurs. [45-46]

This curve, see Figure 3.5.1.2, was simply chosen as a lower bounding curve to all data pulling the curve downwards leading to large amounts of conservatism in safety assessments. As more toughness test programme results were published, it became obvious that there were large amounts of scatter in the toughness data and the lower bounding curve philosophy could no longer give a believable explanation of the toughness properties of ferritic steels.

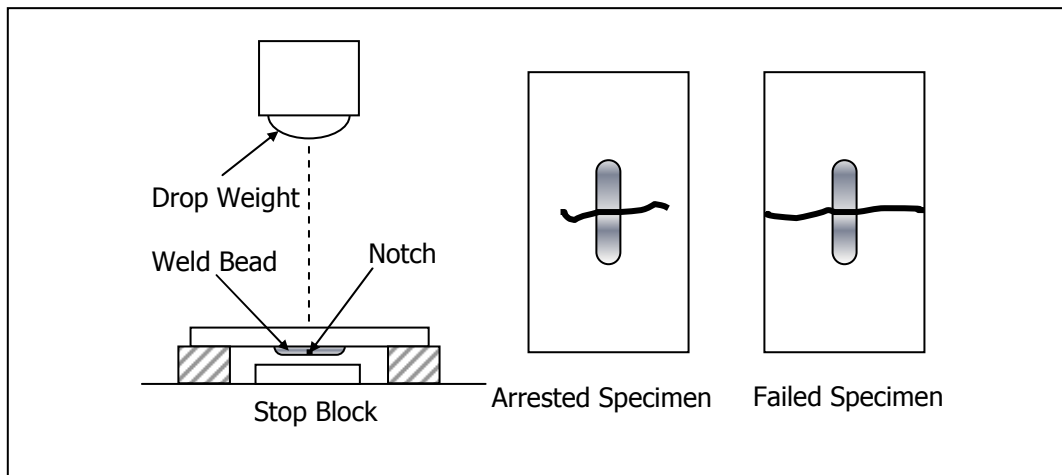


Figure 3.5.1.1 Pellini Drop Weight Test Apparatus and Specimens

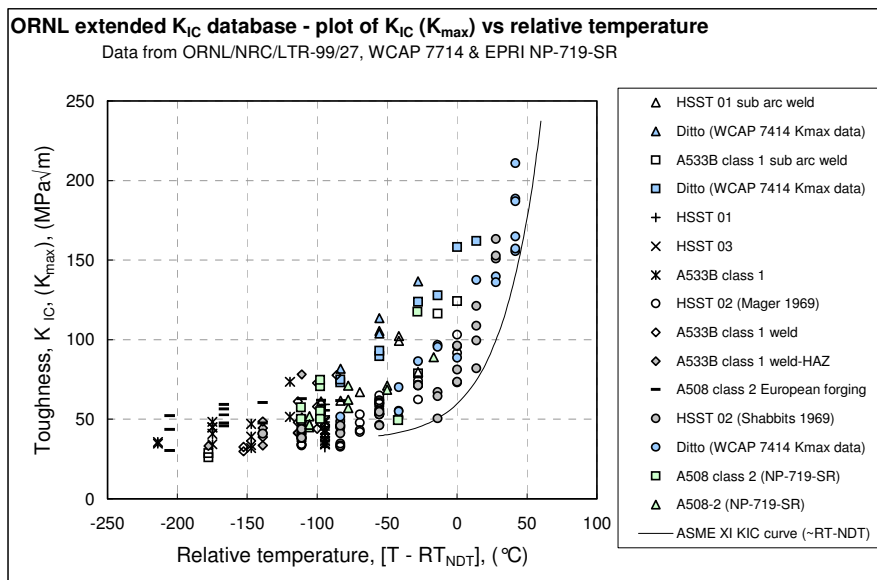


Figure 3.5.1.2 Extended EPRI Database Normalised By Nil-Ductility Temperature

(Plot supplied Dave Swan, R-R OE & T)

### 3.5.2 Master Curve

The eye-ball curve drawn under the initial data does not stand up well when scrutinised, a new approach was needed with increased mechanistic understanding removing some of the conservatism associated with the ASME code. The master curve was initially dismissed by many but has now become the best estimation of the toughness of ferritic materials and has been adopted as an American standard, ASTM E1921-02. <sup>[47]</sup> The main theory of the master curve model is a weakest link



argument; much like a chain a material is made up of links, when one link fails all surrounding links fail as well. This allowed the use of a Weibull distribution to model the scatter in the data and to give a probability of failure associated with an applied load. [48-49] This can then be used in an incredibility of failure argument, where it can be proved that failure is so improbable to occur through out the life of the vessel that it may be operated in its current state without further justifications until the end of the plants life.

It became apparent that a three-parameter Weibull distribution would be required to describe the toughness at a given temperature, two parameters to scale the distribution and one to locate it on the toughness axis. By defining the one of the scale parameters and the location parameter, at least in part, as fixed constants for all ferritic steels it is possible to establish the third by using a small number of tests. By taking the test results at one temperature it is possible to fit the probability density function (pdf), Eq 3.5.2.1, curve to available data by changing the  $K_0$ , or alternatively the  $K_0$  can be calculated from the data by using a maximum likelihood method, Eq 3.5.2.2. The  $K_0$  value, corresponding to roughly a 63<sup>rd</sup> percentile of the distribution can be used to calculate the median of the pdf distribution,  $K_{Jc(med)}$ , Eq 3.5.2.3. [47]

$$\text{Eq 3.5.2.1} \quad pdf = 1 - \exp\left(-\left(\frac{K_{Jc} - K_{MIN}}{K_0 - K_{MIN}}\right)^4\right)$$

$$\text{Eq 3.5.2.2} \quad K_0 = \left[ \sum_{i=1}^N \frac{(K_{Jc(i)} - K_{MIN})^4}{N - 0.3068} \right]^{\frac{1}{4}} + K_{MIN}$$

$$\text{Eq 3.5.2.3} \quad K_{Jc(med)} = (K_0 - K_{MIN})[\ln(2)]^{\frac{1}{4}} + K_{MIN}$$

The MC held onto the idea that the shape of the toughness transition is unaffected by the chemistry of the steel as long as it had a ferritic, bcc, atomic structure. Instead of using the  $RT_{NDT}$  established from the Pellini drop weight test, it was proposed that a reference temperature calculated from the toughness curve should be used. The so-called  $T_0$  value is the temperature at which the median toughness of a 25 mm specimen is equal to 100 MPam<sup>0.5</sup>. This can be calculated from as little as

six tests allowing a complete transition toughness curve to be produced including probability bounds for a very small expense.<sup>[47]</sup>

The definition of specimen size is allowable due to the use of a Weibull 'weakest link' argument. By using this failure model a statistical link can be made between specimen size and toughness. Several proposals have now been made that the size effect may not be consistently modelled for all steels that the MC is claimed to provide accurate toughness data.<sup>[50, 51]</sup> These proposals tend to be commonly for very long crack lengths, such as a complete crack around a circumferential weld in a vessel leading to very low expected toughness.

A failure analysis procedure has been developed around the MC known as SINTAP, the toughness estimation procedure is outlined in Appendix B. This provides users with a simple systematic method to produce a  $T_0$  value based on the worst material data available. By doing this the homogeneity of the material can be checked and toughness estimation is less prone to being dragged upwards by bad test piece location selection.<sup>[52]</sup> If the data is found to be inhomogeneous then a metallographic examination would be recommended in order to allow testing of the worst microstructure.

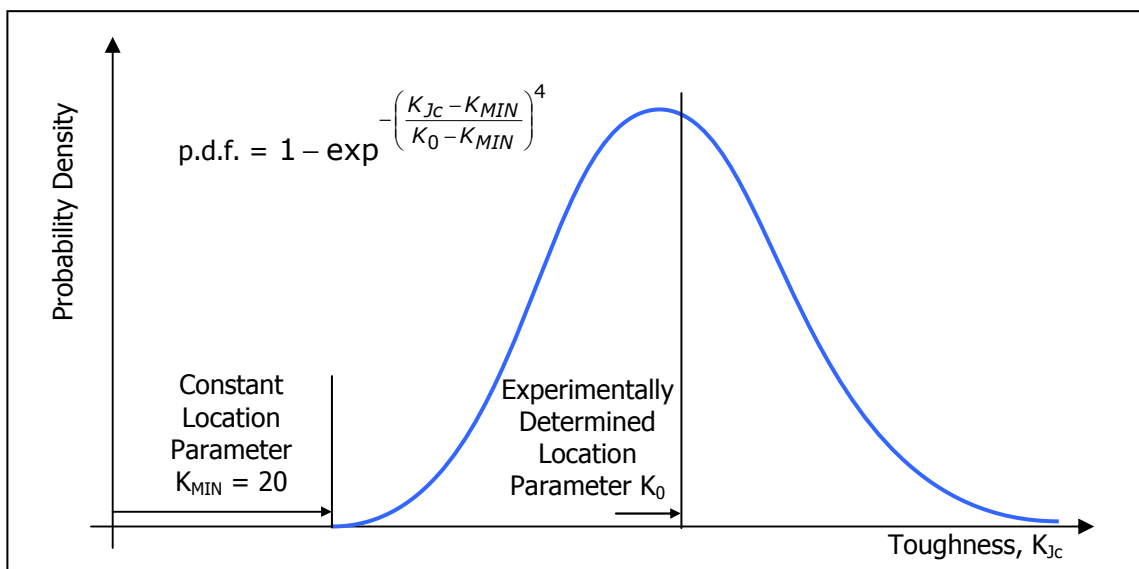


Figure 3.5.2.1 Master Curve Probability Density Function

### 3.5.3 Unified Curve

It has been noted that the MC does not provide a good description of the transition toughness of PVS in the highly embrittled state. This is not commonly a problem for western reactors due to improved chemistry control but former USSR and eastern block reactors were made from steels prone to large amounts of embrittlement.<sup>[53]</sup> However, the development of a model for these steels is difficult due to the small volume of material available in the brittle condition, and so very small samples must be used. Even from this small sample size, it was obvious that the shape of the transition curve was no longer constant.

A new model proposed by Margolin et al. has been created and validated against 2.5Cr-Mo-V and 3Cr-Ni-Mo-V steels in the initial condition.<sup>[53,54]</sup> This model is described below as it is presently the only successful model based on a physical understanding of the conditions of brittle fracture. The model does not predict the shape and temperature shift condition, as is done by the MC, and so the curve is allowed to change shape at various irradiation shifts. The model is based on seven assumptions:

1. Material is polycrystalline and properties are an average of the unit cell properties. Within the unit cell stress and strain are considered homogenous.

2. Local criterion for failure of a unit cell:

$$\text{Equ 3.5.3.1} \quad \sigma_1 + m_{T\epsilon} \sigma_{eff} \geq \sigma_d \quad (\text{nucleation of microcrack})$$

$$\text{Equ 3.5.3.2} \quad \sigma_1 \geq S_c(\epsilon) \quad (\text{propagation of microcrack})$$

$$\text{Equ 3.5.3.3} \quad S_c(\epsilon) = [C_1 + C_2 \exp(-A_d \epsilon)]^{\frac{1}{2}} \quad (\text{critical brittle fracture stress})$$

Where;

$\sigma_1$  = maximum principle stress

$\sigma_{eff} = \sigma_{eq} - \sigma_y$  = effective stress

$\sigma_{eq}$  = equivalent stress,  $\sigma_y$  = yield stress

$\alpha = \int d\varepsilon_{eq}^p$  = Odqvist's parameter

$d\varepsilon_{eq}^p$  = equivalent plastic strain increment

$\sigma_d$  = strength of carbide/matrix interface

$m_{T\varepsilon} = m_T(T)m_\varepsilon(\alpha)$  = parameter dependent on temperature and plastic strain

$m_T(T) = m_0\sigma_{ys}(T)$ ,  $m_\varepsilon(\alpha) = \frac{S_0}{S_c}(\alpha)$

$S_0 \equiv S_c(\alpha = 0)$

$m_0$  = experimentally determined constant

$\sigma_{ys}$  = temperature dependent component of yield stress

$C_1, C_2$  and  $A_d$  are materials constants

3. Assumed that  $\sigma_d$  is stochastic and all other parameters are deterministic.
4. A Weibull distribution is used to describe  $\sigma_d$ , and so the minimum bonding strength of carbides in the unit cell on which cleavage microcracks are nucleated can be established.

$$\text{Equ 3.5.3.4} \quad P(\sigma_d) = 1 - \exp\left[-\left(\frac{\sigma_d - \sigma_{d0}}{\tilde{\sigma}_d}\right)^\eta\right]$$

Where  $P(\sigma_d)$  is the probability of finding in each unit cell a carbide with minimum strength less than  $\sigma_d$ .  $\sigma_{d0}$ ,  $\tilde{\sigma}_d$  and  $\eta$  are Weibull parameters.

5. A weakest link model is used to describe brittle fracture of the polycrystalline material.
6. Brittle fracture may only occur in unit cells where  $\sigma_{eq} \geq \sigma_y$ .
7. Equ 3.5.3.5  $P(\text{Survival of a unit cell}) = 1$  if  $\sigma_1 < S_c(\alpha)$ .

The assumptions have been combined into a probabilistic model with the following parameters:

1. Local criterion outlined above.
2. Brittle fracture is controlled by unit cells in a semi-circular zone near the crack tip with radius  $= r_p + \frac{\delta}{2}$ ; where  $r_p$  = minimum size of the plastic zone,  $\delta$  = crack tip opening displacement (see Figure 3.5.3.1).
3. All unit cells in the same ring will have the same  $P_f$ .
4. Stress and strain on the line are calculated by approximate analytical solutions.

The brittle fracture probability of a cracked specimen,  $P_f$ , can be determined from the above by calculation of the non-fracture probability of all cells. The brittle fracture probability for the cracked specimen can be calculated by the summation of the non-fracture probability for each of the rings. This gives the survival probability of the specimen, hence subtracting from unity gives the brittle fracture probability.

$$\text{Equ 3.5.3.6} \quad P_f(K_I)_T = 1 - \exp \left[ - \frac{\omega}{(\tilde{\sigma}_d)^\eta} \pi \sum_{i=1}^k \left( \frac{\delta}{2\rho_{uc}} + i - \frac{1}{2} \right) (\sigma_{nuc}^i - \sigma_{d0})^\eta \right]$$

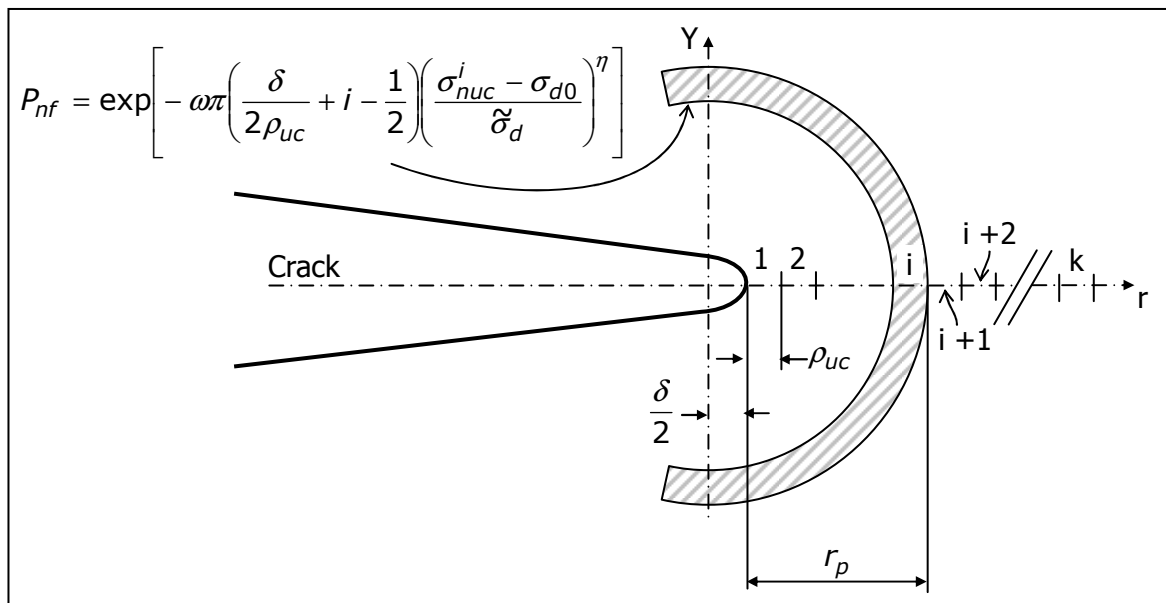


Figure 3.5.3.1 Unified Curve Probabilistic Failure Model

### 3.5.4 Micro Arrest

Actual data shows that the 1 % MC bound is not an accurate representation of the data, in reality a 1.8 % MC bound is equivalent to 1% of the data. A reasonable explanation for this feature is the Micro Arrest (MA) concept.<sup>[51]</sup> If initiation events do conform to a weakest link argument then arrest of the cracks produced by these events must be the lower bounding mechanism. In order for a crack to propagate through the steel it must first break out from the initiation locality, to do this requires energy and there is an energy hump associated with the first and second grain boundary. If the micro-crack has insufficient energy to climb the hump then it will arrest in a micro event.<sup>[44]</sup> The MA concept uses the macro properties of initiation and arrest toughness to describe these micro events.

By using the macro properties MA can be expressed as a crossing of the arrest and initiation distributions. Both of these have been successfully described by probability distributions; Weibull for initiation, log normal for arrest. Dependent on the location parameters ( $T_0$  for initiation,  $T_{kia}$  for arrest) the distributions cross by differing amounts for a given material condition.<sup>[51]</sup> A possible additional benefit of the concept is that  $T_0$  is affected by irradiation and  $T_{kia}$  is not, so as irradiation dose increases the distributions will actually become more crossed and MA will play a larger role in the lower tail of the MC.

For low toughness material the use of MA may be necessary to comply with 'fitness for purpose' and incredibility of failure type safety assessments. In order to use MA it must first be proved to exist and this the subject of one of the current projects discussed latter in this report. To have the best possible chance of discovering MA with a limited number of tests a better understanding of how the distributions cross is needed. In order to assess how MA would affect the lower tail of a toughness distribution a Monte Carlo simulation was conducted, known as the Simulakrum model. By comparing randomly generated initiation and toughness values, it is possible to see how the lower tail is cut off, increasing lower bound toughness (Figure 3.5.4.1).<sup>[51]</sup>

By approaching the distributions in a different way it is possible to calculate the likelihood of MA at a given test temperature and applied stress intensity factor. By

selecting the above and by simple rearrangement of the underlying MC function the probability of MA can be obtained.

$$\text{Equ 3.5.4.1} \quad P(MA) = P(K_{Jc} < K) \times P(K < K_{Ia})$$

$$\text{Equ 3.5.4.2} \quad P(K_{Jc} < K) = 1 - \exp \left[ - \left( \frac{B_x}{B_0} \right) \left( \frac{K_{Jc} - K_{\min}}{11 + 77 \exp[0.019(T - T_0)]} \right)^4 \right]$$

$$\text{Equ 3.5.4.2} \quad P(K < K_{Ia}) = 1 - P(\ln(K); \ln(30 + 70 \exp[0.019(T - T_{KIa})]), 0.18)$$

Where  $P(\ln(K); \ln(30 + 70 \exp[0.019(T - T_{KIa})]), 0.18)$  conforms to the cumulative normal distribution function with mean =  $\ln(30 + 70 \exp[0.019(T - T_0)])$  and standard deviation = 0.18.

If the material parameters,  $T_0$  and  $T_{KIa}$ , are known a probability of MA plot can be constructed (Figure 3.5.4.2). By varying the temperature and crack front length,  $B_x$ , an appreciation of their effect on the likelihood of MA can be obtained. It is observed that MA is more likely at lower temperatures and when a larger crack front length is employed. The first of these is explained by the fact the distributions cross by an increasing amount as lower temperatures are utilised; the second is of more use in safety justifications. The crack arrest property is un-affected by crack front length whereas initiation toughness is greatly reduced by an increased length. This acts as a factor in equation 3.5.4.2 as the  $\frac{B_x}{B_0}$  term and by using possible crack lengths of several meters the effect of MA on real world cases can be established (figure 3.5.4.3)

By including MA in a safety justification it is possible to limit the crack front length correction and so no matter the size of a real world defect the actual level of critical stress intensity factor is reduced. For MA to be accepted it must be proven to exist and this is the subject of one of the current projects detailed in a later section of this report.

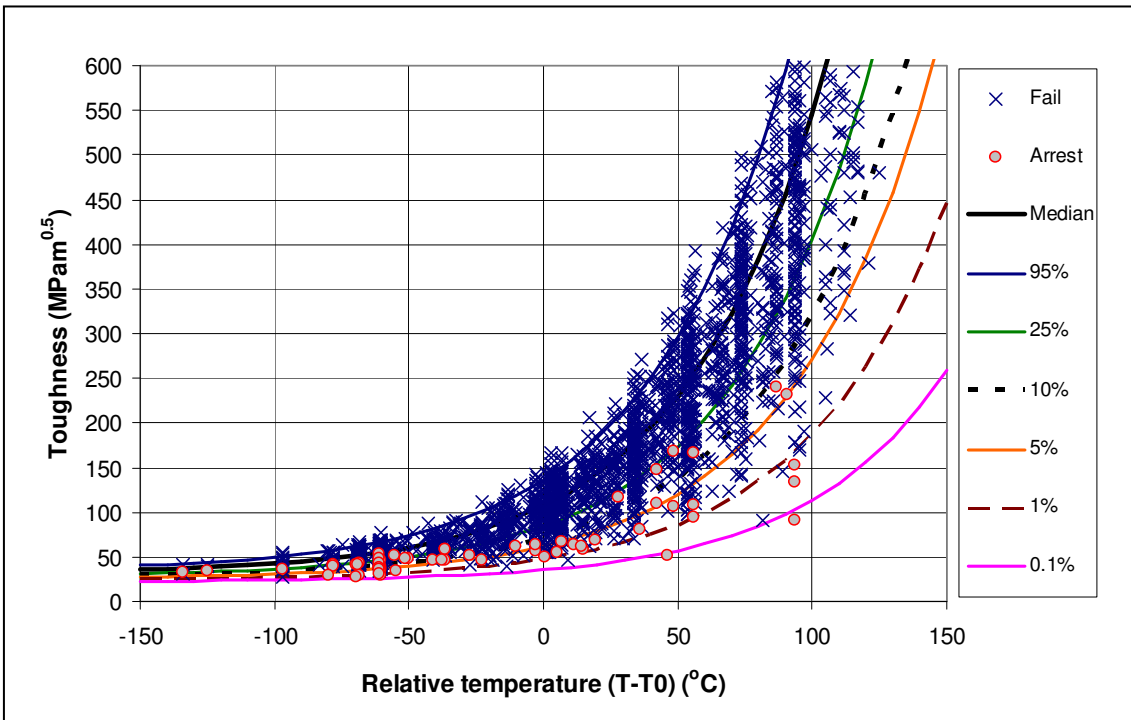


Figure 3.5.4.1 Results of the Simulakrum Simulation



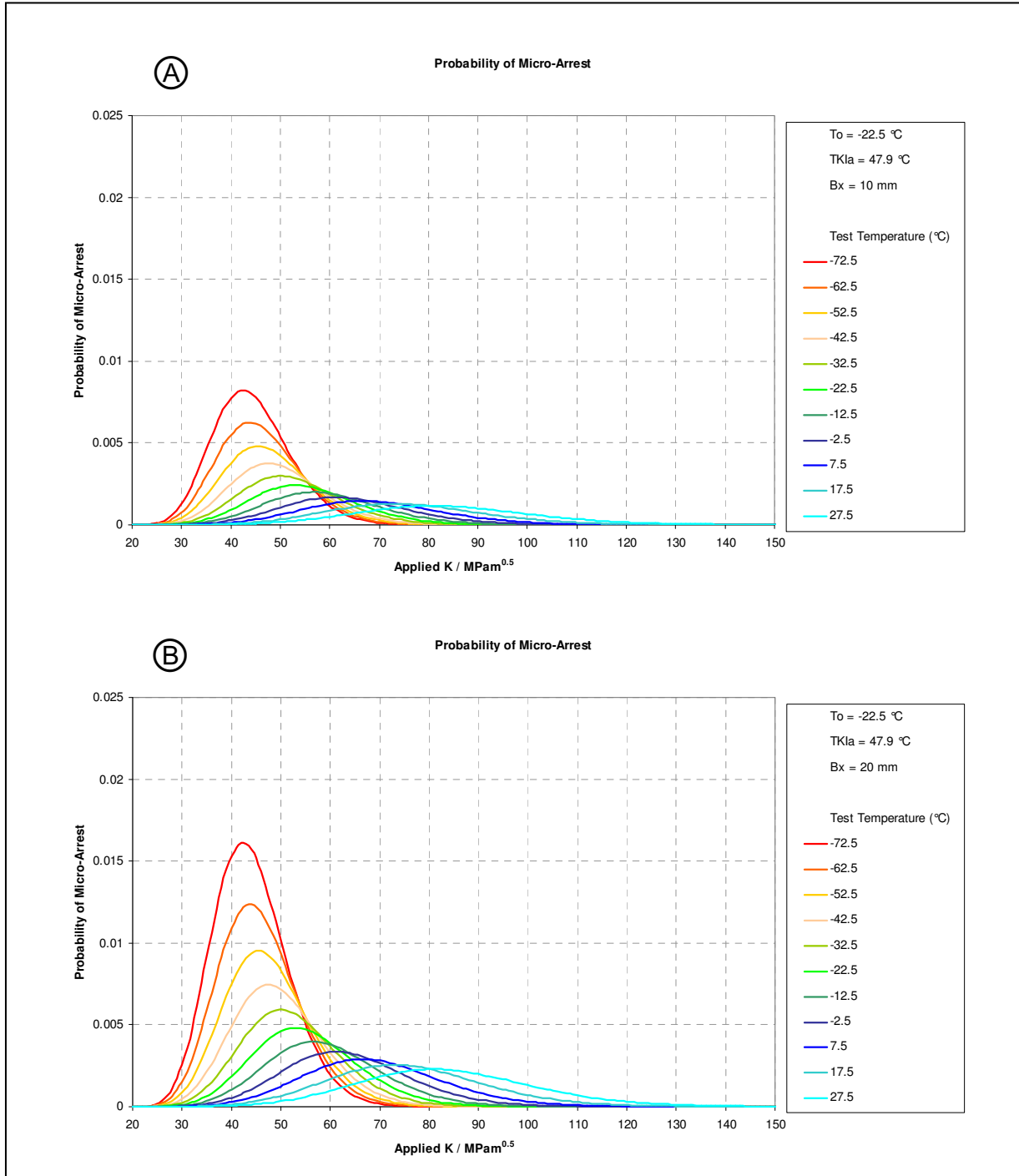


Figure 3.5.4.2 Probability of Micro Arrest plots.

a,  $B_x = 10$  mm; b,  $B_x = 20$  mm.

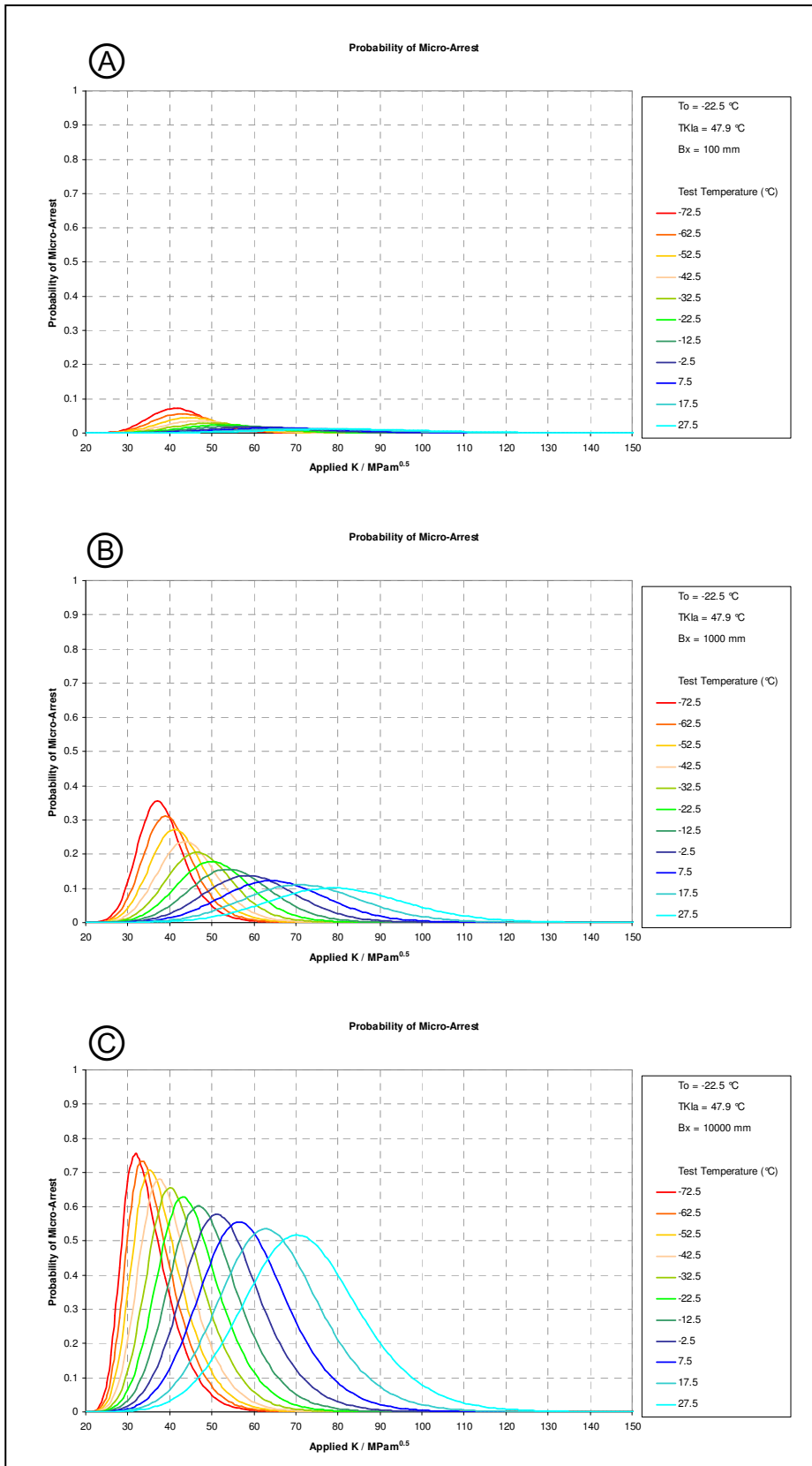


Figure 3.5.4.3 Effect of Micro Arrest on long crack front lengths.

a,  $B_x = 100$  mm; b,  $B_x = 1,000$  mm; c,  $B_x = 10,000$  mm.

### **3.5.5 Other Models**

Many other toughness models exist, however as the actual process of initiation is not completely understood no model can be justified to an extent where it could be proven that it is the 'true' toughness model. Several models are based on best estimation and data fitting (such as the MC) and others provide a complete structural assessment, not just the brittle fracture probability of the material. A new breed of 'multi-scale multi-physics' models are now being produced combining microstructure information with powerful finite element analysis to assess the global stress and strain effects on the local area in front of the micro-crack.

Most countries have their own approved toughness model for civil operation; many based on the ASME pressure vessel code and more recently the MC concept has become more widely accepted as the best fit to available data.

## **4. Business Context of the Project**

Submarines are used in a wide variety of roles from attacking surface ships to land attack. In land attack conventional weapons can be used, such as cruise missiles fired through the torpedo launchers as seen in recent military actions, or the use of atomic weapons deployed using intercontinental ballistic missiles. At present, the Royal Navy submarine fleet provides the United Kingdoms only means of deploying nuclear weapons and as such is the sole nuclear deterrent for the nation. Keeping these submarines available for use by the Royal Navy and on station is of the highest importance. In order to do this the safe continued operation of the submarine power plant must be demonstrated.

Many nations operate submarine fleets but the majority use a combined diesel-electric power supply, which requires the submarine to be at the surface for the diesel engines to be used for propulsion and charge the batteries needed for submerged operation. The range under water is limited by battery capacity and by having to surface the submarine loses its major advantage of stealth, in fact the best way to find and hunt a submerged submarine is using one which is just as undetectable as the first. By switching to nuclear propulsion the submerged range of the submarine is only limited by the endurance of the crew, as demonstrated by the first nuclear submarine the USS Nautilus when it traversed the North Pole, being the first ship to travel from the Atlantic to the Pacific. Nuclear submarines can operate for long periods at sea with little or no support and so become more difficult to detect by not having to meet supply ships that are easy to track. Due to these attributes the use of nuclear submarines has become key to the United Kingdom defence policy.

Rolls-Royce is the sole supplier and provides technical support of marine nuclear power plants to the Ministry of Defence. R-R is the Design Authority for the nuclear steam raising plant (NSRP) used for submarine propulsion, and hence receives all contracts related to design, development, procurement and support of the NSRP. This does mean that it is the burden of R-R to prove the continued safe operation of all running plants, in order to fulfil this role the company invests heavily in experimental programmes. To justify the use of a nuclear reactor a fitness for

purpose assessment must be conducted, this has three parts supported by experimentally determined mechanical properties.

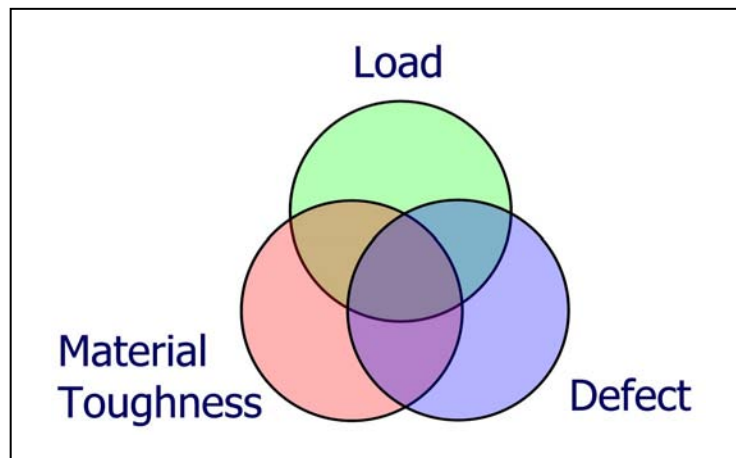


Figure 4.1 Schematic Representation Of The Areas That Combine To Form A Fitness For Purpose Assessment

In order for a safety case to be well defined, each of the three areas must also be well defined. The area this project is concerned with is that of fracture toughness of the steel being used for heavy section forgings such as the reactor vessel. Providing the most accurate estimation of the toughness of the reactor pressure vessel (RPV) material has a direct relation to submarine availability as once a critical value of toughness is reached the reactor must be shut down for fear of public safety. If the toughness is underestimated then valuable years of operation could be lost, also most submarines are unique in the equipment that they have on board and it may be imperative that a particular submarine is available for a particular mission. A submarine costs a large amount of taxpayers money and the more operational years that can be obtained the more cost effective the submarine becomes.

## 5. Current Projects

### 5.1 High $T_0$ Investigation

This project is being conducted to discover why forgings recently procured by R-R are of a lower toughness than those manufactured to a similar specification previously. If it can be discovered which properties are linked to the toughness of a forging it may be possible to devise a composition and processing route that will give improved toughness and increased reliability. Several properties and microstructural features are believed to be related to toughness, although as yet no recognised mathematical correlations exist. Two questions need to be answered in order to increase the understanding of the effect these properties and features have on the toughness of the material.

Question 1. How much does the material remember of previous processing? What is the effect of unit size and orientation?

To answer this question the following must be known about the forgings:

1. Prior Austenite Grain Size

This is considered the unit cell of the material and can be measured in a variety of ways using simple and complex techniques. Various chemical etches (see Appendix C) have been employed to reveal the underlying microstructure of the forgings, however due to the very low concentration of impurities (especially Phosphorus) on the grain boundaries this has proved ineffective. Electron Back Scatter Diffraction (EBSD) should provide better results but has not yet been attempted due to the high cost and time that it is required to obtain accurate measurements. Inducing intergranular fracture by stress corrosion cracking (SCC) has also been considered as a way of obtaining an accurate measurement, some doubts exist if this will actually provide an intergranular surface suitable for measurement as SCC also requires impurities on the grain boundaries.

2. Grain Boundary Angles

If the material has been over/under worked the material may have formed patches where the grains are aligned and hence the grain boundaries offer lowered resistance to the propagation of cleavage, reducing the toughness compared to a randomly orientated structure. The only way to accurately measure this is by EBSD although some tint etchants can provide a qualitative indication of the orientations within the material.

3. Facet Size Measurement

Measurement of the cleavage facet size distribution for comparison with the prior austenite grain size distribution. The fracture surface is produced by breaking a simple saw cut specimen at -196 °C. This may conform/deny the theory that the prior austenite grain size is the unit cell with respect to cleavage failure.

Question 2. Has the prolonged heat treatment applied to these forgings caused unusual carbide growth and morphology?

1. Effect of Carbide Size and Morphology

In order to obtain a carbide distribution the carbides must first be revealed. Two methods are/will be available to separate or view carbides; TEM examination of materials will produce accurate data but will take many months to provide the required distribution, SEM examination of ductile fracture surfaces looking for carbides in the base of voids (will not provide distribution but will give indication of the maximum size).

2. Effect of Alloying Composition on Carbide Size and Morphology

Literature search on the effect of micro-alloying elements and processing on the growth of unwanted and detrimental phases and inclusions in the forgings.

This investigation is due to be reported in early 2006 once all samples have been investigated, some initial results are shown in Appendix D. Presently it appears that the concentration of micro-alloying elements (Ti, V, Nb) is suitably low that, combined with a low forging ratio, is sufficient to cause large prior austenite grain

growth during the forging process. This large inherent grain size is not subsequently removed by the quality heat treatment applied to these forgings.



## 5.2 Micro Arrest Testing

In order for MA arguments to be used to truncate the lower tail of the MC toughness, it must be proven to exist. For the majority of materials the likelihood actually obtaining MA in a test is extremely low but for low toughness material, the odds are improved. By choosing the correct test temperature and maximising the specimen thickness it is possible to greatly increase the chance of obtaining MA in a test. However, material is limited and the largest sample size available provides a crack front length of only 20 mm. This is not sufficient to raise the probability of MA to a level where it can be tested for using a small number of specimens. This can be negated by the use of cyclic loading to increase the number of initiation events.

Currently, initial tests of the micro-arrest concept have been completed with little success. However it is expected that one micro arrest event will be seen in  $\sim 100,000$  loading cycles, so at present the concept can neither be proved nor disproved. In order to undertake MA testing several pieces had to be specified and purchased (see Appendix D), including a liquid nitrogen fed low temperature chamber providing excellent temperature control ( $\pm 1$  °C) over extended periods (up to 6 hrs at  $-50$  °C).

## 6. References

1. Charles Clover, 'Capturing carbon may be answer to global warming', 03/02/2005,  
<http://www.telegraph.co.uk/money/main.jhtml?xml=/money/2005/05/21/ccnuc21.xml>
2. Neil Collins, 'Byers must listen to global warming experts, not his master's voice', 07/02/2005,  
<http://www.telegraph.co.uk/opinion/main.jhtml?xml=/opinion/2005/02/07/do0702.xml>
3. 'Energy White Paper – A Summary', 2003, [www.dti.gov.uk/publications](http://www.dti.gov.uk/publications)
4. Aaron Patrick, 'Wind energy endures a gale of hostility', 26/03/05,  
<http://www.telegraph.co.uk/money/main.jhtml?xml=/money/2005/03/26/ccwind23.xml>
5. W. Schönharting and S. Nettesheim, 'RES2H2 a European hydrogen project: Hydrogen generation from wind energy', 2003, [ww.res2h2.com](http://www.res2h2.com)
6. L.J. Fingersh, 'Optimized Hydrogen and Electricity Generation from Wind', 2003, NREL/TP-500-34364, National Renewable Energy Laboratory, USA
7. R. Kottenstette and J. Cotrell, 'Hydrogen Storage in Wind Turbine Towers', 2003, NREL/TP-500-34656, National Renewable Energy Laboratory, USA
8. G.R. Odette et al, 'On the transition toughness of two RA martensitic steels in the irradiation hardening regime: a mechanism-based evaluation', 2002, Journal of Nuclear Materials, Vol. 307-311, Pg. 1011-1015
9. G.R. Odette et al, 'Cleavage fracture and irradiation embrittlement of fusion reactor alloys: mechanisms, multiscale models, toughness measurements and implications to structural integrity assessment', 2003, Journal of Nuclear Materials, Vol. 323, Pg. 313-340
10. 'Society and Nuclear Energy: Towards a Better Understanding', Nuclear Energy Agency Organisation for Economic Co-operation and Development

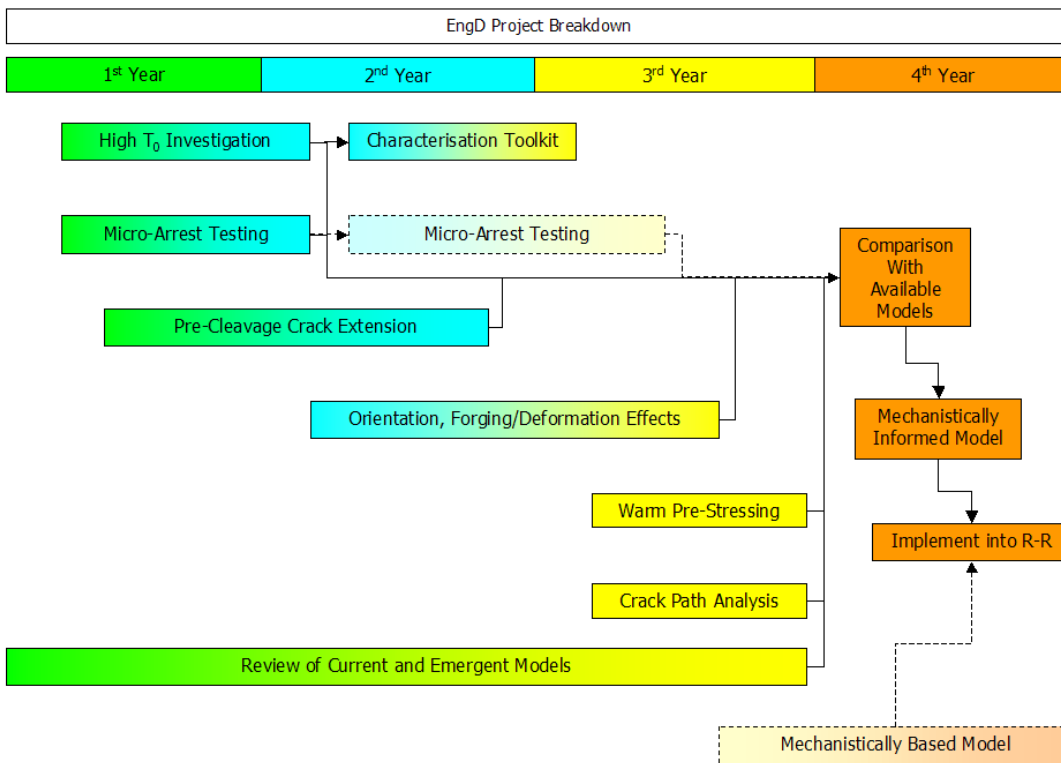
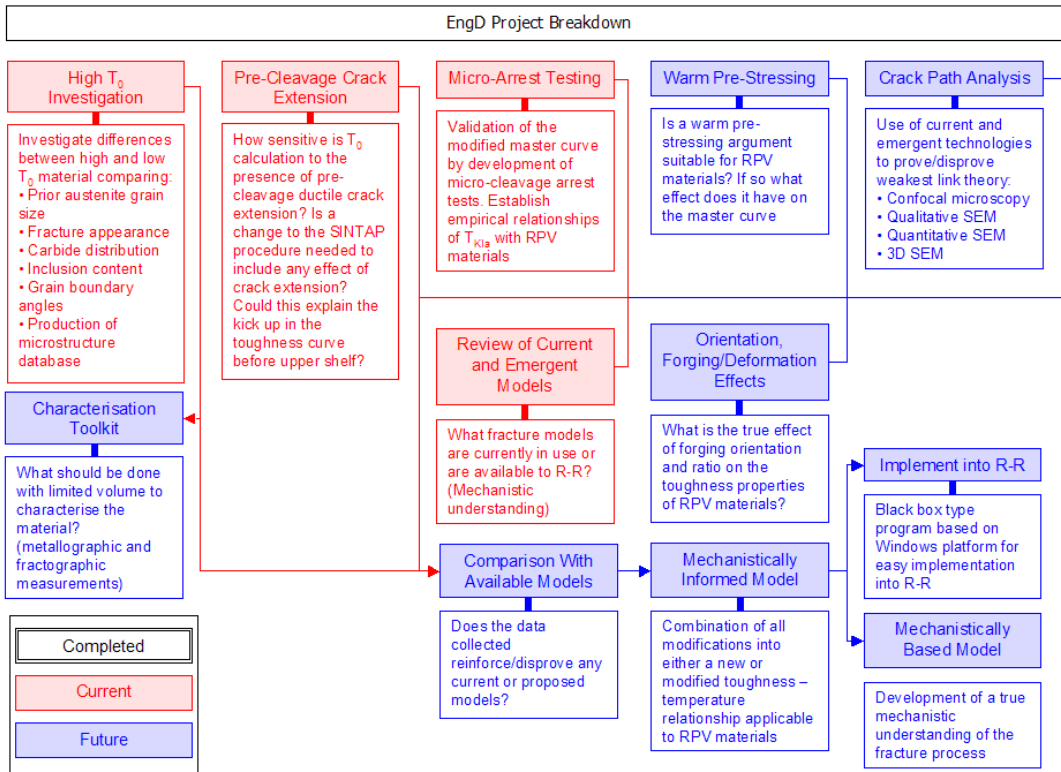
11. 'Nuclear Power: Keeping the Option Open', 2003, Institute of Physics
12. Aaron Patrick, 'Nuclear lobby gathers steam but can expect severe reaction', 21/05/2005,  
<http://www.telegraph.co.uk/money.main.jhtml?xml=/money/2005/05/21/ccnuc21.xml>
13. I. Hore-Lacy, 'Nuclear Electricity', 2003, Uranium Information Centre Ltd.
14. Reactor Design Pocket Guide, 2003, World Nuclear Organisation
15. R.W. Hertzberg, 'Deformation and fracture mechanics of engineering materials', 1996, John Wiley and Sons
16. K. Felkins et al, 'The Royal Mail Ship Titanic: Did a Metallurgical Failure Cause a Night to Remember?', 1998, Journal of Materials, Vol. 50(1), Pg. 12-18
17. 'NRC Bulletin 2002-01: Reactor Pressure Vessel Head Degradation and Reactor Coolant Pressure Boundary Integrity', 2002, <http://www.nrc.gov/reading-rm/doc-collections/gen-comm/bulletins/2002/>
18. 'Davis-Besse: 1Q/2005 Plant Inspection Findings', 2005, <http://www.nrc.gov/NRR/OVERSIGHT/ASSESS/>
19. 'Issuance of order establishing interim inspection requirements for reactor pressure vessel heads at pressurized water reactors', 2003, NRC EA-03-009
20. F.M. Haggag, "Effects of Irradiation Temperature on Embrittlement of Nuclear Pressure Vessel Steels," Effects of Radiation on Materials: 16 th International Symposium, ASTM STP 1175, Arvind S. Kumar, David S. Gelles, Randy K. Nanstad, and Edward A. Little, Eds., American Society for Testing and Materials, Philadelphia, 1993
21. R.G. Carter et al, 'Microstructural characterization of irradiation-induced Cu-enriched clusters in reactor pressure vessel steels', 2001, Journal of Nuclear Materials, Vol. 298, Pg. 211-224
22. A.V. Barshev et al, 'Copper precipitation in Fe-Cu alloys under electron and neutron irradiation', 2004, Acta Materialia, Vol. 52, Pg. 877-886

23. F. Christien and A. Barbu, 'Modelling of copper precipitation in iron during thermal ageing and irradiation', 2004, Journal of Nuclear Materials, Vol. 324, Pg. 90-96
24. C.A. Hipplesley and S.G. Druce, 'The influence of strength and phosphorus segregation on the ductile fracture mechanism in a Ni-Cr steel', 1986, Acta Metall., Vol. 34, No. 7, Pg. 1215-1227
25. D. Cogswell et al, '(P029) The possibility of irradiation-enhanced tempering in RPV steels', 2005, IGRDM-12, Arcachon, France
26. M. Aminal Islam, 'Intergranular fracture in 2.25Cr-1Mo steel at low temperature', PhD thesis, University of Birmingham, 2001
27. I.J. O'Donnel and R. Crombie, 'On the  $\Delta T_{41}$  criterion for irradiation shift', 1996, International Journal of Pressure Vessels and Piping, Vol. 67, Pg. 299-306
28. U.S. Congress, Office of Technology Assessment, 'Aging Nuclear Power Plants: Managing Plant Life and Decommissioning', OTA-E-575 (Washington, DC: U.S. Government Printing Office, September 1993)
29. U.S. Nuclear Regulatory Commission, 'Regulatory guide 1.99 Radiation embrittlement of reactor vessel materials, 1988
30. 'ASTM E23 – 96 Standard Test Methods for Notched Impact Testing of Metallic Materials', American Society for Testing and Materials, 1998
31. 'ASTM E399 – 90 Standard Test Method for Plane-Strain Fracture Toughness of Metallic Materials', American Society for Testing and Materials 1998
32. 'BS 7448 – 1:1991 Fracture mechanics toughness tests — Part 1: Method for determination of  $K_{Ic}$ , critical CTOD and critical J values of metallic materials', British Standards Institute, 2002
33. T.U. Marston, EPRI Report NP-719-SR, 1978
34. H.J. Rathbun, 'Size Effects on Toughness for Fracture in the Elastic Plastic Cleavage Initiation Region', 2002, PhD Dissertation, University of California, Santa Barbara

35. J. E. Srawley, 'Wide range stress intensity factor expressions for ASTM E399 standard fracture toughness specimens' , 1976, International Journal of Fracture, Vol. 12, No. 3, Pg. 475
36. 'ASTM E1737 – 96 Standard Test Method for J-Integral Characterization of Fracture Toughness', American Society for Testing and Materials, 1998
37. J.R. Rice, 'A path independent integral and the approximate analysis of strain concentration by notches and cracks', 1968, Journal of Applied Mechanics, Vol. 35, Pg. 379
38. W. Bolton, 'Engineering Materials', 2000, Newnes
39. A.L. Gurson, 'Continuum theory of ductile rupture by void nucleation and growth: Part I – Yield criteria and flow rules for porous ductile media', 1977, Transactions of the ASME
40. P. Bowen, S.G. Druce, J.F. Knott, 'Micromechanical modelling of fracture toughness', Acta Metallurgica, 1986, Vol. 35(7), Pg. 1735-1746
41. T. Saario, K. Wallin, K. Torrónen, 'On the microstructural basis of cleavage fracture initiation in ferritic and bainitic steels', Journal of Engineering Materials and Technology, 1984, Vol. 106, Pg. 173-177
42. T.L. Anderson, D. Stienstra, R.H. Dodds Jr, 'A theoretical framework for addressing fracture in the ductile-brittle transition region', American Society for Testing and Materials, ASTM STP 1207, 1994, Pg. 186-214
43. K. Wallin, 'Statistical model for carbide induced brittle fracture in steel', Metal Science, 1984, Vol. 18, Pg. 13-18
44. M. Gell and E. Smith, 'The propagation of cracks through grain boundaries in polycrystalline 3% silicon-iron', Acta Metallurgica, 1966, Vol. 15, Pg. 253-258
45. W.S. Pellini, 'Guidelines for fracture-safe and fatigue reliable design of steel structures', The Welding Institute, 1983
46. Section XI, ASME Boiler and Pressure Vessel Code, American Society of Mechanical Engineers, New York, 1986

47. E 1921 - 02 Standard test method for determination of reference temperature, T<sub>0</sub>, for ferritic steels in the transition range', ASTM Standards, 2002, Vol. 03.01
48. K. Wallin, 'Statistical model for carbide induced brittle fracture in steel', Metal Science, 1984, Vol. 18, Pg. 13-18
49. K. Wallin, 'The size effect in KIC results', Engineering Fracture Mechanics, 1985, Vol. 22(1), Pg. 149-163
50. F.M. Burdekin, J.F. Knott, J.D.G. Sumpter, A.H. Sherry, 'TAGSI views on aspects of crack arrest philosophies for pressure vessels with thicknesses up to 100 mm', International Journal of Pressure Vessel & Piping, 1999, Vol. 76, Pg. 879-883
51. T. Williams, D. Swan, G. Dixon, 'Modification of the lower tail of the master curve distribution', IAEA Specialists Meeting, Moscow, 2004
52. S. Webster and A. Bannister, 'A structural integrity approach arising from the SINTAP project', American Society for Testing and Materials, ASTM STP 1417, 2002, Pg. 73-100
53. B.Z. Margolin, V.A. Shvetsova, A.G. Gulenko, A.V. Ilyin, V.A. Nikolaev, V.I. Smirnov, 'Fracture toughness predictions from a reactor pressure vessel steel in the initial and highly embrittled states with the master curve approach and a probabilistic model', International Journal of Pressure Vessel & Piping, 2002, Vol. 79, Pg. 219-231
54. B.Z. Margolin, A.G. Gulenko, V.A. Nikolaev, L.N. Ryadkov, 'A new engineering method for prediction of the fracture toughness temperature dependence of RPV steels', International Journal of Pressure Vessel & Piping, 2003, Vol. 80, Pg. 817-829

## **Appendix A – EngD Project Work Breakdown**



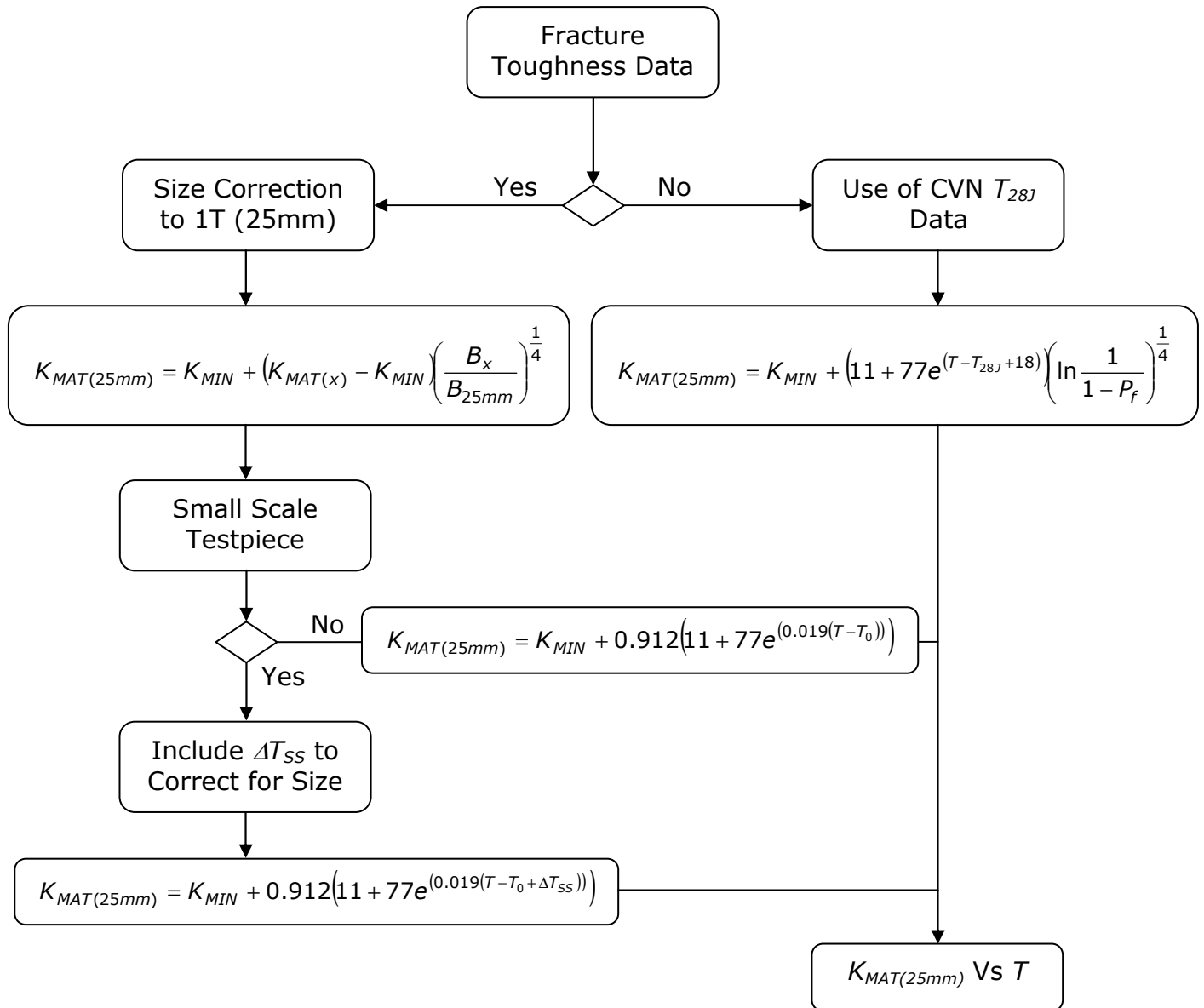


## **Appendix B – SINTAP $K_{MAT}$ Estimation**

The SINTAP estimation process allows the homogeneity of the data collected to be assessed. This method produces a deterministically established  $T_0$  by using the lowest toughness values from the material tested.

## SINTAP: $K_{MAT}$ Estimation

Establishing  $K_{MAT}$  For Test Temperature  $T$



$T_{28J}$  = Temperature corresponding to an impact energy (CVN) of 28J

$K_{MAT(25mm)}$  = Stress intensity factor to cause failure when a 25mm defect is present  $\equiv K_{Jc(50\%)}$

$K_{MIN}$  = Minimum toughness

$K_{MAT(x)}$  = Measured toughness for a defect size  $x$

$B_x$  = Defect of size  $x$

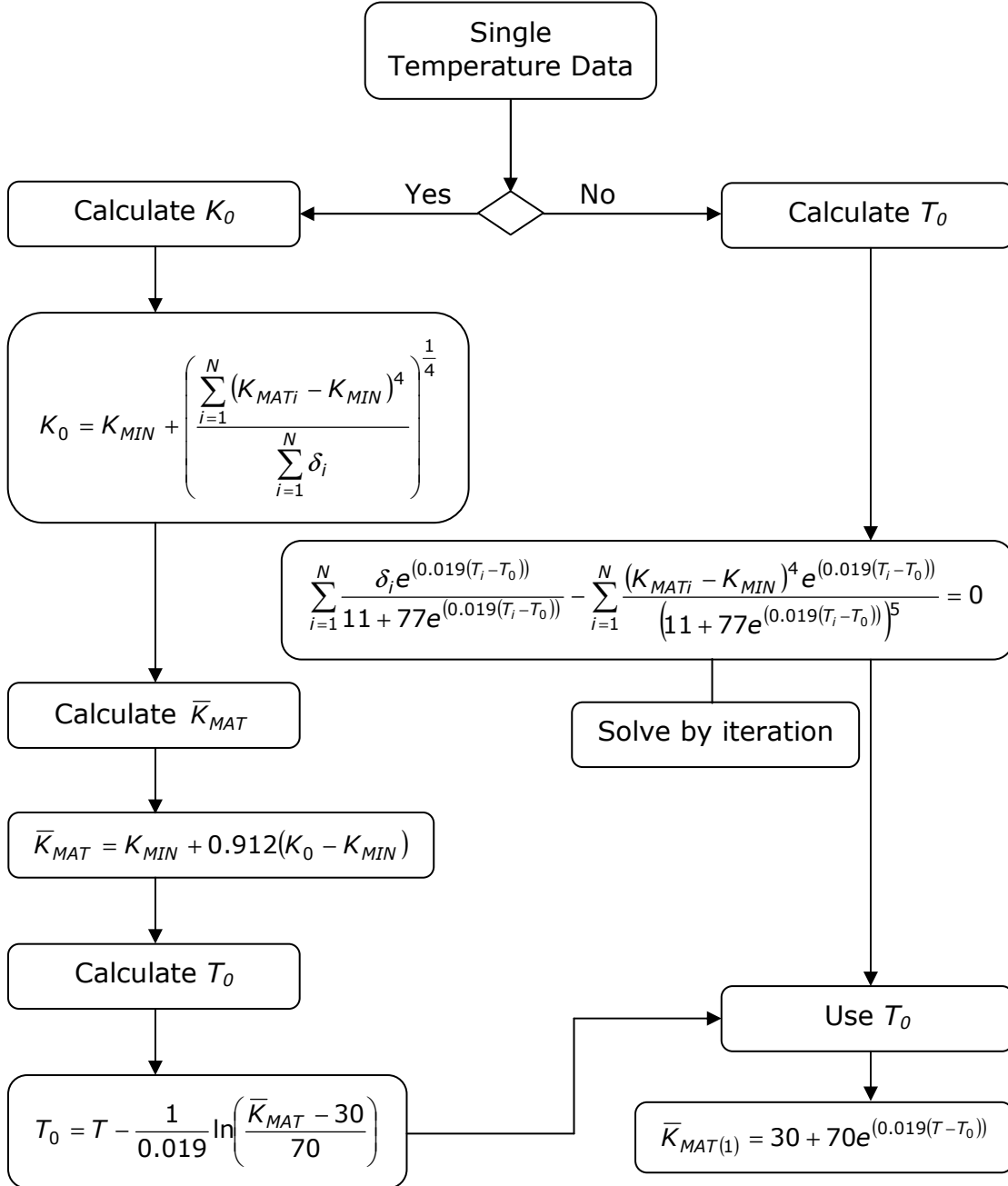
$P_f$  = Probability of failure

$T_0$  = Reference temperature for material ( $K_0 = 100 \text{ MPam}^{1/2}$ )

$$\Delta T_{SS} = 51.4 \ln \left( 2 \left( \frac{B}{10} \right)^{\frac{1}{4}} - 1 \right)$$

## Step 1: Normal Maximum Likelihood Estimator

All available data is used to estimate the  $K_{MAT}$  except those tests where the specimen has failed in a ductile manner at end of test, or the specimen has exceeded its measuring capacity limit.



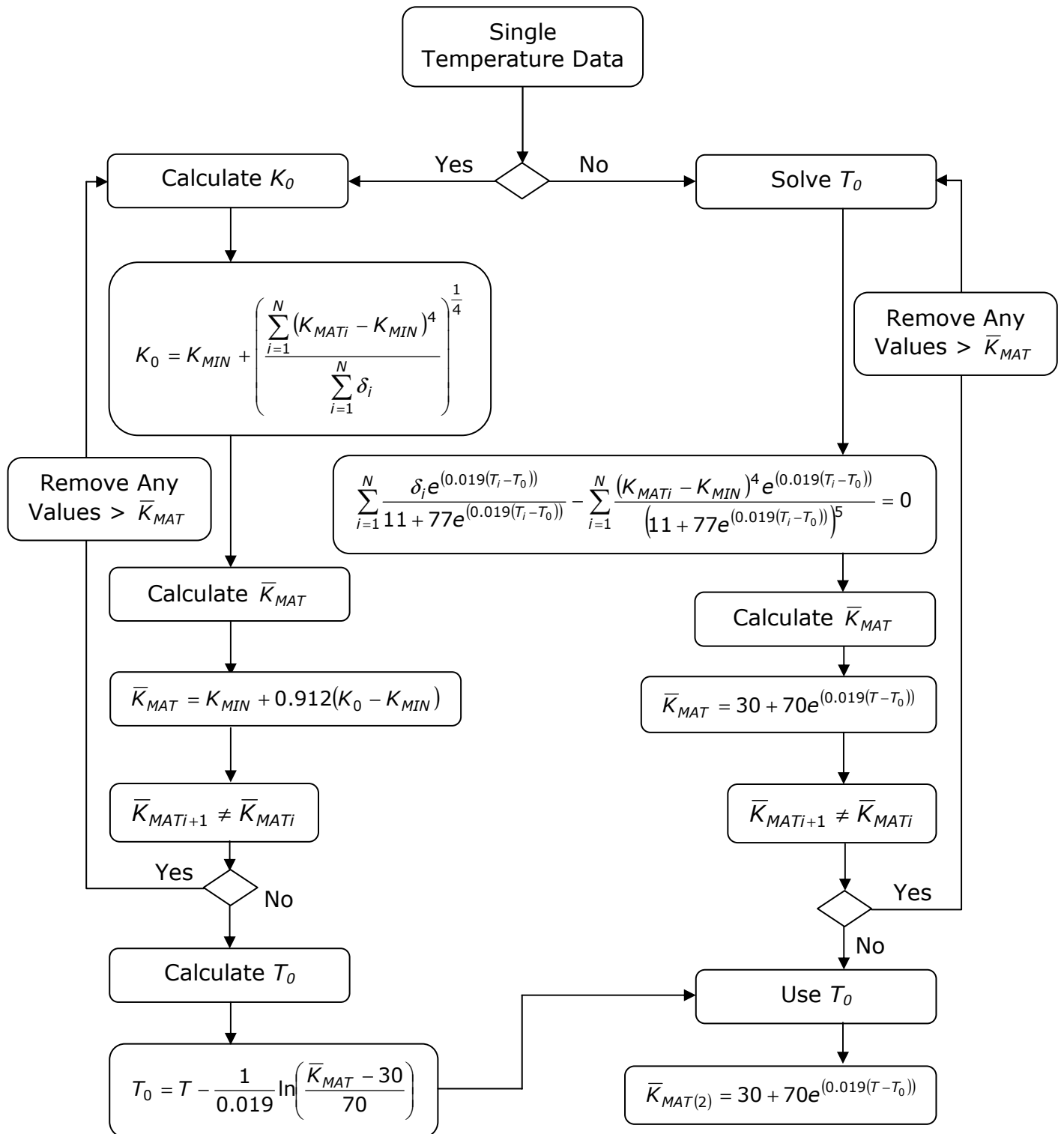
$\delta$  = censoring parameter,  $\delta = 1 \Rightarrow K_{MAT} \leq \left( \frac{E \times b_0 \times \sigma_{YS}}{M} \right)^{\frac{1}{2}}$ , where  $E$  = Young's Modulus,

$b_0$  = size of uncracked ligament ( $=W-a_0$ ),  $\sigma_{YS}$  = yield strength at temperature,  
 $M$  = measuring capacity of specimen;  $\delta = 0 \Rightarrow$  ductile at end of test, beyond measuring capacity of specimen

$\bar{K}_{MAT}$  = Median  $K_{MAT}$  value  $\equiv K_{Jc(med)}$  (MC)

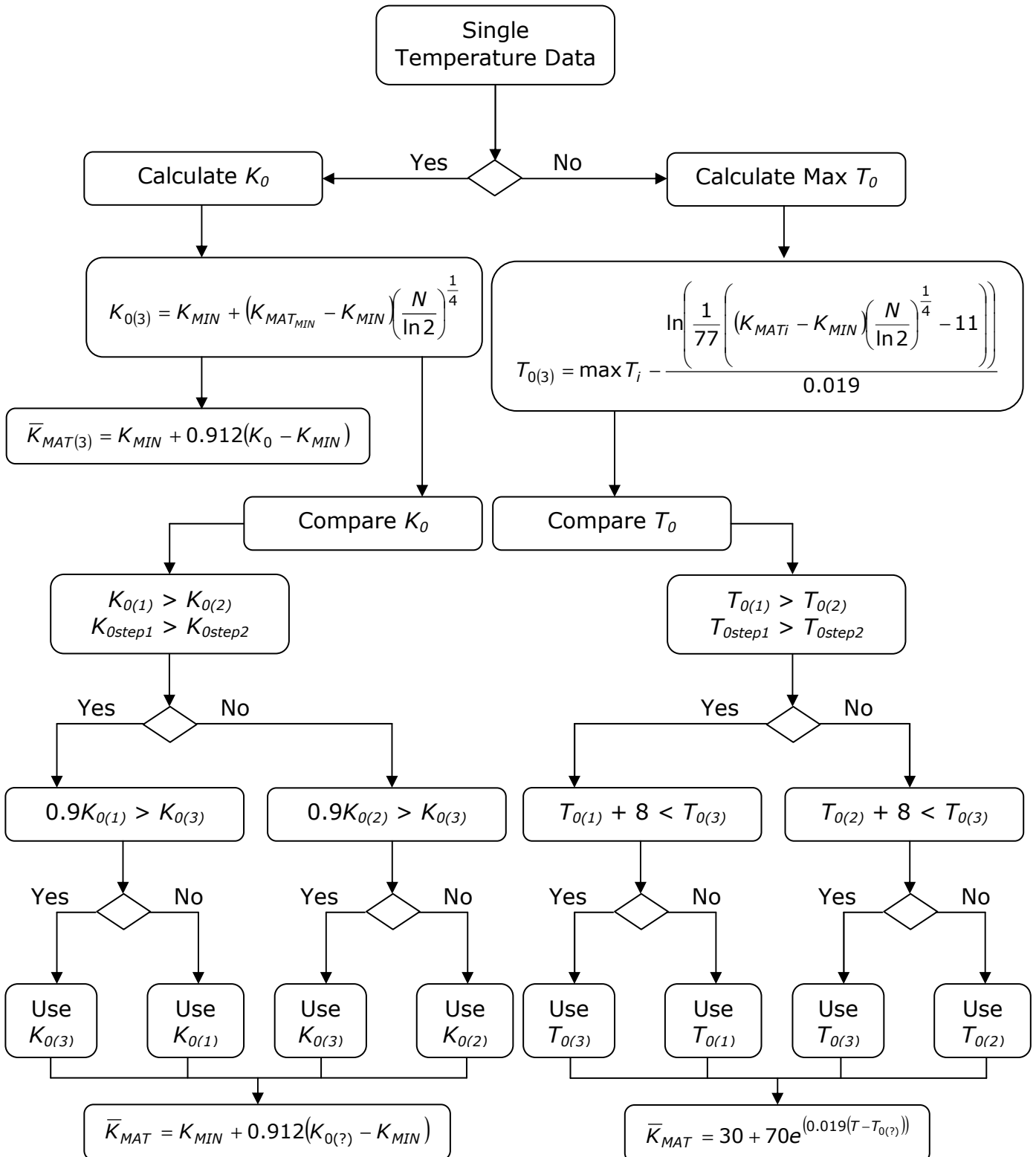
## Step 2: Lower Tail Maximum Likelihood Estimator

The upper tail (50%) is censored, removing specimens which may have exhibited constraint loss, and the  $T_0$  or  $\bar{K}_{MAT}$  is recalculated in an iterative manor until a limiting value is reached.



### Step 3: Minimum Value Estimator

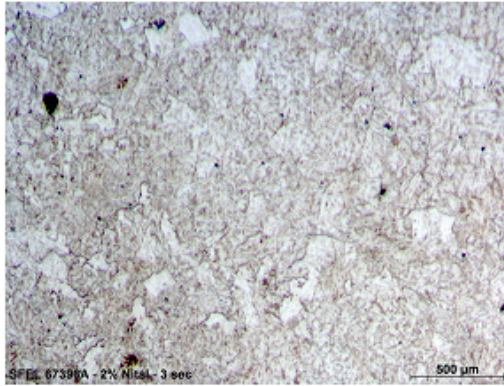
The minimum value of  $K_{MAT}$  is used to estimate  $\bar{K}_{MAT}$  for the material. The purpose of this is to check the homogeneity of the material, done to avoid overly conservative values that may arise from using the median value alone (only used when less than 10 toughness measurements have been taken).



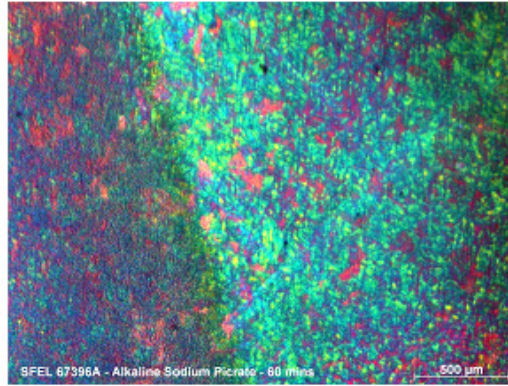
## **Appendix C – High $T_0$ Investigation Initial Etchant Results**

<b>Heat Treatment</b>	
<b>Name</b>	<b>Description</b>
AR	As received
McQuaid & Ehn	Pack carburising 8 hrs @ 925 °C
TE	Temper embrittlement 72 hrs @ 520 °C

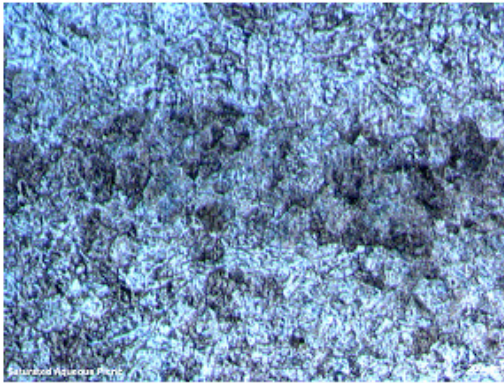
<b>Etch</b>			
<b>Name</b>	<b>Composition</b>	<b>Procedure</b>	<b>Comments</b>
2 % Nital	2 ml HNO <sub>3</sub> 98 ml methanol	Immersion; 2-5 sec	Standard etch for all steels. Reveals some grain boundaries.
		Electrolytic; low voltage 2-30 sec	Very deep etch
Alkaline Sodium Picrate	2 g picric acid 25 g NaOH 100 ml water	Immersion in boiling solution (105-110 °C) for 2-60 mins	Oxide forms over sample and in some areas a film forms showing the underlying orientations. Area is very small and does not allow accurate measurement this has also been reproduced on other samples.
Viella's Etch	1 g picric acid 5 ml HCl 100 ml ethanol	Immersion; 3-5 sec	Most successful etchant for defining microstructure. Some delineation of the grain boundaries but becomes obscured by the contrast produced between the ferrite grains and bainite packets.
		Polish and etch cycles	No improvement over the single cycle. As the etch is very shallow and there is no deep grain boundary attack a gentle polish removes the first etch.
Saturated Aqueous Picric Acid	100 ml Saturated aqueous picric acid	Immersion; 30-90 sec	Showed banding in the order of 0.3 mm thick dark and light bands. Delineation of grain boundaries apparent but not continuous and image is cluttered by grain centre artefacts.



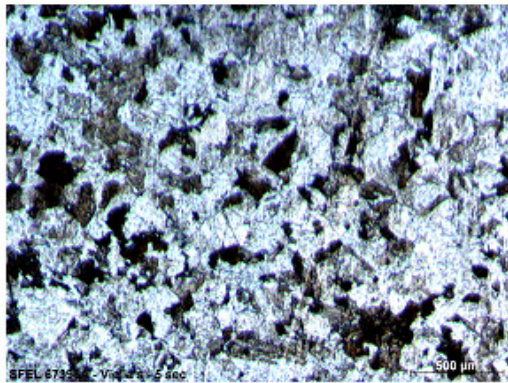
As received – 2% Nital – 3 sec immersion



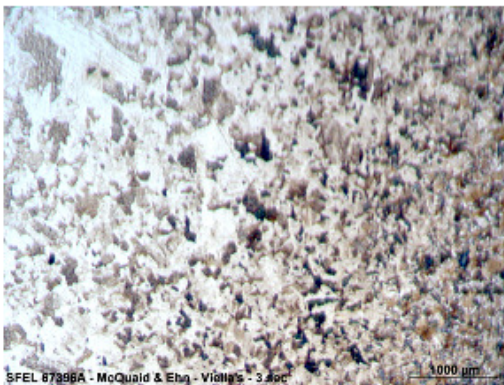
As received – Alkaline Sodium Picrate – 60 mins



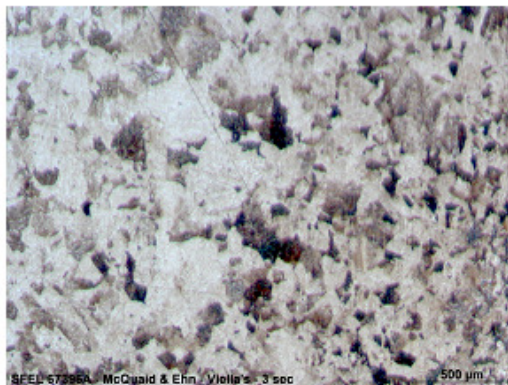
As received – Aqueous Picric Acid – 30 sec immersion



As received – Viella's – 5 sec immersion



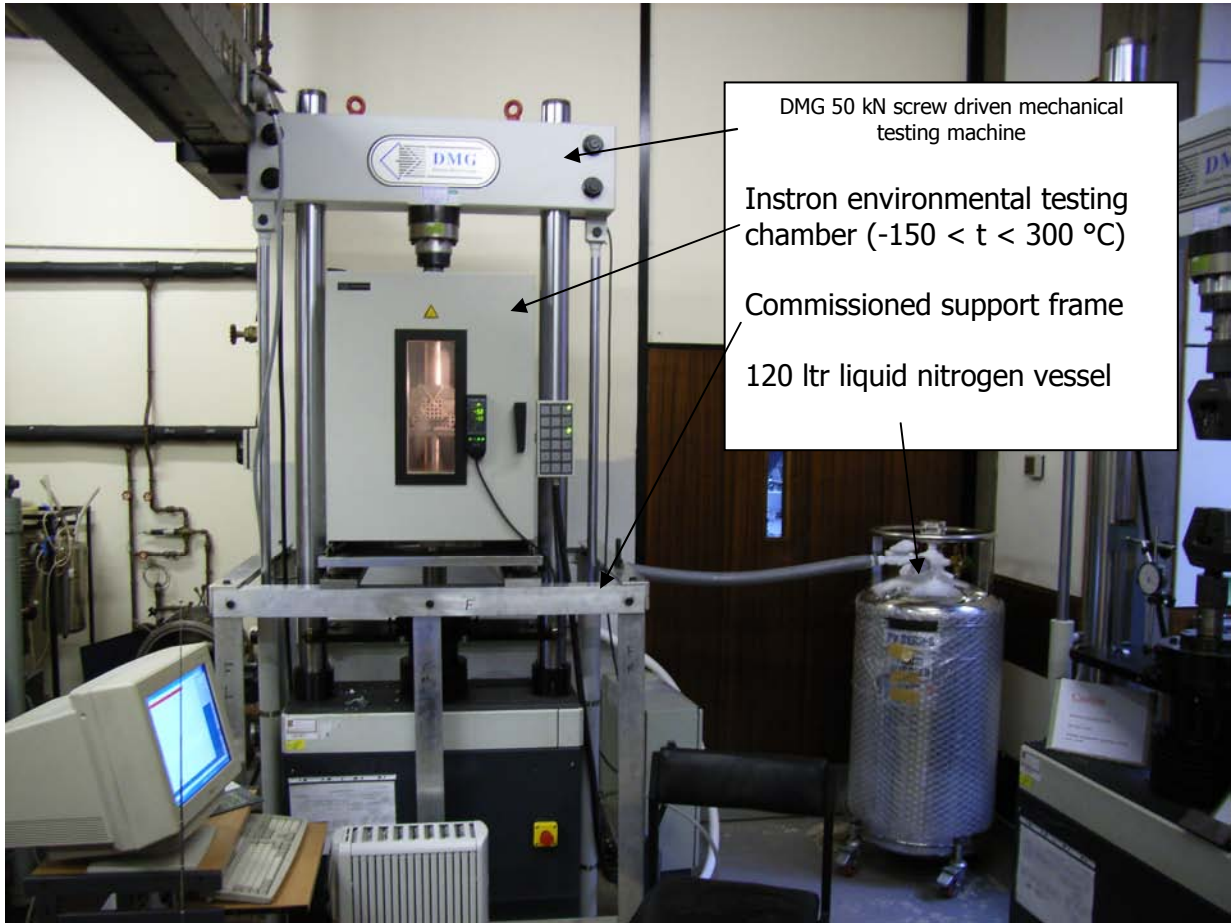
McQuaid & Ehn – Viella's – 3 sec immersion



McQuaid & Ehn – Viella's – 3 sec immersion



## **Appendix D – Micro-Arrest Equipment Set Up**



## **Appendix E – EngD Conference 2004 Presentation**

Presentation given to EngD Conference 2004 held at the Department of Metallurgy and Materials, the University of Birmingham on the 14<sup>th</sup> October 2004



# Probabilistic Methods For Structural Integrity Assessment In Naval Marine Nuclear Power Generation

Daniel Cogswell

Supervisors: P. Bowen (UoB), J. Knott (UoB) and T. Williams (RR)



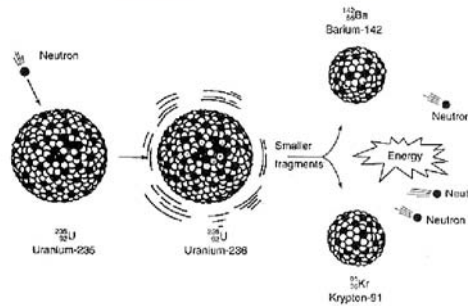
- Nuclear Power Generation
- Pressurised Water Reactor
- Irradiation Embrittlement
- Methods For Toughness Prediction
- Probabilistic Risk Assessment

## Nuclear Industry



- 438 utility scale reactors in operation
- 16% of world power from nuclear reactor
- First utility scale reactor
  - Calder Hall, Sellafield 1956
  - Shut down 2003
- Ageing of safety critical components limits life of reactor

## The Fission Reaction



## Key Reactor Components



- Fuel
  - Natural or enriched Uranium
- Moderator
  - Slows the fast neutrons to allow chain reaction
- Control Rods
  - A neutron absorptive material to control or stop reaction
- Coolant
  - Used to transfer heat energy to generate steam
- Pressure Vessel
  - Contains reactor core

## Pressurised Water Reactor (PWR)



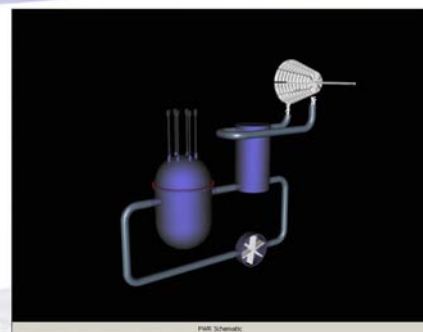
- 263 civil reactors operational worldwide
- Fuel
  - Enriched Uranium
- Moderator and Coolant
  - Light water, H<sub>2</sub>O, containing Boric acid
- Control Rods
  - Boron containing materials
- Ferritic steel pressure vessel
- Indirect steam generation

## PWR Schematic



- Control rods
- Closure studs
- Closure head
- Fuel rods
- Inlet and outlet nozzles
- Vessel

## PWR Power Plant Overview



## Irradiation Embrittlement

- ♦ Matrix Damage
  - Neutrons from reaction process, not slowed by the moderator, displace a primary knock on atom

- The primary can then go on to hit a secondary and so on, leading to a cascade
- This creates a distribution of vacancies and point defect clusters, locally disordering the matrix and raising  $\sigma_y$

9 Daniel Cogswell – EngD Conference 14<sup>th</sup> Oct 2004

## Irradiation Embrittlement (cont.)

- ♦ Cu/Ni Precipitation
  - Copper initially used as a coating on weld filler rods and now found as an impurity; Nickel added to the RPV composition to improve strength, both have a precipitation hardening effect
  - Due to low concentrations no over-ageing occurs
  - This raises the  $\sigma_y$
- ♦ Impurity Segregation
  - Impurities, especially Phosphorus, may migrate to the grain boundaries leading to grain boundary embrittlement
  - This can change the failure mode from transgranular cleavage to intergranular brittle failure, lowers the fracture stress  $\sigma_f$

10 Daniel Cogswell – EngD Conference 14<sup>th</sup> Oct 2004

## Through-Wall Neutron Dose

11 Daniel Cogswell – EngD Conference 14<sup>th</sup> Oct 2004

## Effect of Irradiation on $\sigma_y$ and $\sigma_f$

12 Daniel Cogswell – EngD Conference 14<sup>th</sup> Oct 2004

## Industry Specific Problem

15 Daniel Cogswell – EngD Conference 14<sup>th</sup> Oct 2004

## Effect of Irradiation on Toughness Transition

14 Daniel Cogswell – EngD Conference 14<sup>th</sup> Oct 2004

## Effect of Irradiation on Ductile to Brittle Transition

13 Daniel Cogswell – EngD Conference 14<sup>th</sup> Oct 2004

## Obtaining a $K_{IC}$ Transition

- ♦ ASME curve
  - Bounding curve drawn to limited data (~170 valid tests at time) normalised to a nil-ductility reference temperature,  $RT_{NDT}$
  - Gives overly conservative values
- ♦ Master curve (ASTM E1921-02)
  - Statistical method based on 'Weakest Link' theory
  - Allows extrapolation of curve from only a small amount of data
  - Validated against a large database of toughness data for RPV steel

16 Daniel Cogswell – EngD Conference 14<sup>th</sup> Oct 2004

## Weakest Link Theory

- Like a chain, a material is only as strong as its 'weakest link'
- If the weak link fails then brittle fracture propagates through-out material
- A weak link has to be sampled in a specific area ahead of the crack tip for brittle failure
- If the requirements are not met then slow stable crack growth dominates (ductile)

17 Daniel Cogswell - EngD Conference 14<sup>th</sup> Oct 2004

## Weakest Link Theory (cont.)

18 Daniel Cogswell - EngD Conference 14<sup>th</sup> Oct 2004

## Fitting to Weibull Distribution

- The values of  $K_{Jc}$  conform to a Weibull distribution
- To validate this and create a probability distribution from the data it needs to be ranked and plotted
- The data is ranked by the following method:
  - Sort  $K_{Jc}$  data, low to high
  - Give each a ranked probability using  $\frac{i-0.3}{N+0.4}$
  - Plot probability Vs.  $K_{Jc}$  on probability paper

19 Daniel Cogswell - EngD Conference 14<sup>th</sup> Oct 2004

## Probability Vs. $K_{Jc}$ Plot

- The plot can be used to make statements about the material property
- I.e: It is 97.5% probable that the  $K_{Jc}$  of the material will be greater than x

20 Daniel Cogswell - EngD Conference 14<sup>th</sup> Oct 2004

## The Master Curve (ASTM E1921-02)

- The Master Curve uses the probabilistic approach to predict the  $K_{Jc}$  of a ferritic steel from limited test data (only 6 valid tests)
- It assumes that the shape of the curve is material independent
- The curve is located using a reference temperature,  $T_0$ 
  - $K_{Jc} @ T - T_0 = 100 \text{ MPam}^{3/2}$
- A size correction for various sized test specimens is included in the standard

21 Daniel Cogswell - EngD Conference 14<sup>th</sup> Oct 2004

## Steps to Produce Master Curve

$$K_{Jc} = \sqrt{J_e \frac{E}{1-\nu^2}}$$

$$K_{Jc(x)} = K_{MDV} + (K_{Jc(0)} - K_{MDV}) \left(\frac{B_0}{B_x}\right)^{1/4}$$

$$K_0 = \left( \sum_{i=1}^N \frac{(K_{Jc(i)} - K_{MDV})^4}{N} \right)^{1/4} + K_{MDV}$$

$$K_{Jc(med)} = K_{MDV} + (K_0 - K_{MDV}) (0.9124)^{1/4}$$

22 Daniel Cogswell - EngD Conference 14<sup>th</sup> Oct 2004

## Steps to Produce Master Curve (cont.)

$$T_0 = T - \frac{1}{0.019} \ln \left( \frac{K_{Jc(med)} - 30}{70} \right)$$

$$K_{Jc(med)} = 30 + 70 e^{(0.019)(T - T_0)}$$

$$K_{Jc(0.xx)} = 20 + \left( \ln \left( \frac{1}{1 - 0.xx} \right) \right)^{1/4} (11 + 77 e^{(0.019)(T - T_0)})$$

23 Daniel Cogswell - EngD Conference 14<sup>th</sup> Oct 2004

## How Does the Master Curve Link to Experimental Data?

24 Daniel Cogswell - EngD Conference 14<sup>th</sup> Oct 2004

## Nuclear Industry View Of Risk

- Probabilistic methods used in all risk assessments
- Probability of failure calculated on years of reactor operation I.e. 1 failure causing more than 50 deaths in 5,000 reactor years (HSE)
- Risk to public calculated by irradiation at the boundary fence
- Failure is calculated on a worst case scenario basis

25 Daniel Cogswell – EngD Conference 14<sup>th</sup> Oct 2004

## Worst Case Scenario

- Loss of Coolant Accident (LOCA)
- Relatively cold coolant added in large quantities
- Gives large thermal stresses throughout vessel (Pressurised Thermal Shock event)
- Assume
  - Worst possible crack shape (semi circular surface crack)
  - Worst location (weld microstructure in beltline region)
  - Defect size from NDE

26 Daniel Cogswell – EngD Conference 14<sup>th</sup> Oct 2004

## Pressurised Thermal Shock Event

```

    graph LR
      A[PTS Event Sequence] --> B[Thermal Analysis]
      B --> C[Stress Analysis]
      C --> D[Probability of Through-Wall Cracking from event, CPF]
      E[Frequency of event, fe] --> D
      D --> F[Frequency of Through-Wall Cracking, CPF x fe]
  
```

27 Daniel Cogswell – EngD Conference 14<sup>th</sup> Oct 2004

## Probabilistic Risk Assessment Model

```

    graph LR
      PM[Probabilistic Model] --> TSM[Thermal Stress Model]
      PM --> DDM[Defect Distribution Model]
      PM --> IM[Irradiation Model]
      PM --> MPM[Material Properties Model]
      TSM --> PTT[Pressure and Temperature Vs. Time]
      DDM --> DLS[Density, Location and Shape]
      IM --> FOV[Fluence on vessel]
      MPM --> YFT[Yield Strength, Fracture Toughness]
      PTT --> EICM[Embrittlement and Crack Initiation Model]
      DLS --> PICI[Probability of Crack Initiation]
      FOV --> CAM[Crack Arrest Model]
      YFT --> PTC[Probability of Through-Wall Cracking, CPF]
      EICM --> PICI
      CAM --> PTC
      FE[Frequency of Event, fe] --> PTC
      PTC --> FTWC[Frequency of Through-Wall Cracking, CPF x fe]
  
```

28 Daniel Cogswell – EngD Conference 14<sup>th</sup> Oct 2004

## Summary

- Nuclear reactor pressure vessel material properties
- Industry specific problems with material toughness
- Toughness modelling
- Probabilistic approach to data analysis
- Use of models to conduct risk assessment

29 Daniel Cogswell – EngD Conference 14<sup>th</sup> Oct 2004

## Acknowledgements

- EPSRC
- Project Supervisors
- Dave Swan (RR)
- Milorad Novovic (UoB)
- Tom Jarvis (animation specialist)

30 Daniel Cogswell – EngD Conference 14<sup>th</sup> Oct 2004

## **Appendix F – EngD Conference 2005 Poster**

Poster presented at the EngD Conference 2005 held at the Department of Metallurgy and Materials, the University of Birmingham on the 21-22 November 2005



# Nuclear Power Generation

Daniel Cogswell, EngD Research Engineer, Rolls-Royce Plc



USS Nautilus, the first nuclear powered submarine. This photograph was taken shortly after the Nautilus traversed the Arctic ocean.

## Uses of Nuclear Power

There has been much talk in the media recently about the need to switch to non-carbon dioxide (CO<sub>2</sub>) producing power generation. It has been reported that if there is not a change in the use of fossil fuels in the near future, then global warming may become a run-away effect. Fossil fuels are also a non-renewable resource and will eventually run out. Some predictions state that if current usage continues, the world oil supply will be used up within a century and the supply of coal and gas within 400 years. Many governments have been conducting studies on how they can change energy policies to meet agreements made at an international level, such as the Kyoto agreement, for the use of fossil fuels and pollution control. One way that targets for CO<sub>2</sub> reduction can be met is by the use of alternative sources of energy that are CO<sub>2</sub> neutral and will have no effect on global warming.

The use of wind farms and hydroelectric power has become an attractive option recently and many governments have switched to wind turbines as the front-runner for meeting CO<sub>2</sub> targets. However, both wind farms and hydroelectric power have their drawbacks. Hydroelectric power requires large amounts of water to generate energy on a utility scale, in order to produce a steady supply a dam is commonly used, flooding large areas and changing the natural environmental cycle of the river downstream. Wind farms, by their nature, produce a random supply of electricity and hence cannot be used to supply base load or be relied on for peak loading of a power grid.

The only power source currently available that can meet the short-term requirements of low CO<sub>2</sub> emissions and a steady and predictable power supply is nuclear fission. The problems associated with nuclear power generation are by no means small and the legacy of nuclear waste will be of concern for many years to come. Until nuclear fusion can be demonstrated at a utility scale to provide clean power then nuclear fission is the only option, radioactive materials are still produced in a fusion reactor but only a small fraction compared to nuclear fission. However, this is only a small part of the structure and is not a consumable in the same way that fuel rods/pellets are for fission reactors; hence, the waste is greatly reduced. A large amount of research is being conducted into low activation materials, i.e. those that have very short radiation half-lives, to reduce the legacy of radioactive waste.

Public perceptions of nuclear power are very low, due largely to the Chernobyl incident of 1986. It is now understood that the incident was caused by a combination of poor design and by inexperienced operators under pressure to perform a series of reactor test operations without the necessary safety procedures being taken into account. Given the concerns of the public nuclear energy policy in the UK is a contentious issue and the process of deciding to build a new reactor to actual construction takes approximately ten years. Within this time, at least one general election will take place and

recommending nuclear new-build while public opinion is so heavily against it will certainly be damaging to any governments chances of re-election, so at present nuclear power in the UK will be limited to the ageing reactors currently in operation. A similar situation exists across the world and as of 2003, there are 438 nuclear reactors producing electricity on a utility scale worldwide, there are also many reactors used for maritime power generation all utilised for military purposes.

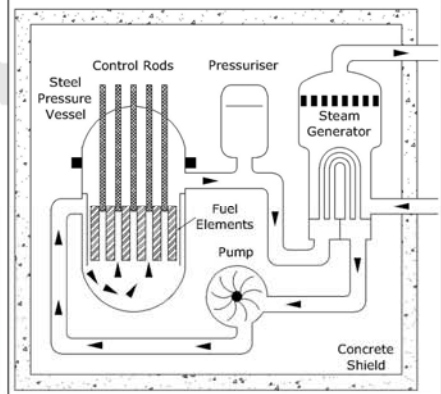
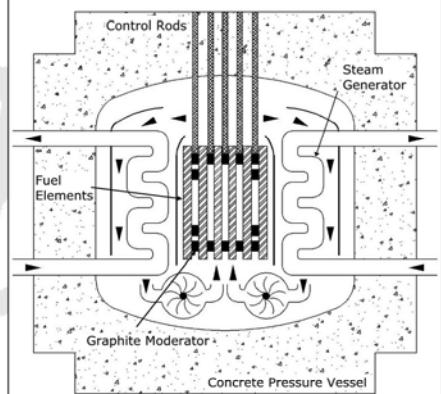
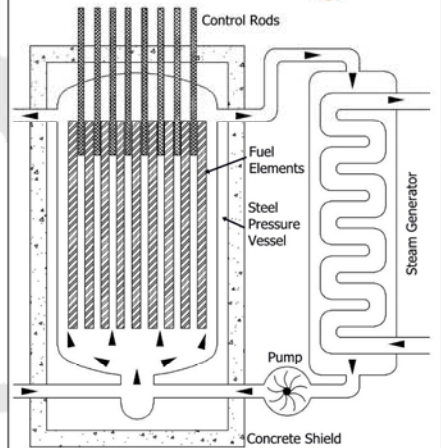
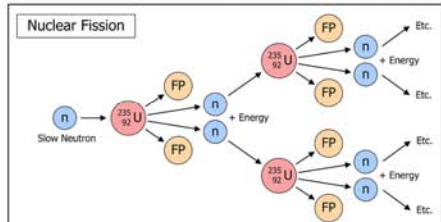
There are several different reactor designs currently in use and some new designs considered for new-build by 2010. By far the most common reactor type is the pressurised water reactor (PWR); used in both utility and marine power generation. The PWR design uses an enriched uranium oxide fuel and light water (H<sub>2</sub>O) as a moderator and coolant. Steam generation is indirect; heat is transferred from the primary coolant, which is kept liquid by maintaining a high pressure into a secondary system via a heat exchanger. The controlling factor for the safe operation of these reactors is the fitness for purpose of the main containment shield, in most cases a low alloy steel reactor pressure vessel.

## Properties of Low Alloy Steel

Low alloy steels are used in a large variety of applications but all suffer from a similar problem. Due to the body centred cubic atomic structure of these steels a transition is observed in the toughness, most commonly described by the ductile-brittle transition temperature (DBTT) found in impact testing. Misunderstanding of the toughness properties has caused many large-scale accidents, some well reported and in others, the cause of failure has not become apparent until recently. The wide spread use of low alloy steels due to their low price and good tensile properties has lead to a variety of failures.

The sinking of the Titanic following a collision with an iceberg on its maiden voyage in 1912 was largely a mystery. Until recently only survivors statements were all that were available to piece together what happened. However, in 1985 a group using deep-sea submersibles catalogued and photographed the remains of the Titanic. It was found to be in two sections a large distance apart on the sea floor. A section of the hull plating was lifted allowing experimental work to be conducted. Charpy impact testing has been used to determine the DBTT of the material and it was concluded that at the ambient temperature of the water on that night, -1 °C, the hull plate was in the brittle region. Current belief is that striking the iceberg caused water to be taken on in vast quantities submerging the bow of the ship, this caused the stern to be lifted out of the water putting a great deal of stress on the mid point of the ship, as it was now effectively in three point bend. The ship then fractured in two starting near the top deck and several features have been observed on the wreck which corroborates the above; buckling is noted in the keel which corroborates the above; buckling is noted in the keel at the mid point and the fracture line above it simply runs through plate boundaries and no localised plastic deformation is seen at the rivets, implying brittle failure.

Many other examples exist from bridge failures to molasses containers where brittle failure has resulted in the loss of life. The most demanding application for these steels also has the greatest potential for tragedy. Ferritic steel is used as the main structural material in the construction of nuclear pressure vessels; this is a very demanding role as the pressure vessel is the first, and commonly the only form of containment for the reactor core. In normal operation the pressure stresses on the vessel are low, however during a loss of coolant accident (LOCA) large amounts of cold coolant are added creating thermal gradients across the vessel wall resulting in an increase in stress due to contraction of the inner surface. For a vessel to withstand these high stresses it must conform to a minimum toughness that is safe to operate, however the mechanical properties of the steel are degraded over time by several mechanisms.



The three reactor designs used in the UK. Top, Magnox type; Middle, Advanced Gas Cooled Reactor (AGR); Bottom, Pressurised Water Reactor (PWR).



The power station at Sizewell comprises two reactor designs. On the left is a Magnox type and on the right is the most recent of the UK utility scale reactors, utilising a PWR design.

The author is sponsored in this work by



EngD Conference 2005

21<sup>st</sup> - 22<sup>nd</sup> November 2005

Department of Metallurgy and Materials, University of Birmingham, UK



# Plant Life Extension for Nuclear Reactors

Daniel Cogswell, EngD Research Engineer, Rolls-Royce Plc

## Plant Life Limiting Factors for Nuclear RPV's

As well as suffering from the usual problems with fatigue and corrosion a reactor pressure vessel (RPV) is also effected by neutrons emitted by the reaction process. This is the key area of concern for RPV degradation during the operational life of the reactor; due to irradiation embrittlement changes to the microstructure which would normally be seen at higher temperatures are found in the operating window of most reactor types. The following changes result in detrimental changes to the RPV:

- Matrix damage

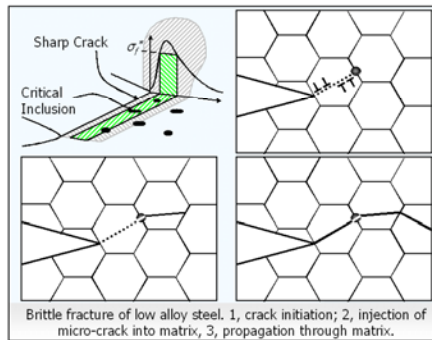
Fast neutrons released from the reaction process knock atoms out of the regular body centred cubic (BCC) structure causing vacancies or point defect clusters, the atoms knocked from position can then hit other atoms in the matrix causing further damage, this process is known as a cascade. This has the effect of locally disordering the matrix on an atomic scale, raising the yield stress,  $\sigma_y$ , and decreasing the work hardening rate. The following effects are a direct result of the increased vacancy concentration allowing substitutional diffusion of atoms in the matrix at the operating temperature of the reactor, which is far below the temperature normally associated with thermal diffusion.

- Copper / Nickel precipitation

Copper initially found in scrap metal used to make the PVS and used as a coating on weld filler rods to prevent corrosion has a precipitation hardening effect on the steel. This was discovered in the late 1960's/early 1970's when the problem of irradiation embrittlement became apparent. At present, the amount of copper is strictly controlled and only found as a trace impurity. Nickel added in small quantities, ~0.75% weight for A508-3-1, to improve the strength and toughness also has a precipitation hardening effect on the PVS. Due to the small concentrations of each, no over-aging occurs and the RPV remains in a peak aged condition, this raises the  $\sigma_y$ .

- Segregation of impurities

Impurities may migrate to the grain boundaries and cause grain boundary embrittlement, of most concern is phosphorus. This may cause a change in the failure mechanism from trans-granular cleavage to inter-granular



fracture if the concentration of phosphorus at the grain boundaries is high enough to promote grain boundary embrittlement. This can dramatically lower the fracture toughness of the material. The processing routes of modern pressure vessel steels are much more restrictive than those of the past, meaning cleaner steels containing fewer impurities, negating this issue.

## Brittle Fracture

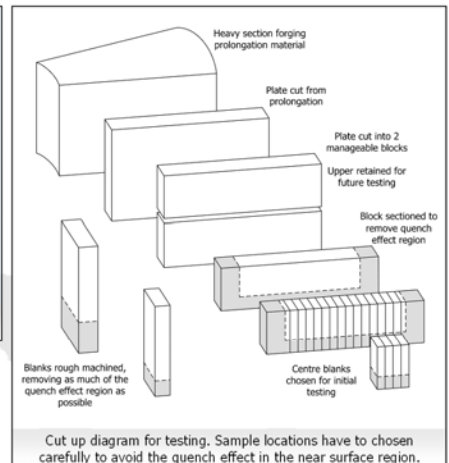
Brittle failure is catastrophic, i.e. it may happen with out warning. The material property that controls the resistance to fracture appears to have a random nature and conforms to a distribution; when loaded the user is effectively sampling from this distribution, which has very large variability, compared to  $\sigma_y$ . This random sampling can result in very low resistance to fracture and once one small packet of material fractures the rest of the component will also fail, the crack front will travel through the material at close to the speed of sound resulting in a very sudden failure. Unlike ductile failure where load is still supported by the remaining ligament, brittle failure results in complete breaking of the component, i.e., there is no remaining ligament to support any load, so when brittle failure occurs it will begin at an unpredictable point and proceed too rapidly for the load to be removed. It is therefore very difficult to design against brittle failure as commonly the trigger event is only known after a catastrophic failure has occurred, only then can the component be redesigned to reduce the potency of the initiator.

## Modelling Brittle Fracture

The master curve (MC) was initially dismissed by many but has now become the best estimation of the toughness of ferritic materials and has been adopted as an American standard, ASTM E1921-02. The main theory of the MC model is a weakest link argument; much like a chain a material is made up of links, when one link fails all surrounding links fail as well. This allowed the use of a Weibull distribution to model the scatter in the data and to give a probability of failure associated with an applied load. This can then be used in an incredible of failure argument, where it can be proved that failure is so improbable to occur through out the life of the vessel that it may be operated in its current state without further justifications until the end of the plants life.

It became apparent that a three-parameter Weibull distribution would be required to describe the toughness at a given temperature, two parameters to scale the distribution and one to locate it on the toughness axis. By defining one of the scale parameters and the location parameter, at least in part, as fixed constants for all ferritic steels it is possible to establish the third by using a small number of tests. The MC does have one major failing; it is overly conservative in the lower tail of the distribution used in a probabilistic safety assessment. One possible explanation for this conservatism is the overlap between the arrest and initiation toughness distribution. By combining the two distributions it is possible to extrapolate the effect the arrest distribution has initiation for various conditions.

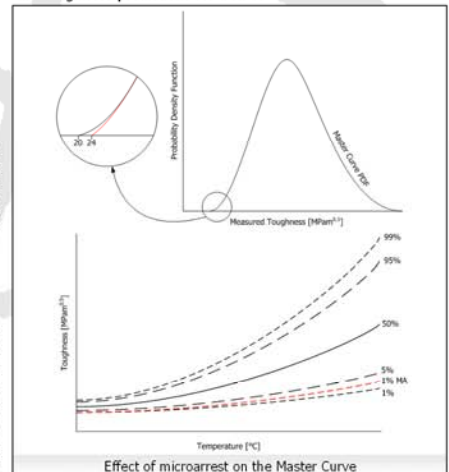
It is hoped that microarrest can be used to truncate the low values of toughness predicted by the MC at low probability bounds. As the arrest toughness, unlike the initiation toughness, is not size dependent so the likelihood of



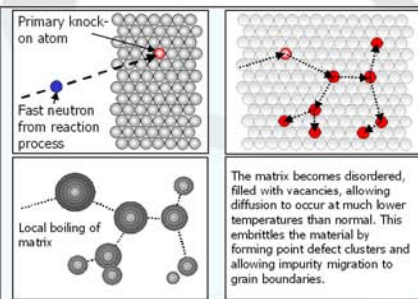
Blanks rough machined, removing as much of the quench effect region as possible. Cut up diagram for testing. Sample locations have to be chosen carefully to avoid the quench effect in the near surface region.

microarrest is greatly increased when real world defects are considered.

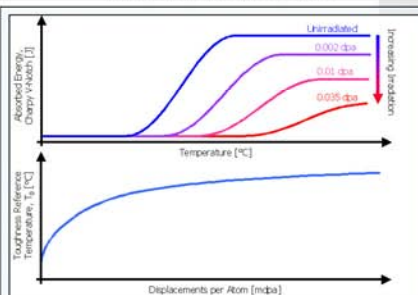
The total effect of microarrest is dependent on the initiation and arrest reference temperatures; the smaller the difference between them the larger the effect. The arrest reference temperature ( $T_{ar}$ ) is believed to be unaffected by irradiation, whereas the initiation toughness temperature ( $T_0$ ) is increased by irradiation damage. An accurate model of microarrest then becomes important for reducing conservatism in the through-life toughness predictions for a RPV.



Effect of microarrest on the Master Curve

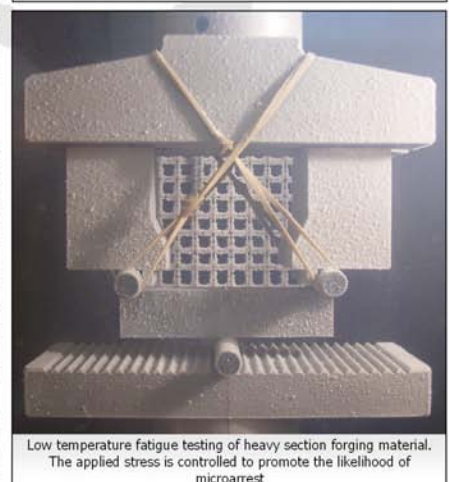


Cascade event; fast neutrons collide with primary knock-on atoms which in turn collide with others, etc.



The irradiation damage is commonly quantified by a change in toughness caused by the number of displacements per atom (dpa).

The author is sponsored in this work by  
**Rolls-Royce** **EPSRC** Engineering and Physical Sciences Research Council



Low temperature fatigue testing of heavy section forging material. The applied stress is controlled to promote the likelihood of microarrest.



*Appendix B*

**Fracture of Low Alloy Steel: 2<sup>nd</sup>  
Year Report**



UNIVERSITY OF  
BIRMINGHAM

# ***FRACTURE OF LOW ALLOY STEEL***

**Daniel Cogswell**

Submitted to the  
**Department of Metallurgy and Materials, School of Engineering,  
The University of Birmingham**

For the degree of  
**Engineering Doctorate in Engineered Materials for High Performance  
Applications in Aerospace and Related Technologies**

5,579 Words

***2<sup>ND</sup> YEAR REPORT***

**EPSRC**  
Engineering and Physical Sciences  
Research Council



**Rolls-Royce**



# 1 Contents

## 1.1 Sections

1	Contents.....	i
1.1	Sections.....	i
1.2	Tables.....	ii
1.3	Figures.....	ii
1.4	Appendices.....	iii
2	Introduction.....	1
3	Historical Developments Of Toughness Curves.....	1
3.1	HSST Programme.....	1
3.2	ASME XI Code.....	1
3.3	Master Curve.....	2
4	Database Analysis.....	3
4.1	Database.....	3
4.2	Datasets.....	4
4.2.1	Material Condition.....	4
4.2.2	Irradiation Condition.....	5
4.2.3	Crack Geometry.....	5
4.2.4	Dataset Sorting Within Database.....	5
4.3	Reference Temperature Calculation.....	6
4.4	Results of Database Analysis.....	11
4.5	Further Work.....	13
5	Summary.....	14

6	Tables .....	15
7	Figures .....	19
8	References.....	25
9	Appendices .....	26

**1.2 Tables**

Table 1 - Description of headings for Appendix B .....	15
Table 2 - Description of headings for Appendix C .....	15
Table 3 - Description of headings for Appendix D.....	16
Table 4 - Description of headings for Appendix E and Appendix F .....	17
Table 5 - Lookup table for standard deviation of distribution based on $K_{JcEqmed}$ .....	17
Table 6 - Actual/expected analysis of database for $-50 < T - T_0 < 50$ temperature range ....	18

**1.3 Figures**

Figure 1 - HSST Programme plate 2 just before quenching (picture taken from ref 1) .....	19
Figure 2 - Range of specimen sizes tested using drop weight testing (picture taken from ref 1).....	19
Figure 3 - Pellini drop weight Test.....	20
Figure 4 - ORNL extended $K_{Ic}$ database normalised by $RT_{NDT}$ .....	20
Figure 5 - Effect of changing parameters on Weibull distribution .....	21
Figure 6 - Variation of three parameter Weibull distribution with shape and offset parameters fixed.....	21
Figure 7 - PEAI database plotted using $T_0$ as reference temperature .....	22
Figure 8 - All data, valid datasets in colour invalid datasets in grey .....	22
Figure 9 - Valid data sets, $-50 < T - T_0 < 50$ temperature range .....	23
Figure 10 - Expected and actual number below Master Curve bound (1 - 10 % bounds).....	23



Figure 11 - Expected and actual number below Master Curve bound (0.01 - 0.5 % bounds) 24

### **1.4 Appendices**

Appendix A - Master Curve $T_0$ Calculation As Per ASTM E1921-05 .....	26
Appendix B - Sources of Data for PEAI Database .....	27
Appendix C - Specimen Geometries in Database .....	29
Appendix D - Third Order Polynomial Fit to Strength Data for Database .....	31
Appendix E - All Dataset Information.....	37
Appendix F - Valid Dataset Information .....	47
Appendix G - Visual Basic Macro Used to Calculate SINTAP Step 1,2 and 3 Values of $T_0$ and Error on $T_0$ .....	51
Appendix H - Visual Basic Macro Used to Automatically Generate Plots of Valid Data.....	56
Appendix I - Output of Visual Basic macro in Appendix G .....	57

## **2 Introduction**

The following is a summary of the work conducted on the analysis of the modified Electric Power Research Institute (EPRI) database supplied informally to Rolls-Royce Plc (R-R) by Mark EricksonKirk of the United States Nuclear Regulatory Commission (NRC). The database was originally produced in the late 1990's to provide sufficient evidence for the use of the Master Curve (MC) concept in regulatory codes. The MC concept is now being widely adopted by many countries into their own regulatory codes following the USA's lead; R-R has used the MC for several years as a key argument for safety justifications and continued plant operation. A large database containing all toughness points available to R-R was used to develop a series of different modifications to the MC to increase accuracy of estimation, especially in the lower tail of the distribution where significant gains can be made. The EPRI database has some overlap with the R-R but also contains a large amount of information not previously analysed by R-R.

## **3 Historical Developments Of Toughness Curves**

### ***3.1 HSST Programme***

When it became apparent that brittle failure was a very real and dangerous failure mechanism that could present itself in the steels used in primary containment of nuclear reactors large testing programmes were commissioned. The Heavy Section Steel Technology (HSST) programme was the original attempt at generating sufficient data to provide some confidence in the estimation of reactor pressure vessel (RPV) materials <sup>[ref 1]</sup>. In order to produce valid toughness data very large test specimens were created. Some of these reached sizes of 10T or more, i.e. 10 inches or 254 mm. In order to produce specimens with uniform properties across these large distances very large forgings were produced and heat-treated. Figure 1 shows the scale of the very large plates used in the HSST programme. Figure 2 shows the large sizes of test pieces used, in this case the largest shown is a 8 inch thick drop weight specimen.

### ***3.2 ASME XI Code***

By normalising the results from the HSST and other programmes it was possible to plot all data on a single chart. This normalisation procedure used the Nil Ductility Temperature (NDT) as a reference temperature for each heat of material. The NDT is established by Pellini drop weight testing which utilises a weld bead on a plate. This weld bead provides an initiation point for a fast running cleavage crack into the underlying plate of material to be tested.<sup>[ref 2]</sup>

The NDT is then established by dropping a weight on to the reverse side of the plate to the weld bead at various temperatures. If the crack propagates to either side of the specimen

then the specimen is considered to have failed. The NDT is the lowest temperature where the crack is arrested on both sides of the plate (see Figure 3)

The NDT of the material can be used to normalise toughness data if it is used as a reference temperature for the material,  $RT_{NDT}$ . By subtracting the  $RT_{NDT}$  from the temperature used for the toughness test it is possible plot all toughness data on a single plot (see Figure 4).

Although the drop weight test provides a comparable parameter it is related to the materials ability to withstand and arrest a fast running crack in a thin plate. In reality the danger from cleavage failure is that the crack cannot be arrested in a thick section as there is insufficient local plastic strain to allow arrest. The thin sections used in this type of test aid the arrest mechanism by allowing plasticity to escape to the free surfaces leading to large amounts of dislocation movement and crack arrest. The size of the specimens also limit the distance that the running crack can be arrested in, so the NDT is a measure of a specific geometry as well as material and temperature effects.

### **3.3 Master Curve**

In recent years a large amount of data has become available in the literature. In the future, as the relative cost of producing suitable and valid results reduces, even more will become freely available. The importance of toughness data to the continued safe operation of nuclear plants has become more prevalent as less reliance is put on impact toughness measurements that cannot be directly related to the materials ability to withstand postulated or real defects. Kim Wallin proposed a new methodology using the toughness data itself to provide a reference temperature for the material<sup>[ref 3,ref 4]</sup>. In order to generate this reference temperature several key assumptions about the toughness distribution need to be made:

1. For all steels conforming to the MC a standard curve shape and distribution applies
  - a. The shape of the toughness vs. temperature curve does not change with material type or condition it is simply translated on the temperature axis
  - b. The distribution of values around the toughness curves is the same for materials and this is modelled by a three parameter Weibull distribution
2. Most ferritic steels with room temperature yield strengths within set limits (275 to 825 MPa)[ can modelled by the MC
3. Failure in these steels is controlled by a weakest link mechanism
  - a. Initiation happens once caused by a favourably orientated grain boundary carbide

- b. The micro crack is injected into the surrounding matrix and propagates across the grain boundary into the material
- c. Cleavage failure propagates completely without obstruction leading to failure

The weakest link mechanism allows the use of a Weibull distribution. This simplifies the mathematics involved in both generating the distribution and the development of a maximum likelihood expression to estimate values. The three-parameter distribution is needed to set the distribution in an x-y co-ordinate system (see Figure 5) so the minimal amount of numerical transformations need to be applied to the toughness values generated during testing. The parameters are used to control shape, scale and offset. The MC method sets the shape and offset to known values allowing the offset to vary with temperature (see Figure 6).

The offset value ( $K_{min}$ ) has been chosen as  $20 \text{ MPam}^{0.5}$  as no valid toughness value has been recorded in the steels used to validate the MC approach below  $20 \text{ MPam}^{0.5}$ . The shape parameter has been set at 4 following database analysis. As a Weibull distribution with a shape factor of 4 is nearly indistinguishable from a normal distribution this has caused some discussion between experts as to whether the Weibull distribution provides a physical description of the data. The scale parameter ( $K_0$ ) is allowed to vary by fitting this parameter to data it is possible to determine where the data is located in relation to the toughness curve.

By setting two out of the three parameters in the Weibull distribution to known values it is possible to generate the third by maximum likelihood methods. It is possible to generate the scale parameter in two ways dependent on the type of data available. If replicate testing has been utilised a single temperature method can be used, which simply utilises an equation to calculate the  $K_0$ . If a multi temperature dataset is available then a more complex iterative method is used (see Appendix A).

## **4 Database Analysis**

### **4.1 Database**

The database is a compendium of data available in the literature and privately collected by Mark EricksonKirk, at present no Rolls-Royce proprietary data has been included (see Appendix B). The database contains 6561 data points: 5419 unirradiated, 1142 irradiated. All information was originally supplied in imperial units (ksi, °F, etc) and required conversion to SI units, however there appears to be no errors due to this conversion. A large number of different specimen geometries are included in the database that in the future will allow comparison of analysis techniques and the suitability of small specimens and low constraint geometry specimens to the estimation of toughness curves (see Appendix C). Strength data

has also been collected for each material type (see Appendix D). This, as would be expected with data from the literature, is of varying quality as identified in Appendix D. The yield and ultimate tensile strengths have both been modelled by a three-order polynomial of the form:

**Equation 1**      $\sigma_y = C_0 + C_1.T + C_2.T^2$

Where  $\sigma_y$  = yield strength

$C_0$ ,  $C_1$  and  $C_2$  = material constants

$T$  = test temperature

Description of headings for Appendix B, Appendix C and Appendix D can be found in the Tables section below.

## **4.2 Datasets**

The information contained in the database must first be divided into datasets before calculation of a reference temperature. The database is divided into datasets by the following criteria:

### **4.2.1 Material Condition**

This encompasses a very wide range of different properties that describe an individual heat of material. Most importantly the microstructure of the material will be a controlling factor for the toughness. Current multi-scale multi-physics modelling techniques assume that grain boundary carbides acted upon by cross grain dislocation pile-ups initiate cleavage failure. However there are many different ways in which the microstructure can be affected by the chemistry, thermal and mechanical history of the material. The production of each heat of material is different from another in some way; even those of the same specification will have variations in heat treatment, composition and forging route. A small difference in either or a combination of these may have a large effect on the resulting microstructure of the heat. This leads to a unique microstructure for each heat, hence the variability between forgings of inherently the same composition and forging route.

Orientation can also affect the recorded toughness of a material and it is important to remember this when performing toughness estimates for a component with a complex geometry. The underlying texture of the material may not be clearly visible when studying the microstructure however orientation can have a noticeable effect on the toughness of RPV steels and this must be taken into account when analysing results.

#### *4.2.2 Irradiation Condition*

The effects of irradiation on ferritic steels are well documented in the literature, yet a complete understanding of the mechanisms of irradiation damage are yet to be developed. In general the yield strength of the material is increased, while the fracture strength can be decreased as well. This leads to a large embrittlement of the material with only few observable changes to the microstructure. Neutron damage causes local disordering of the lattice structure allowing diffusion of impurities at much lower temperatures than can be expected due to thermal diffusion. These changes can only be noted on the nano and atomistic scales using very specialised equipment to look for the creation of point defects within the matrix or the formation of copper rich clusters and precipitates.

#### *4.2.3 Crack Geometry*

In the real world cracks come in a variety of different morphologies. A test specimen is a representation of the most damaging type of crack at the most damaging location. To achieve this a sharp crack is introduced via fatigue and the crack front is located at the centre of the specimen. The shape crack raises the local stresses to the highest possible level and by placing the crack at the centre of the specimen the small plastic zone ahead of the crack is contained. Preventing the plastic zone from escaping to free surfaces maintains the high stresses at the crack tip that will induce cleavage failure.

In the real world many defects are in fact shallow or embedded and the stress intensities at the crack tip are much lower than the test specimens used. A material can resist a shallow flaw more easily than a deep flaw with equivalent stress intensity due to the lower constraint. By allowing the plastic zone to escape back to the free more mechanical work can be absorbed into the material lowering the stresses at the crack tip and promoting a ductile failure mechanism.

#### *4.2.4 Dataset Sorting Within Database*

By selecting data points that have the same criteria as above, it is possible to divide the database into datasets. This is achieved by using the following parameters from the database:

1. Mat ID

Each heat of material in the database has a unique identifier.

2. Irrad ID

Each irradiation condition in the database has a unique identifier, when combined with the Mat ID a unique identifier for the tensile properties of the material is created.

3. Geometry ID

Each specimen geometry has a unique identifier. The type of specimen and specimen thickness can affect the measured toughness so the data is grouped accordingly.

4. Orientation

To eliminate the texture effects data points are grouped according to the orientation of the crack plane in the specimen.

5. Sort A/W

The crack depth in the specimen determines constraint, if constraint is lost then the test result will be effected. Shallow and deep defects are grouped separately to allow calculation for low and high constraint geometries.

6. Static Test

If the test has been conducted at a dynamic rate then the effective yield stress of the material will be increased; this is a significant difference for a dataset containing only static data points.

### ***4.3 Reference Temperature Calculation***

In order to speed the process of reference temperature calculation a Visual Basic macro was written (see Appendix G) to perform the calculation of the following reference temperatures and associated information:

1. Reference temperatures

- a.  $T_0$  as per ASTM E1921-05
- b. SINTAP Step 2 and Step 3 as per SINTAP recommendations

2. Associated information

- a. Error on  $T_0$  as per ASTM E1921-05
- b. Validity of  $T_0$  calculation

An example of the output of the macro can be found in Appendix I. Appendix I will be used as an example of how the calculation is performed and the equations used. The example will be described on a calculation-by-calculation then column-by-column basis. These have been labelled in the appendix as Calc 1 to 8 and columns have been numbered 1 to 59. In this example it has taken 8 calculations to supply all of the required information above, for other datasets it may require much more. Due to censoring procedures there are iterative steps in the determination of two of the reference temperatures ( $T_0$  and SINTAP Step 2) and hence it may take several iterations before the exit criteria is reached.

**Calc 1 – Columns 1-29 1<sup>st</sup> estimate of reference temperature,  $T_0$**

**Columns 1-6** This is a direct copy of the relevant information for this dataset from the database.

**Column 7** The Geometry ID (Col 3) is used look up reference to provide the specimen thickness.

**Column 8** The 1T equivalent toughness calculated using Equation 2.

**Equation 2** 
$$K_{Jc25mm} = K_{\min} + (K_{Jcmeas} - K_{\min}) \left( \frac{B}{B_0} \right)^{\frac{1}{4}}$$

Where  $K_{Jc25mm}$  = 1T equivalent

$K_{\min}$  = assumed constant 20 MPam<sup>0.5</sup>

$K_{Jcmeas}$  = measured toughness

$B$  = specimen thickness

$B_0$  = reference thickness, 25mm

**Column 9** Remaining ligament of specimen calculated using Equation 3.

**Equation 3** 
$$b = \frac{1}{1000} \left( \frac{B}{W} (1 - a/W) \right)$$

Where  $b$  = ligament

$a$  = crack depth

$W$  = specimen width

**Column 10** Yield strength at test temperature calculated using Equation 1.

**Column 11** Young's modulus at test temperature (Col 4) calculated using Equation 4.



**Equation 4**  $E = 207200 - 57.1T$

Where  $E$  = Young's modulus

**Column 12** The Geometry ID (Col 3) is used look up reference to provide the specimen thickness.

**Column 13** Poisson's ratio for steel, assumed constant at 0.3 mm/mm.

**Column 14** Measuring limit of the specimen calculated using Equation 5.

**Equation 5** 
$$K_{Jc\text{limit}} = \sqrt{\frac{b \cdot \sigma_y \cdot E}{M(1 - \nu^2)}}$$

Where  $K_{Jc\text{limit}}$  = measuring capacity for specimen size and geometry

$M$  = measure of lateral constraint on plastic zone due to specimen geometry

$\nu$  = Poisson's ratio, assumed constant 0.3 mm/mm

**Column 15** Validity check on measuring capacity of specimen, 1 if Col 6 < Col 14, else 0.

**Column 16** Minimum of Col 6 and size corrected (Equation 2) Col 14 to be used in subsequent calculations.

**Column 17** Relative temperature (Col 4 - Col 29) calculated using Equation 6.

**Equation 6**  $RT = T - T_0$

Where  $RT$  = relative temperature

$T_0$  = reference temperature

**Column 18** Validity check on relative temperature, set to 1 for first calculation. 1 if  $-50 < \text{Col 17} < 50$ , else 0.

**Column 19-29** Maximum likelihood calculation of reference temperature using Microsoft Excel Goal Seek to minimise difference between Col 26 and Col 27.

**Result** Produces  $T_0$  estimate to allow censoring to relative temperature

**Calc 2 – Columns 1-29 2<sup>nd</sup> estimate of reference temperature,  $T_0$**

**Column 1-17** Copy of Calc 1 Columns 1-17.

**Column 18** Validity check on relative temperature, 1 if  $-50 < \text{Col } 17 < 50$ , else 0. Uses previously calculated  $T_0$  as reference temperature.

**Column 19-29** Maximum likelihood calculation of reference temperature using Microsoft Excel Goal Seek to minimise difference between Col 26 and Col 27.

**Result** Produces  $T_0$  estimate to allow censoring to relative temperature

### **Calc 3 Column 1-29 Final estimate of reference temperature, $T_0$**

Calc 2 is repeated until the calculated reference temperature is equal to the previous reference temperature. The  $T_0$  calculated uses only data points that are valid to both the measuring capacity and relative temperature.

### **Calc 4 Column 30-33 Reference temperature validity check**

**Column 30** 1 if  $-14 < \text{Relative temperature (Col 17)} < 50$ , else 0.

**Column 31** 1 if  $-35 < \text{Relative temperature (Col 17)} < -15$ , else 0.

**Column 32** 1 if  $-50 < \text{Relative temperature (Col 17)} < -36$ , else 0.

**Column 33** Weighted sum of Col 30 - 31 as it is believed that data points with lower relative temperatures contribute to greater accuracy, calculated using Equation 7.

**Equation 7**

$$Col33 = \frac{Col30}{6} + \frac{Col31}{7} + \frac{Col32}{8}$$
$$r_i \cdot N_i = \sum Col33$$

Where  $r_i$  = weighting factor

$N_i$  = number of data points contributing to  $T_0$  estimate within relative temperature range

**Result** If  $\sum Col33 > 1$  then the  $T_0$  estimate is considered valid.

### **Calc 5 Column 34-37 Estimate of $\epsilon T_0$**

**Column 34** Median toughness at relative temperature calculated using Equation 8. If Col 15 or Col 18 = 0 then Col 34 =0.

**Equation 8**  $K_{Jcmed} = 30 + 70e^{0.019(T-T_0)}$

Where  $K_{Jcmed}$  = median toughness

**Column 35** Equivalent median toughness calculated using Equation 9.

**Equation 9**  $K_{JcEqmed} = \frac{\sum K_{Jcmed}}{r}$

Where  $K_{JcEqmed}$  = equivalent median toughness

$r$  = number of valid data points in set

**Column 36** An estimated standard deviation for the mean based on the equivalent median toughness, values looked up using Table 5.

**Column 37** Estimate of error on  $T_0$  calculation, equivalent to 1 standard deviation, calculated using Equation 10  $\sigma = \frac{\beta}{\sqrt{r}}$ .

**Equation 10**  $\sigma = \frac{\beta}{\sqrt{r}}$

Where  $\sigma$  = standard deviation of  $T_0$  distribution

$\beta$  = standard deviation of parent toughness distribution

**Calc 6 Column 38-39 Estimate of SINTAP step 3 reference temperature**

**Column 38** Step 3  $T_{0i}$  calculated using Equation 11.

**Equation 11**  $Step_3 T_{0i} = T - \frac{\ln \left( \frac{(K_{Jc25mm} - K_{min}) \left( \frac{N}{\ln(2)} \right)^{\frac{1}{4}} - 11}{77} \right)}{0.019}$

Where  $Step_3 T_{0i}$  = reference temperature calculated from single data point

**Column 39** Maximum of Col 38.

### **Calc 7 Column 40-59 1<sup>st</sup> estimate of SINTAP Step 2 reference temperature**

**Column 40-41** Copy of Col 29 and Col 4 from Calc 3.

**Column 42** Reference temperature calculated using Equation 6 and the  $T_0$  from Calc 3.

**Column 43** Copy of Col 8 from Calc 3.

**Column 44** Median toughness calculated using Equation 8.

**Column 45** Minimum of Col 43 and Col 44 to be used in subsequent calculations.

**Column 46** Validity check on median toughness, 1 if Col 43 < Col 44, else 0.

**Column 47** Copy of Col 18 from Calc 3.

**Column 48-59** Maximum likelihood estimator for  $T_0$ . similar to that used in Calc 1-3, however censoring is based on  $K_{Jcmed}$  as opposed to  $K_{Jclimit}$ .

**Result** 1<sup>st</sup> estimate of SINTAP Step 2 reference temperature.

### **Calc 8 Column 40-59 Final estimate of SINTAP Step 2 reference temperature**

Repetition of Calc 7 Col 40-59 however values previously copied from Calc 3 are now copied from Calc 7. This process is repeated until the current and previously calculated Step 2 values are equal or the current value is lower than the previous value.

#### ***4.4 Results of Database Analysis***

Once reference temperatures are calculated for all datasets (see Appendix E) the toughness values for each point can now be plotted against relative temperature. With all data plotted (see Figure 7) it can be seen that the large number of invalid  $T_0$  estimates creates a chaotic plot, however the majority of data clearly lies within the bounds of the MC. By plotting the valid datasets in colour and the invalid datasets in grey (see Figure 8) the trends become more obvious. It can be seen from Figure 8 that once the criteria used for dataset selection is taken into account then the MC, at least visually, provides a good representation of the data across a wide temperature range. The effect of the onset of large-scale plasticity and tearing can be seen in the upper transition as the data points and estimation curves begin to significantly diverge.

In order to check the quality of fit to the data a simple analysis was conducted comparing the actual number of data points below a MC bound to that which could be expected from the statistics of the MC distribution. The ASTM standard E1921-05 recommends the use of the MC in the relative temperature region of  $-50 < T - T_0 < 50$ . Beyond this region the accuracy of the MC is considered to diminish as the toughness estimates are extrapolated to a point where, even if data was available, no information was used in the  $T_0$  calculation. The database has been replotted with just valid data sets over the above temperature region in Figure 9. Simple counting of the number of points below each bound has been conducted (see Table 6) and has produced some interesting results. It can be seen from Figure 10 and Figure 11 that the number of recorded data points below the MC bounds up to 8 % is less than expected. This implies that the MC is overly conservative in the lower tail of the distribution.

There are several explanations for this observation:

1. The observed difference is real
  - a. The MC assumption of a Weibull distribution is wrong and a different type of statistical distribution is required, such as a log normal distribution (Moskovic approach)<sup>[ref 6]</sup>.
  - b. The MC assumption of a Weibull distribution is correct and the lower tail is being affected by the arrest distribution (Microarrest approach)<sup>[ref 7]</sup>.
  - c. The assumption of  $K_{min}$  across the temperature range is incorrect and a temperature dependent  $K_{min}$  needs to be derived from the database.
2. The observed difference is not real
  - a. The database is simply 'one throw of the dice' for the materials tested. If the toughness tests were repeated the result may be different. This can be assessed using the Simulakrum spreadsheet developed by Tim Williams.
  - b. Even though the database is large it is not of sufficient size to provide confidence in the analysis.

This observation was also made by David Swan of R-R when analysing the internal R-R database, as stated early there is some overlap between these databases so this result was not unexpected. The data also clear shows a large up swing above  $T - T_0$  of +50, this observation has also been made previously and as yet remains unexplained or quantified.

#### **4.5 Further Work**

The above statements need to be proved or disproved in order to provide confidence in new analysis and estimation methodologies based on the results of a database analysis. These can be solved by:

1. Difference is real
  - a. Asses the suitability of Weibull, normal and log normal distributions to the modelling of the data base. The development of maximum likelihood estimators for normal distributions is not trivial, as shown by Moskovic, and may take considerable development.
  - b. Further study into the micro mechanisms of fracture are required to understand the effect that microarrest may have on the lower tail of the distribution. Development of the local approach modelling techniques may help to provide a solution for how this complex yet subtle effect influences the toughness distribution.
  - c. Continued database analysis fitting the current MC distribution to the database but allowing the offset parameter,  $K_{min}$ , to vary. However, this type of analysis may only show a significant difference in the  $50 < T - T_0$  temperature region.
2. Difference is not real
  - a. The format of the database may need to altered to allow easy insertion into the Simulakrum spreadsheet, however once included the analysis is heavily automated and is not labour intensive.
  - b. The size of the database needs to be increased dramatically. Further data is available both from internal and external sources, this is believed to be ~2500 data points. Although insufficient to prove the suggestion of over conservatism if the trend continues then the inference can still be made. This step should be completed before the more complicated analysis methods above are considered.

The data already contained in the database also needs to be checked against the originally reported data for errors.

## **5 Summary**

A first pass analysis of the PEAI database as supplied by Mark EricksonKirk has been shown to provide an invaluable source of information for justification of the aster curve methodology and will be a highly useful tool in the future. The database is currently of sufficient size to allow inference of concepts but not large enough to provide definitive proof of these concepts.

## 6 Tables

**Table 1 - Description of headings for Appendix B**

<b>Heading</b>	<b>Description</b>
Primary Author [#]	Only the first named author has been shown for clarity.
Title [#]	Title of paper, report or presentation containing the data in either tabulated or graphical format.
Society [#]	Professional society, company or university that published the data.
Pages [#]	Page reference in document.
Date [#]	Year of publication.

**Table 2 - Description of headings for Appendix C**

<b>Heading</b>	<b>Description</b>
Geometry ID [#]	Unique identifier for specific geometry.
Specimen Type [#]	Defines specimen type and side grooving: Compact tension, bend bar or wedge opening load
Full Thickness [mm]	Thickness of specimen in millimetres.
Net Thickness [mm]	Thickness of specimen once side grooving has been taken into account in millimetres.
Sort Thickness [mm]	Due to conversion from metric to imperial, and vice versa, small errors (of the order of 0.01 mm) are generated. The sort thickness, in millimetres, is a rounding of the thickness to allow grouping of data.
B/W [mm/mm]	The ratio of specimen thickness to height (unitless)



**Table 3 - Description of headings for Appendix D**

<b>Heading</b>	<b>Description</b>
Mat ID [#]	Unique identifier for material heat.
Irrad ID [#]	Unique identifier for irradiation condition.
Name [#]	Combination of <Mat ID>.<Irrad ID> to allow searching within database.
RT YS [MPa]	Room temperature yield strength in MPa.
RT UTS [MPa]	Room temperature ultimate tensile strength in MPa.
YS $C_0$ , $C_1$ and $C_2$	Constants used to fit yield data with a three order polynomial, with the equation: $YS = C_0 + C_1.T + C_2.T^2$
UTS $C_0$ , $C_1$ and $C_2$	Constants used to fit UTS data with a three order polynomial, with the equation: $UTS = C_0 + C_1.T + C_2.T^2$
Yield Data Quality [#]	Quality of source data use to generate the polynomial.

**Table 4 - Description of headings for Appendix E and Appendix F**

<b>Heading</b>	<b>Description</b>
Dataset ID [#]	Unique identifier for dataset.
Dataset [#]	Dataset name, combination of <Mat ID>,<Irrad ID>,<Orientation>,<Sort A/W>,<Static Test>
N [#]	Total number of points in dataset.
r [#]	Number of valid points in dataset, i.e. number used in calculation. Assumed that test terminated with cleavage.
T <sub>0</sub> [°C]	Reference temperature of dataset (equivalent to SINTAP step 1).
ri.Ni [#]	Validity check on T <sub>0</sub> calculation. Dataset valid if >1.
εT <sub>0</sub> [°C]	Error on calculated T <sub>0</sub> .
Step 2 [°C]	SINTAP Step 2 reference temperature calculated by censoring to median toughness as oppose to specimen limit.
Step 3 [°C]	SINTAP Step 3 reference temperature calculated using the lowest point in the dataset.
Step 3 Significant [#]	Step 3 value is considered significant if Step 3 > Max (Step 1, Step 2) + 8
MAX Step1, 2, 3 [°C]	Maximum value of Step 1, 2, or 3.
SINTAP T <sub>0</sub> Final [°C]	Reference temperature recommended by SINTAP to be used in toughness estimation. SINTAP T <sub>0</sub> Final = MAX(Step 1, 2, 3) + 14/√r

**Table 5 - Lookup table for standard deviation of distribution based on K<sub>JcEqmed</sub>**

<b>Equivalent median toughness rounded to nearest integer</b> <b>K<sub>JcEqmed</sub></b>	<b>Standard deviation of parent population</b> <b>β</b>
83 < K <sub>JcEqmed</sub>	18
66 < K <sub>JcEqmed</sub> < 83	18.8
58 < K <sub>JcEqmed</sub> < 65	20.1

**Table 6 - Actual/expected analysis of database for  $-50 < T - T_0 < 50$  temperature range**

<b>Master Curve % Bound</b>	<b>Number Expected Below Bound</b>	<b>Actual Number Below Bound</b>	<b>Actual / Expected</b>
0.01	0.2546	0	0
0.02	0.5092	0	0
0.03	0.7638	0	0
0.04	1.0184	0	0
0.05	1.273	1	0.785545954
0.1	2.546	3	1.178318932
0.2	5.092	4	0.785545954
0.3	7.638	7	0.91647028
0.4	10.184	9	0.883739199
0.5	12.73	9	0.706991359
1	25.46	19	0.746268657
2	50.92	38	0.746268657
3	76.38	65	0.851008117
4	101.84	92	0.903377848
5	127.3	120	0.942655145
6	152.76	152	0.995024876
7	178.22	173	0.970710358
8	203.68	200	0.981932443
9	229.14	232	1.012481452
10	254.6	256	1.005498822
50	1273	1338	1.051060487
95	2418.7	2383	0.985240005
99	2520.54	2479	0.983519405
100	2546	2546	1

## 7 Figures

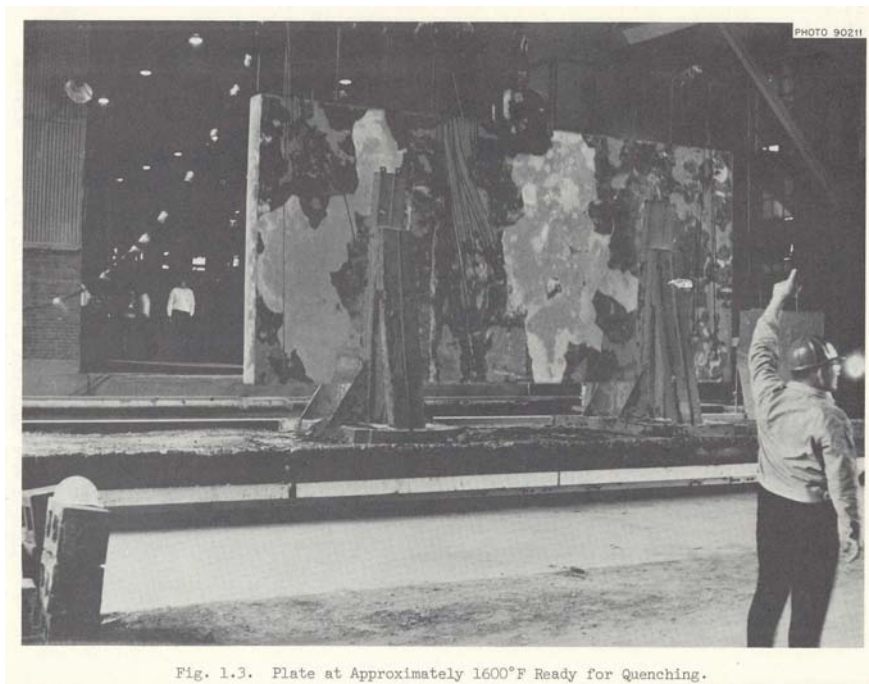


**Figure 1 - HSST Programme plate 2 just before quenching (picture taken from ref 1)**

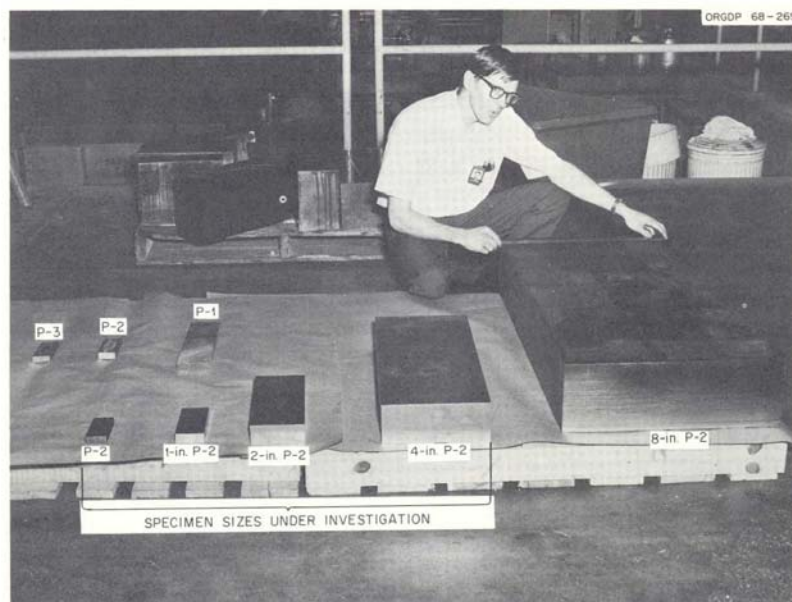
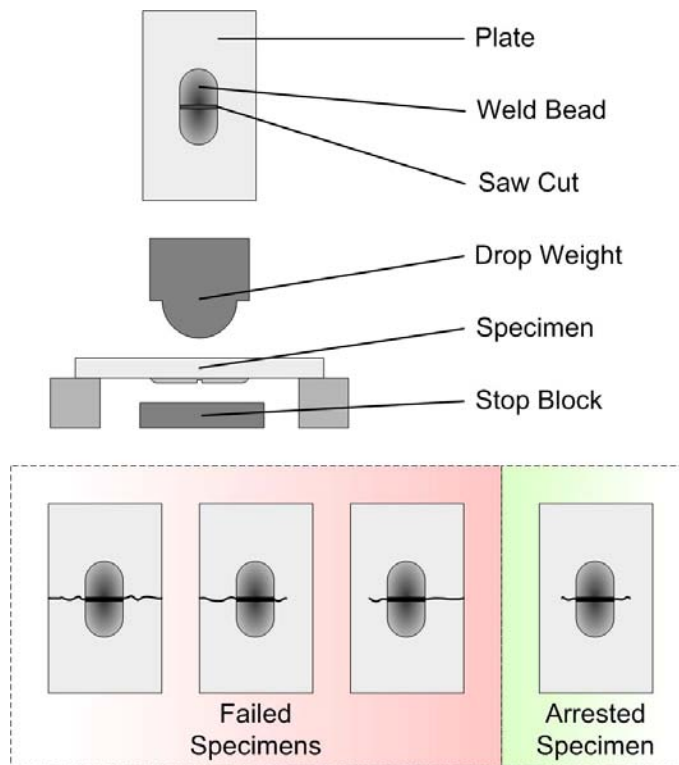
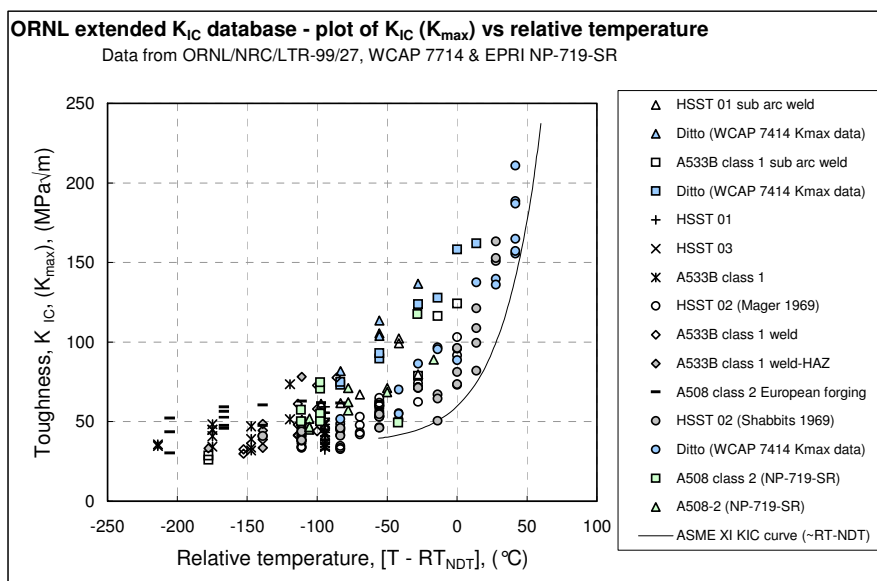


Fig. 2.11. Comparison of Drop-Weight NDT Specimens.

**Figure 2 - Range of specimen sizes tested using drop weight testing (picture taken from ref 1)**



**Figure 3 - Pellini drop weight Test**



**Figure 4 - ORNL extended  $K_{IC}$  database normalised by  $RT_{NDT}$**

Plot supplied by David Swan, Rolls-Royce Plc

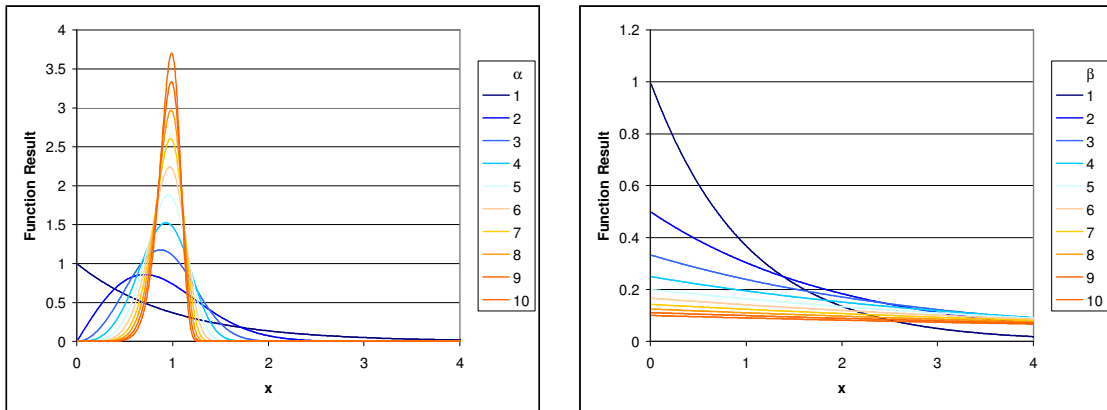
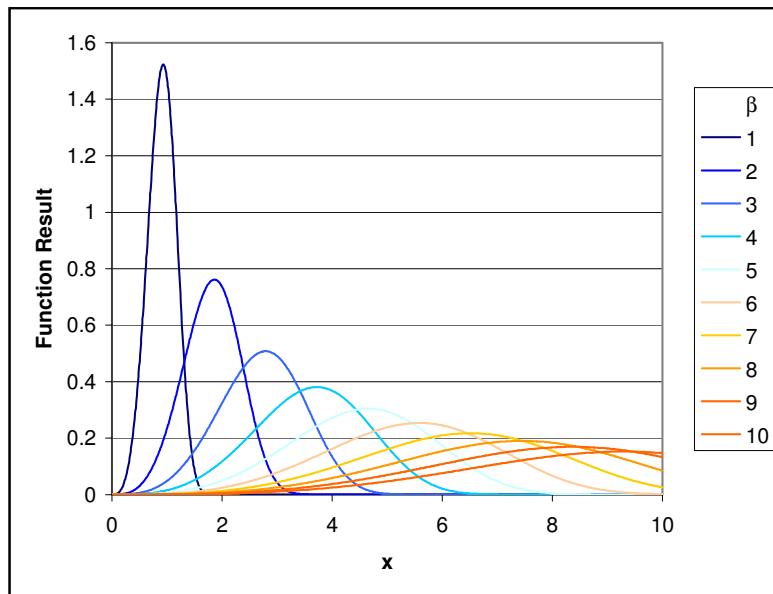


**Figure 5 - Effect of changing parameters on Weibull distribution**



Offset fixed at 0, shape parameter fixed at 4.

**Figure 6 - Variation of three parameter Weibull distribution with shape and offset parameters fixed**

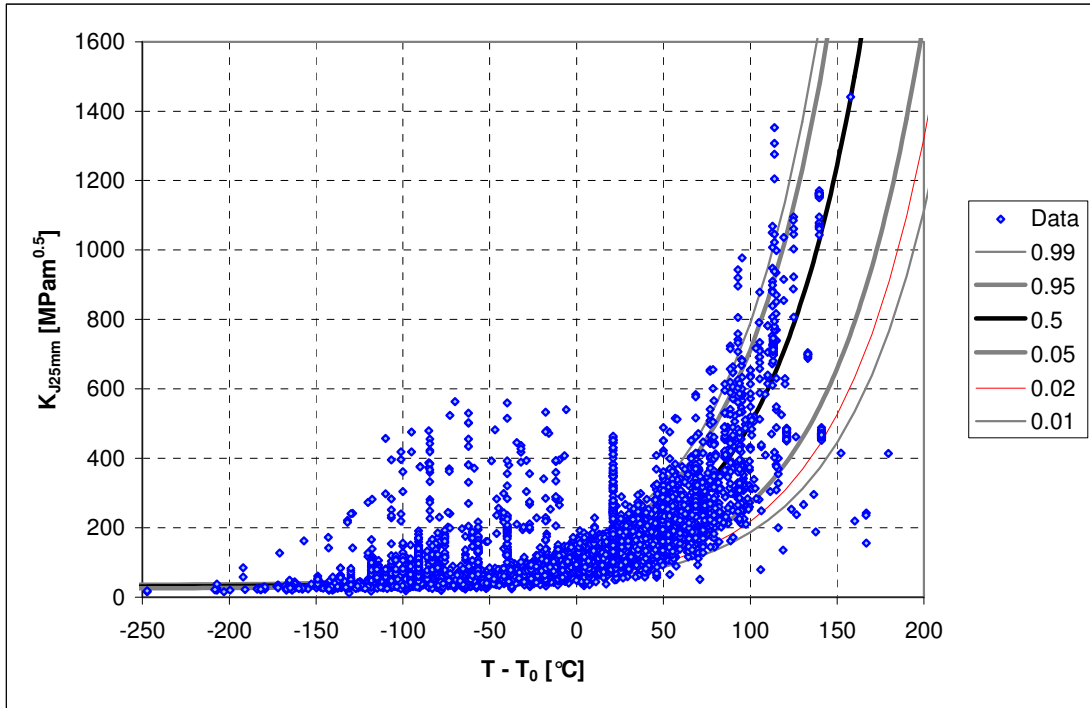


**Figure 7 - PEAI database plotted using  $T_0$  as reference temperature**

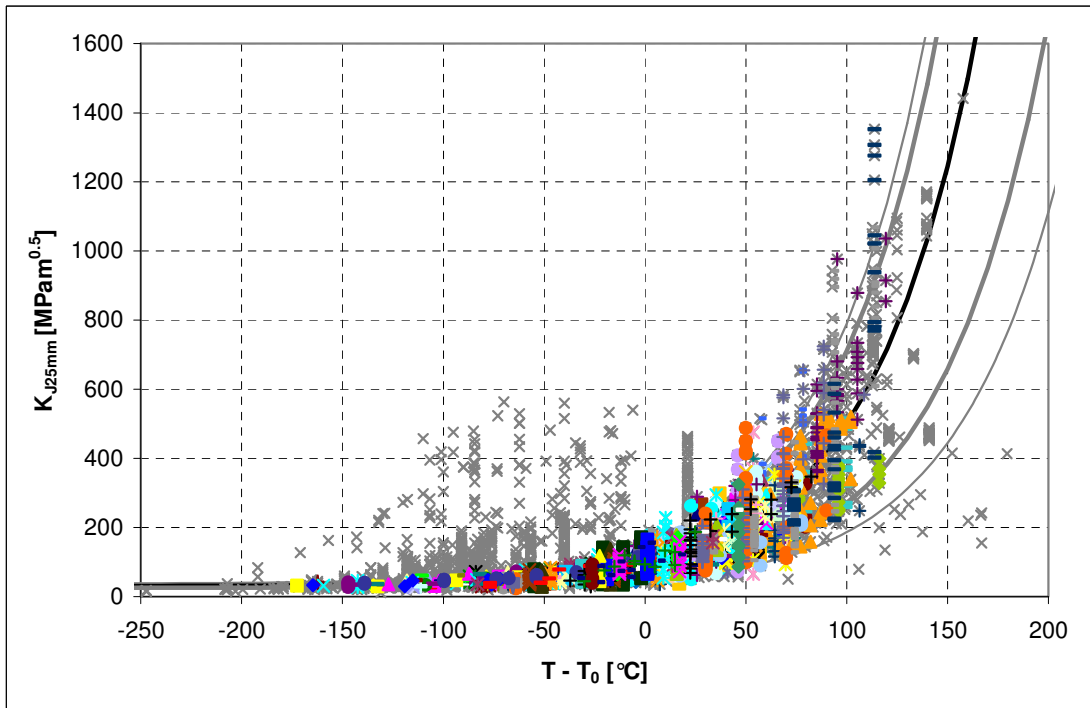
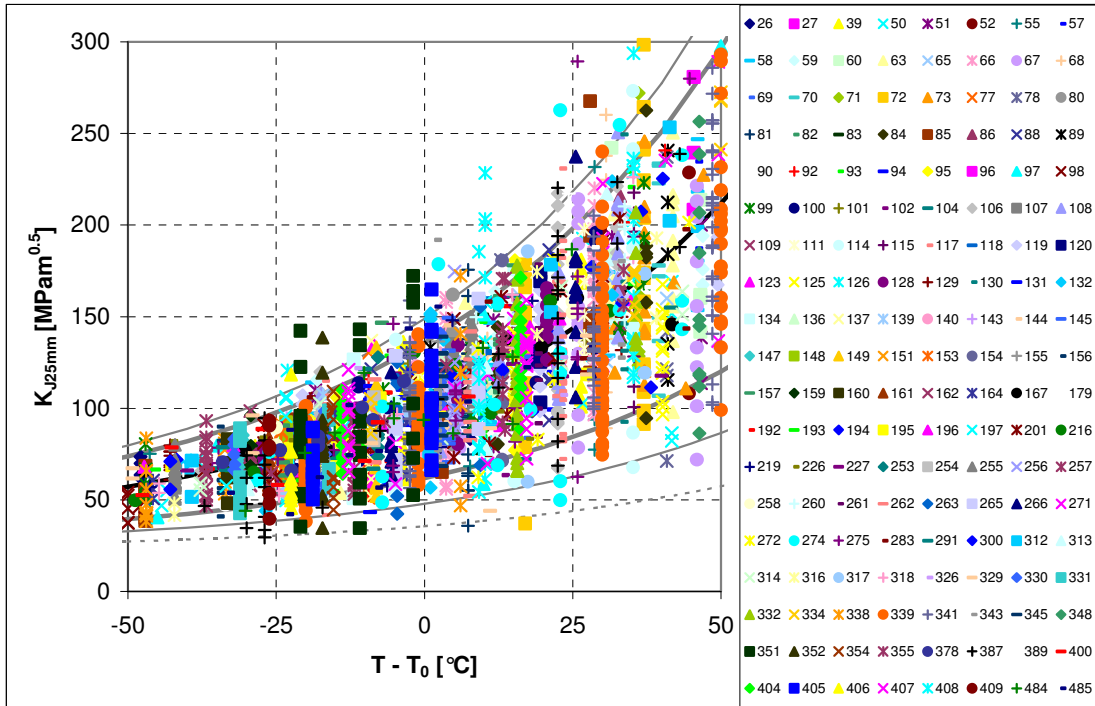


**Figure 8 - All data, valid datasets in colour invalid datasets in grey**



Series names correspond to Dataset ID found in Appendix F.

**Figure 9 - Valid data sets,  $-50 < T - T_0 < 50$  temperature range**

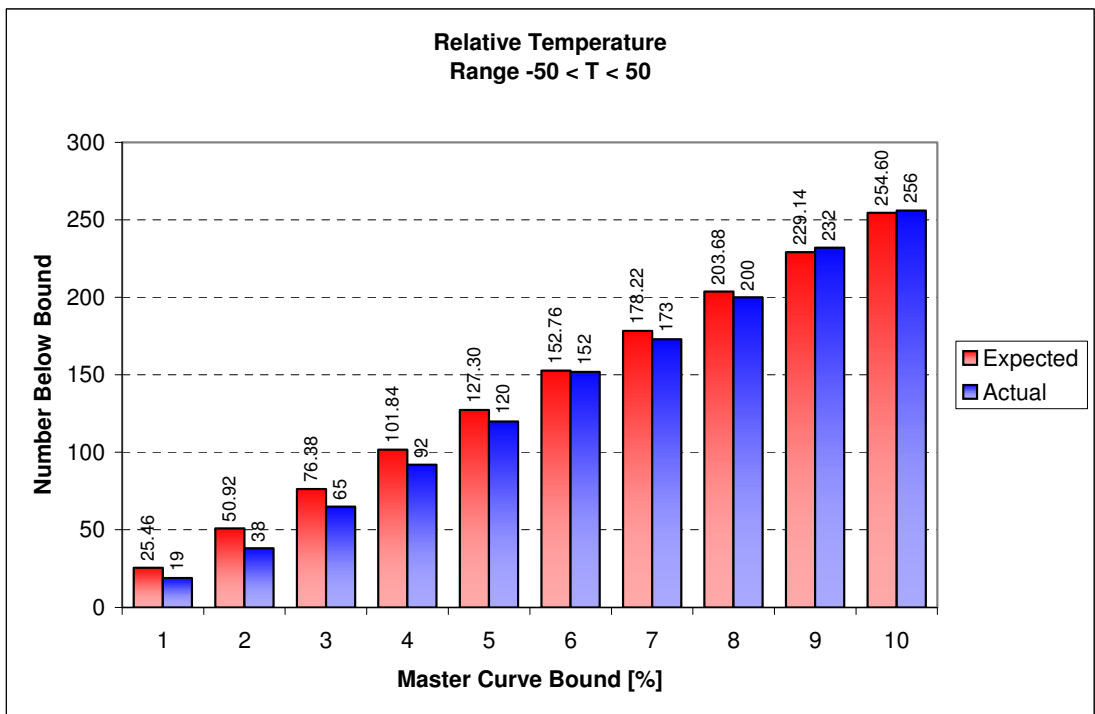


**Figure 10 - Expected and actual number below Master Curve bound (1 - 10 % bounds)**



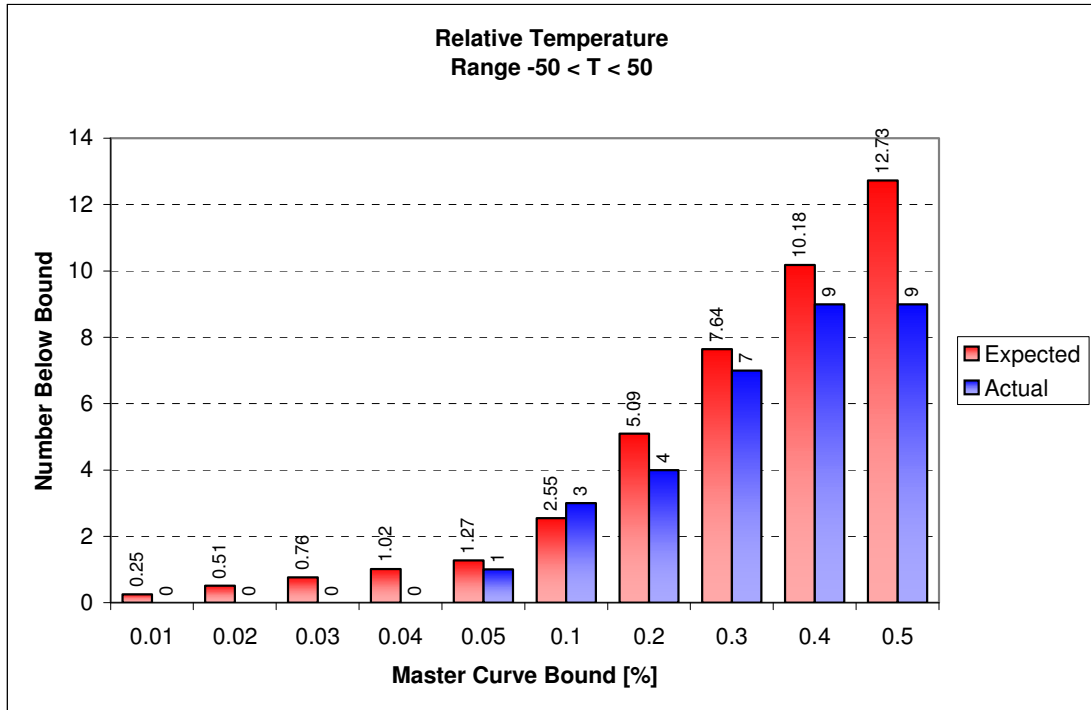


**Figure 11 - Expected and actual number below Master Curve bound (0.01 - 0.5 % bounds)**

## 8 References

- ref 1 F.J. Witt, Heavy-Section Steel Technology Program semiannual progress report for period ending February 29, Oak Ridge National Laboratory, 1968
- ref 2 William S. Pellini, Guidelines for fracture-safe and fatigue-reliable design of steel structures, The Welding Institute, 1983
- ref 3 K. Wallin, 'Statistical model for carbide induced brittle fracture in steel', Metal Science, 1984, Vol. 18, Pg. 13-18
- ref 4 K. Wallin, 'The size effect in KIC results', Engineering Fracture Mechanics, 1985, Vol. 22(1), Pg. 149-163
- ref 5 E 1921 - 05 Standard test method for determination of reference temperature,  $T_0$ , for ferritic steels in the transition range', ASTM Standards, 2002, Vol. 03.01
- ref 6 J. Heerens et al, 'Fracture toughness characterisation in the ductile-to-brittle transition and upper shelf regimes using pre-cracked Charpy single-edge bend specimens, International Journal of Pressure Vessels and Piping, 2005, Vol. 82, Pg. 649-667
- ref 7 T. Williams, D. Swan, G. Dixon, 'Modification of the lower tail of the master curve distribution', IAEA Specialists Meeting, Moscow, 2004

## 9 Appendices

### Appendix A - Master Curve $T_0$ Calculation As Per ASTM E1921-05

Measuring capacity 
$$K_{Jc\ limit} = \sqrt{\frac{b \cdot \sigma_y \cdot E}{M(1 - \nu^2)}}$$

Measuring capacity validity 
$$\begin{aligned} K_{Jc\ meas} \leq K_{Jc\ limit} &\Rightarrow \delta = 1 \\ K_{Jc\ meas} > K_{Jc\ limit} &\Rightarrow \delta = 0 \end{aligned}$$

Toughness value for calculation 
$$\begin{aligned} \delta = 1 &\Rightarrow K_{Jci} = K_{Jc\ meas} \\ \delta = 0 &\Rightarrow K_{Jci} = K_{Jc\ limit} \end{aligned}$$

Size correction 
$$K_{Jc25mm} = K_{\min} + (K_{Jci} - K_{\min}) \left( \frac{B}{B_0} \right)^{\frac{1}{4}}$$

Maximum likelihood estimator 
$$\sum_{i=1}^N \delta_i \frac{e^{0.019[T-T_0]}}{11 + 77e^{0.019[T-T_0]}} - \sum_{i=1}^N \frac{(K_{Jci} - K_{\min})^4 e^{0.019[T-T_0]}}{(11 + 77e^{0.019[T-T_0]})^5} = 0$$

Tolerance bounds 
$$K_{Jc(0.xx)} = 20 + \left( \ln \left( \frac{1}{1 - 0.xx} \right) \right)^{\frac{1}{4}} (11 + 77e^{0.019(T-T_0)})$$

Where  $xx$  = percentage bound required, i.e. 2%  $\Rightarrow 0.xx = 0.02$

## Appendix B - Sources of Data for PEA I Database

Primary Author	Title	Society	Pages	Date
#	#	#	#	#
Marston, T.U.	Flaw Evaluation Procedures, Background and Application of ASME Sec. XI App. A	EPRI		1978
Nanstad, R.K.	Irradiation Effects on Fracture Toughness of Two High-Copper Submerged-Arc Welds, HSSI Series 5	USNRC		1992
VanDerSluys, W.A.	Results of MPC/JSPS Cooperative Testing Program in the Ductile-to-Brittle Transition Region	ASTM	308-324	1994
Morland, E	Fracture Toughness in the Transition Regime for A533B-1 Steel: The Effect of Specimen Sidegrooving	ASTM	215-237	1990
Alexander, D.J.	Fracture Properties of Specially Heat Treated ASTM A508 Cl. 2 Pressure Vessel Steel	ASTM	365-380	199-+3
McCabe, D.E.	A Comparison of Weibull and Beta-Ic Analysis of Transition Range Fracture Toughness Data	USNRC & ASTM	80-94	1992 & 1993
Ingham, T.	Fracture Toughness in the Transition Regime for A533B Steel: Prediction of Large Specimen Results from Small Specimen Tests	ASTM	368-389	1989
McCabe, D.E.	Unirradiated Material Properties of Midland Weld WF-70	USNRC		1994
McGowan, J.J.	Characterization of Irradiated Current Practice Welds and A533 Grade B Class 1 Plate for Nuclear Pressure Vessel Service	USNRC		1988
Iwazate, T.	An Analysis of Elastic Plastic Fracture Toughness Behavior for J-sub-Ic Measurement in the Transition Region	ASTM	531-561	1983
Lidbury, D.	Assessment of the Ductile-to-Brittle Transition Toughness Behavior of an A508 Cl. 3 PWR Pressure Vessel Steel By a Statistical Approach	ASME	283-294	1993
Sorem, W.A.	The Effect of Specimen Size and Crack Depth on the Elastic-Plastic Fracture Toughness of a Low-Strength High-Strain Hardening Steel	University of Kansas		1989
Nanstad, R.K.	Personal Communication Regarding Midland WF-70 Toughness After Irradiation			1997
CEOG	Fracture Toughness Characterization of C-E RPV Materials	CEOG		1998
Williams, James F.	Determination of Reference Temperature, To, for Nuclear Pressure Vessel Steels in both the Unirradiated and Irradiated Conditions	Westinghouse		1998
Hawthorne, J.R.	Evaluation and Prediction of Neutron Embrittlement in Reactor Pressure Vessel Materials	EPRI		1992
Hawthorne, J.R.	Notch Ductility and Fracture Toughness Degredation of A302-B and A533-B Reference Plates from PSF Simulated Surveillance and Through-Wall Irradiation Capsules	USNRC		1984
Hiser, A.L.	Post-Irradiation Fracture Toughness Characterization of Four Lab-Melt Plates	US-NRC		1989
Hawthorne, J.R.	Influence of Fluence Rate on Radiation-Induced Mechanical Property Changes in RPV Steels	US-NRC		1990
Hawthorne, J.R.	Experimental Assessments of Gundremmingen RPV Archive Material for Fluence Rate Effects Studies	US-NRC		1988
Hawthorne, J.R.	Investigations of Irradiation-Anneal-Reirradiation (IAR) Properties Trends of RPV Welds: Phase 2 Final Report	US-NRC		1990
Chaouadi, Rachid	Fracture Toughness Measurement in the Transition Regime Using Small Specimens	ASTM		1997
Miranda, Carlos	Accuracy in the To Determination: Numerical vs. Experimental Results	ASME		1999
Valo, Matti	Irradiation Response of the IAEA CRP-3 Material FFA Measured by Fracture Toughness Specimens	ASTM	238-248	1993
Aquino, C.T.E.	"An Approach to the Fracture Toughness Variation in the Ductile-Brittle Transition for Nuclear Pressure Vessel Steels (in Portuguese)	IPEN/USP, San Paulo, Brazil		1997
Pavinich, W.A.	Fracture Toughness Testing of Linde 1092 Reactor Vessel Welds in the Transition Range Using Charpy-Sized Specimens	ASTM	157-166	1999
Ishino, S.	The Effect of Chemical Composition on Irradiation Embrittlement	MPS	13.1-13.15	1988
Havel, R.	Fracture Properties of Irradiated A533B Cl.1, A508 Cl. 3, and 15Ch2NMFAA Reactor Pressure Vessel Steel	ASTM	163-171	1993
Havel, R.	Effects of Neutron Irradiation on Advanced CrNiMoV RPV Steel	AASMRT	227-237	
Kodaira, T.	Evaluation of Neutron Irradiation Embrittlement of Heavy Section Nuclear RPV Steels in terms of Elastic-Plastic Fracture Toughness		1-13	1985
Chaouadi, R.	Fracture Toughness of the Ni-Modified A302-B Plate of the BR3 Reactor Pressure Vessel	ASTM		1999
Wallin, K.	Theory Based Statistical Interpretation of Fracture Toughness of Reactor Pressure Vessel Steel 15x2M-phi-A and its Welds	AASMRT	131-136	
Ahlf, Jurgen	Irradiation Programs to Establish the Safety Margins of German Licensing Rules Related to RPV Steel Embrittlement	ASTM	115-129	1989
Link, Richard	Dynamic Fracture Toughness Initiation of A533 Grade B Steel Plate, NUREG, CR-6512	NRC		1997
Wallin, Kim	Master Curve Analysis of Ductile to Brittle Transition Region Fracture Toughness Round Robin Data, The "EURO" Fracture Toughness Curve, VTT-367	VTT		1998
Shabbits, W.O.	Dynamic Fracture Toughness Properties of Heavy Section A533B Class 1 Steel Plate, WCAP 7623, HSST Technical Report #13	Westinghouse & HSST		1970

Primary Author	Title	Society	Pages	Date
#	#	#	#	#
Joyce, James A.	On the Utilization of High-Rate Pre-Cracked Charpy Test Results and the Master Curve to Obtain Accurate Lower Bound Toughness Predictions in the Ductile-to-Brittle Transition	ASTM		1997
Pluvinage, G.	Application of Local Fracture Criteria to Dynamic Fracture Toughness		3151-3158	1984
Marandet, B.	Influence of Loading Rate on the Fracture Toughness of Some Structural Steels in the Transition Regime	ASTM	622-647	1984
Shoemaker, A.K.	The Static and Dynamic Low-Temperature Crack-Toughness Performance of Seven Structural Steels		319-339	1971
Priest, A.H.	Influence of Strain Rate and Temperature on the Fracture and Tensile Properties of Several Metallic Materials	TWI	95-111	1979
Fujii, E.	An Evaluation of Dynamic Fracture Toughness of Type A508 Class 3 Steel	ASTM	181-190	1986
Vacek, Miroslav	Radiation Embrittlement and Annealing Recovery of CrNiMoV Pressure vessel Steel With Different Copper and Phosphorus Content	ASTM	172-182	1993
Holtmann, M.	The Influence of Loading Rate on the Ductile-Brittle Transition and Cleavage Fracture Stress of 2.25Cr-1Mo Steel			
Holzmann, M.	R-Curves and Fracture Toughness Transition Behavior at Static, Rapid, and Impact Loading of CrNiMoV Reactor Pressure Vessel Steel		39-47	1995
Nakano, Y.	Dynamic Fracture Toughness of LWR Pressure Vessel Steel A508 Cl. 3: A Japanese Round Robin Study		255-270	1988
Soulat, P.	The Effect of Irradiation on the Toughness of Pressurized Water Reactor Vessel Steels Under Different Service Conditions		61-68	1984
Krabiell, Armin	(in German)		225-230	1982
Fujii, E.	Effects of Temperature and Strain Rate on Dynamic Fracture Toughness of Steel (in Japanese)		619-629	1985
Onizawa, Kunio	Effect of Irradiation on Fracture Toughness in the Transition Range of RPV Steels	ASTM		1999
Natishan, MarjorieAnn Erickson	Mechanisms of Strength and Toughness in a Microalloyed, Precipitation Hardened Steel	U. Va. Ph. D. Dissertation		1988
Gudas, John P.	Micromechanics of Fracture and Crack Arrest in Two High Strength Steels	DTNSRDC/SME-87-20		1987
Kirk, M.T.	Applicability of ASTM A710 Grade A Class 3 (HSLA-80) Steel for use as Crack Arrestors	DTNSRDC/SME-87-54		1987
Vassilaros, Michael G.	Fracture Behavior of Modern Low-Carbon Steels	Churchill College, Ph.D. Dissertation		1991
Czyryca, E.J.	Fracture Toughness of HSLA-100, HSLA-80, and ASTM A710 Steel Plate	DTRC-SME-88/64		1990
Hasson, D.F.	The Effect of a Higher Loading Rate on the JIC Fracture Toughness Transition Temperature of HY Steels	ASME	133-141	1981
Yoon, K.K.	BWOG To Data (PROPRITARY)			2000
Rathbun, H.J.	Size Scaling of Toughness in the Transition: A Single Variable Experiment and Data Base Assessment	ASME		2000
Wallin, K.	Statistical Aspects of Constraint with Emphasis on Testing and Analysis of Laboratory Specimens in the Transition Region	ASTM	264-288	1993
Joyce, J.	To Evaluation in Common Specimen Geometries	ASME		2000
Joyce, J.	DEVELOPMENT OF THE To REFERENCE TEMPERATURE FROM PRECRACKED CHARPY SPECIMEN	ASME		1999

## Appendix C - Specimen Geometries in Database

Geometry ID	Specimen Type	Full Thickness	Net Thickness	Sort Thickness	B/W
#	#	mm	mm	mm	mm/mm
1	WOL	25.4	25.4	25.4	0.5
2	WOL	50.8	50.8	50.8	0.5
3	C(T)	12.5	12.5	12.7	0.5
4	C(T)	12.5	10	12.7	0.5
5	C(T)	12.7	12.7	12.7	0.5
6	C(T)	12.7	9.525	12.7	0.5
7	C(T)	25.4	25.4	25.4	0.5
8	C(T)	25	25	25.4	0.5
9	C(T)	25	20	25.4	0.5
10	C(T)	25	12.5	25.4	0.5
11	C(T)	25.4	19.05	25.4	0.5
12	C(T)	25.4	20.32	25.4	0.5
14	C(T)	50.8	50.8	50.8	0.5
15	C(T)	50.8	38.1	50.8	0.5
16	C(T)	76.2	76.2	76.2	0.5
17	C(T)	101.6	101.6	101.6	0.5
18	C(T)	101.6	76.2	101.6	0.5
19	C(T)	152.4	152.4	152.4	0.5
20	C(T)	203.2	203.2	203.2	0.5
21	C(T)	254	254	254	0.5
22	Recon SE(B)	10.0076	10.0076	10.0076	1
23	SE(B)	10.0076	10.0076	10.0076	1
24	SE(B)	12.7	12.7	12.7	1
25	SE(B)	12.5	12.5	12.7	0.5
26	SE(B)	31.8	31.8	12.7	0.5
27	SE(B)	25	25	25.4	1
28	SE(B)	31.8	31.8	31.75	1
29	SE(B)	31.8	31.8	31.75	0.5
30	SE(B)	50	50	50.8	1
31	SE(B)	80	80	76.2	1
32	SE(B)	100	100	101.6	1
33	SE(B)	200	200	203.2	1
34	SE(B)	230	230	228.6	1
35	C(T)	279.4	279.4	279.4	0.5
36	C(T)	24.13	24.13	25.4	0.475059382
37	C(T)	12.7	10.16	12.7	0.5
38	C(T)	50.8	40.64	50.8	0.5
39	C(T)	101.6	81.28	101.6	0.5
40	SE(B)	10.0076	8.00608	10.0076	0.5
41	SE(B)	8.9916	8.9916	10.0076	0.5
42	RC(T)	12.7	10.16	12.7	0.5
43	C(T)	99.9998	79.99984	101.6	0.5
44	RC(T)	12.7	12.7	12.7	0.5
45	C(T)	49.9872	49.9872	50.8	0.5
46	C(T)	99.9998	99.9998	101.6	0.5
47	C(T)	75.0062	75.0062	76.2	0.5
48	C(T)	150.0124	150.0124	152.4	0.5
49	SE(B)	25.4	25.4	25.4	0.333333333

Geometry ID	Specimen Type	Full Thickness	Net Thickness	Sort Thickness	B/W
#	#	mm	mm	mm	mm/mm
50	SE(B)	15.0114	15.0114	12.7	1
51	SE(B)	13.0048	13.0048	12.7	0.25
52	C(T)	15.875	12.7	12.7	0.5
53	C(T)	19.05	15.24	19.05	0.5
54	SE(B)	25.4	20.32	25.4	0.5
55	C(T)	49.9999	39.99992	50.8	0.5
56	SE(B)	7.9502	7.9502	10.0076	0.156494523
57	SE(B)	15.875	15.875	15.875	0.3125
58	SE(B)	31.75	31.75	31.75	0.625
59	SE(B)	63.5	63.5	63.5	1.25
60	SE(B)	127	127	127	2.5
61	SE(B)	254	254	254	5
62	SE(B)	7.9502	7.9502	10.0076	0.312998842
63	SE(B)	15.875	15.875	15.875	0.625
64	SE(B)	31.75	31.75	31.75	1.25
65	SE(B)	7.9502	7.9502	10.0076	0.626017278
66	SE(B)	15.875	15.875	15.875	1.25
67	SE(B)	31.75	31.75	31.75	2.5
68	SE(B)	7.9502	7.9502	10.0076	1.252003205
69	SE(B)	15.875	15.875	15.875	2.5
70	SE(B)	31.75	31.75	31.75	5
71	SE(B)	12.7	10.16	12.7	0.5
72	SE(B)	25.4	25.4	25.4	0.5
73	SE(B)	5.0038	3.9878	5.08	0.5
74	SE(B)	25.4	22.86	25.4	1
75	SE(B)	10.0076	8.0264	10.0076	1
76	C(T)	25.4	20.32	25.4	0.625
77	C(T)	24.765	19.685	25.4	0.48756704
78	C(T)	24.13	24.13	25.4	0.5
79	SE(B)	8.0264	8.0264	10.0076	0.802030742
80	SE(B)	20	20	20	1

### Appendix D - Third Order Polynomial Fit to Strength Data for Database

Mat ID	Irrad ID	Name	RT YS	RT UTS	YS, C0	YS, C1	YS, C2	UTS, C0	UTS, C1	UTS, C2	#	Yield Data Quality
#	#	#	MPa	MPa	# (MPa, °C)	# (MPa, °C)	# (MPa, °C)	# (MPa, °C)	# (MPa, °C)	# (MPa, °C)	#	#
1	3	1.3	468.8600	620.5500	487.3329	-0.7878	0.0021	642.4844	-0.8652	0.0025	3	Generic RT data, generic fit
2	3	2.3	468.8600	620.5500	487.3329	-0.7878	0.0021	642.4844	-0.8652	0.0025	3	Generic RT data, generic fit
3	3	3.3	468.8600	620.5500	487.3329	-0.7878	0.0021	642.4844	-0.8652	0.0025	3	Generic RT data, generic fit
4	3	4.3	468.8600	620.5500	487.3329	-0.7878	0.0021	642.4844	-0.8652	0.0025	3	Generic RT data, generic fit
5	3	5.3	468.8600	620.5500	487.3329	-0.7878	0.0021	642.4844	-0.8652	0.0025	3	Generic RT data, generic fit
6	3	6.3	468.8600	620.5500	487.3329	-0.7878	0.0021	642.4844	-0.8652	0.0025	3	Generic RT data, generic fit
7	3	7.3	468.8600	620.5500	487.3329	-0.7878	0.0021	642.4844	-0.8652	0.0025	3	Generic RT data, generic fit
8	1	38.3	468.8600	620.5500	487.3329	-0.7878	0.0021	642.4844	-0.8652	0.0025	1	Fit to directly measured data
9	1	39.3	468.8600	620.5500	487.3329	-0.7878	0.0021	642.4844	-0.8652	0.0025	1	Fit to directly measured data
10	3	10.3	466.9984	621.9980	492.0000	-0.8420	0.0023	646.0000	-0.9390	0.0030	3	Generic RT data, generic fit
10	5	10.6	613.0345	751.0034	630.0001	-0.5470	0.0006	775.0004	-0.8080	0.0019	5	Guess, Should Revise
11	5	11.3	468.8600	620.5500	487.3329	-0.7878	0.0021	642.4844	-0.8652	0.0025	5	Guess, Should Revise
11	1	8811.88	613.6550	#VALUE!	637.8327	-1.0311	0.0027				1	Fit to directly measured data
11	1	8911.89	655.0250	#VALUE!	680.8327	-1.1006	0.0029				1	Fit to directly measured data
12	1	312.3	497.8190	606.0705	505.9999	-0.3808	0.0073	630.0000	-0.8969	0.0024	1	Fit to directly measured data
12	1	412.4	612.9655	714.3220	635.9999	-0.6989	0.0024	734.0003	-0.7314	0.0018	1	Fit to directly measured data
13	2	313.3	489.5450	599.1755	502.0000	-0.4541	0.0061	624.0001	-0.8999	0.0021	2	Forced thru RT data, generic fit.
13	1	513.5	655.0250	743.2810	661.0001	-0.5349	0.0009	756.0003	-0.5656	0.0007	1	Fit to directly measured data
14	1	314.3	455.0700	599.8650	472.9995	-0.7646	0.0020	621.0682	-0.8364	0.0024	1	Fit to directly measured data
15	2	315.3	468.8600	620.5500	483.3943	-0.6941	0.0017	641.0187	-1.0319	0.0007	2	Forced thru RT data, generic fit.
16	1	316.3	544.7050	696.3950	532.8002	-0.6690	0.0064	684.4433	-0.7476	0.0046	1	Fit to directly measured data
17	2	317.3	441.2800	599.8650	458.6662	-0.7415	0.0020	621.0682	-0.8364	0.0024	2	Forced thru RT data, generic fit.
19	2	319.3	406.8050	586.0750	418.1867	-0.8525	0.0031	611.6479	-1.1319	0.0033	2	Forced thru RT data, generic fit.
19	1	1219.12	646.0615	746.7285	671.5160	-1.0856	0.0029	773.1229	-1.0411	0.0030	1	Fit to directly measured data
19	2	1319.13	628.1345	717.0800	652.8827	-1.0554	0.0028	742.4264	-0.9998	0.0029	2	Forced thru RT data, generic fit.
20	1	320.3	544.7050	655.0250	554.4142	-0.7130	0.0016	673.2627	-1.0475	0.0029	1	Fit to directly measured data
20	1	1420.14	701.2215	791.5460	728.8493	-1.1782	0.0031	819.5245	-1.1036	0.0032	1	Fit to directly measured data
22	1	322.3	552.9790	640.5455	580.0000	-1.0750	0.0028	661.9999	-0.8640	0.0025	1	Fit to directly measured data
22	1	722.7	564.0110	645.0273	580.9999	-0.5250	0.0014	668.0000	-0.7410	0.0021	1	Fit to directly measured data
23	1	323.3	638.4770	721.9755	660.0001	-0.9490	0.0024	745.9999	-0.8560	0.0026	1	Fit to directly measured data
23	1	823.8	710.5298	784.0305	729.9998	-0.5890	0.0011	806.0000	-0.6990	0.0018	1	Fit to directly measured data
24	1	324.3	478.0304	594.0043	504.0000	-0.8160	0.0021	621.0000	-0.8680	0.0025	1	Fit to directly measured data
24	1	924.9	534.0178	649.0264	548.0000	-0.5290	0.0009	671.0001	-0.8370	0.0022	1	Fit to directly measured data
25	2	325.3	468.9979	598.9687	493.0000	-0.8410	0.0023	624.0001	-0.8790	0.0025	2	Forced thru RT data, generic fit.
25	3	1025.10	538.9822	649.0264	557.9999	-0.7000	0.0013	673.0001	-0.8780	0.0022	3	Generic RT data, generic fit
26	2	326.3	482.6500	634.3400	501.6662	-0.8110	0.0022	656.7618	-0.8844	0.0025	2	Forced thru RT data, generic fit.
27	2	327.3	468.8600	620.5500	487.3329	-0.7878	0.0021	642.4844	-0.8652	0.0025	2	Forced thru RT data, generic fit.
28	2	328.3	765.3450	868.7700	795.4992	-1.2860	0.0034	899.4781	-1.2113	0.0035	2	Forced thru RT data, generic fit.



Mat ID	Irrad ID	Name	RT YS	RT UTS	YS, C0	YS, C1	YS, C2	UTS, C0	UTS, C1	UTS, C2	#	Yield Data Quality
#	#	#	MPa	MPa	# (MPa, °C)	# (MPa, °C)	# (MPa, °C)	# (MPa, °C)	# (MPa, °C)	# (MPa, °C)	#	#
29		329.3	248.2200	461.9650	257.9998	-0.4171	0.0011	478.2939	-0.6441	0.0019	2	Forced thru RT data, generic fit.
30		330.3	490.2345	595.7280	509.5495	-0.8237	0.0022	616.7850	-0.8306	0.0024	2	Forced thru RT data, generic fit.
31		331.3	442.6590	561.2530	460.0995	-0.7438	0.0020	581.0914	-0.7825	0.0022	2	Forced thru RT data, generic fit.
32		332.3	481.2710	588.8330	500.2329	-0.8087	0.0022	609.6463	-0.8210	0.0024	2	Forced thru RT data, generic fit.
32	18	32.18	791.5460	#VALUE!	822.7326	-1.3300	0.0035				2	Forced thru RT data, generic fit.
33		333.3	451.6225	570.9060	469.4162	-0.7588	0.0020	591.0857	-0.7960	0.0023	2	Forced thru RT data, generic fit.
34		334.3	507.4720	595.0385	527.4661	-0.8527	0.0023	616.0712	-0.8296	0.0024	2	Forced thru RT data, generic fit.
34	17	34.17	590.2120	#VALUE!	613.4661	-0.9917	0.0026				2	Forced thru RT data, generic fit.
35		335.3	509.5405	601.2440	529.6162	-0.8562	0.0023	622.4960	-0.8383	0.0024	2	Forced thru RT data, generic fit.
36		336.3	486.0975	598.4860	505.2495	-0.8168	0.0022	619.6405	-0.8345	0.0024	2	Forced thru RT data, generic fit.
37		337.3	456.4490	570.2165	474.4329	-0.7670	0.0020	590.3717	-0.7950	0.0023	2	Forced thru RT data, generic fit.
38		338.3	439.9010	589.5225	457.2329	-0.7392	0.0020	610.3602	-0.8220	0.0024	2	Forced thru RT data, generic fit.
39		339.3	457.1385	599.1755	475.1496	-0.7681	0.0020	620.3544	-0.8354	0.0024	2	Forced thru RT data, generic fit.
40		340.3	479.2025	629.5135	498.0829	-0.8052	0.0021	651.7647	-0.8777	0.0025	2	Forced thru RT data, generic fit.
41		341.3	456.4490	564.7005	474.4329	-0.7670	0.0020	584.6608	-0.7873	0.0023	2	Forced thru RT data, generic fit.
42		342.3	476.4445	583.3170	495.2162	-0.8006	0.0021	603.9353	-0.8133	0.0023	2	Forced thru RT data, generic fit.
43		343.3	501.2665	617.1025	521.0161	-0.8423	0.0022	638.9150	-0.8604	0.0025	2	Forced thru RT data, generic fit.
44		344.3	471.6180	579.1800	490.1995	-0.7924	0.0021	599.6521	-0.8075	0.0023	2	Forced thru RT data, generic fit.
45		345.3	485.4080	592.2805	504.5329	-0.8156	0.0022	613.2157	-0.8258	0.0024	2	Forced thru RT data, generic fit.
46		346.3	441.2800	#VALUE!	458.6662	-0.7415	0.0020				2	Forced thru RT data, generic fit.
46	15	46.15	464.7230	#VALUE!	483.0329	-0.7809	0.0021				2	Forced thru RT data, generic fit.
47		347.3	370.9510	#VALUE!	385.5663	-0.6233	0.0017				2	Forced thru RT data, generic fit.
47	16	47.16	679.8470	#VALUE!	706.6326	-1.1423	0.0030				2	Forced thru RT data, generic fit.
49		349.3	415.7685	572.2850	432.1496	-0.6986	0.0019	592.5134	-0.7979	0.0023	2	Forced thru RT data, generic fit.
49	19	49.19	455.0700	604.6915	472.9995	-0.7646	0.0020	626.0653	-0.8431	0.0024	2	Forced thru RT data, generic fit.
50		350.3	489.5450	632.9610	508.8328	-0.8226	0.0022	655.3341	-0.8825	0.0025	2	Forced thru RT data, generic fit.
50	20	50.20	564.0110	691.5685	586.2328	-0.9477	0.0025	716.0132	-0.9642	0.0028	2	Forced thru RT data, generic fit.
50	21	50.21	510.9195	646.7510	531.0495	-0.8585	0.0023	669.6115	-0.9017	0.0026	2	Forced thru RT data, generic fit.
50	22	50.22	484.0290	630.8925	503.0995	-0.8133	0.0022	653.1925	-0.8796	0.0025	2	Forced thru RT data, generic fit.
50	23	50.23	516.4355	652.9565	536.7828	-0.8678	0.0023	676.0363	-0.9104	0.0026	2	Forced thru RT data, generic fit.
50	24	50.24	565.3900	703.2900	587.6661	-0.9500	0.0025	728.1490	-0.9806	0.0028	2	Forced thru RT data, generic fit.
51		351.3	442.6590	599.1755	460.0995	-0.7438	0.0020	620.3544	-0.8354	0.0024	2	Forced thru RT data, generic fit.
51	25	51.25	512.9880	650.8880	533.1995	-0.8620	0.0023	673.8947	-0.9075	0.0026	2	Forced thru RT data, generic fit.
51	26	51.26	526.0885	655.0250	546.8162	-0.8840	0.0024	678.1780	-0.9133	0.0026	2	Forced thru RT data, generic fit.
51	27	51.27	535.7415	670.1940	556.8494	-0.9002	0.0024	693.8831	-0.9344	0.0027	2	Forced thru RT data, generic fit.
52		352.3	429.5585	593.6595	446.4829	-0.7218	0.0019	614.6434	-0.8277	0.0024	2	Forced thru RT data, generic fit.
52	28	52.28	606.7600	723.9750	630.6661	-1.0195	0.0027	749.5651	-1.0094	0.0029	2	Forced thru RT data, generic fit.
53		353.3	453.6910	641.2350	471.5662	-0.7623	0.0020	663.9005	-0.8941	0.0026	2	Forced thru RT data, generic fit.
53	29	53.29	570.2165	712.2535	592.6827	-0.9581	0.0026	737.4293	-0.9931	0.0029	2	Forced thru RT data, generic fit.
53	30	53.30	600.5545	732.2490	624.2161	-1.0091	0.0027	758.1315	-1.0210	0.0029	2	Forced thru RT data, generic fit.

Mat ID	Irrad ID	Name	RT YS	RT UTS	YS, C0	YS, C1	YS, C2	UTS, C0	UTS, C1	UTS, C2	#	Yield Data Quality
#	#	#	MPa	MPa	# (MPa, °C)	# (MPa, °C)	# (MPa, °C)	# (MPa, °C)	# (MPa, °C)	# (MPa, °C)	#	#
53	31	53.31	581.2485	729.4910	604.1494	-0.9767	0.0026	755.2761	-1.0171	0.0029	2	Forced thru RT data, generic fit.
53	32	53.32	558.4950	705.3585	580.4994	-0.9384	0.0025	730.2906	-0.9835	0.0028	4	Forced thru RT data, generic fit, DATA AVAILABLE
53	33	53.33	538.4995	682.6050	559.7161	-0.9048	0.0024	706.7328	-0.9517	0.0027	4	Forced thru RT data, generic fit, DATA AVAILABLE
54	34	54.3	437.1430	606.7600	454.3662	-0.7345	0.0020	628.2069	-0.8460	0.0024	4	Forced thru RT data, generic fit, DATA AVAILABLE
54	35	54.34	526.0885	674.3310	546.8162	-0.8840	0.0024	698.1664	-0.9402	0.0027	4	Forced thru RT data, generic fit, DATA AVAILABLE
55	36	55.3	459.2070	628.1345	477.2995	-0.7716	0.0021	650.3370	-0.8758	0.0025	4	Forced thru RT data, generic fit, DATA AVAILABLE
55	37	55.35	665.3675	777.7560	691.5827	-1.1180	0.0030	805.2471	-1.0844	0.0031	4	Forced thru RT data, generic fit, DATA AVAILABLE
56	38	56.3	463.3440	625.3765	481.5995	-0.7785	0.0021	647.4815	-0.8719	0.0025	2	Forced thru RT data, generic fit.
56	39	56.36	683.9840	799.1305	710.9326	-1.1493	0.0031	827.3771	-1.1142	0.0032	2	Forced thru RT data, generic fit.
57	40	57.3	430.9375	581.2485	447.9162	-0.7241	0.0019	601.7937	-0.8104	0.0023	2	Forced thru RT data, generic fit.
57	41	57.37	549.5315	698.4635	571.1828	-0.9234	0.0025	723.1519	-0.9739	0.0028	2	Forced thru RT data, generic fit.
57	42	57.38	492.9925	640.5455	512.4162	-0.8284	0.0022	663.1867	-0.8931	0.0026	2	Forced thru RT data, generic fit.
58	43	58.3	464.0335	623.9975	482.3162	-0.7797	0.0021	646.0537	-0.8700	0.0025	3	Generic RT data, generic fit.
58	44	58.39	577.8010	721.2170	600.5661	-0.9709	0.0026	746.7096	-1.0056	0.0029	4	Forced thru RT data, generic fit, DATA AVAILABLE
58	45	58.40	586.0750	723.9750	609.1661	-0.9848	0.0026	749.5651	-1.0094	0.0029	4	Forced thru RT data, generic fit, DATA AVAILABLE
58	46	58.41	595.7280	732.9385	619.1994	-1.0010	0.0027	758.8455	-1.0219	0.0029	4	Forced thru RT data, generic fit, DATA AVAILABLE
58	47	58.42	615.0340	740.5230	639.2660	-1.0334	0.0028	766.6980	-1.0325	0.0030	4	Forced thru RT data, generic fit, DATA AVAILABLE
58	48	58.43	594.3490	736.3860	617.7660	-0.9987	0.0027	762.4148	-1.0267	0.0030	4	Forced thru RT data, generic fit, DATA AVAILABLE
58	49	58.44	579.1800	719.8380	601.9994	-0.9732	0.0026	745.2819	-1.0037	0.0029	2	Forced thru RT data, generic fit.
58	50	58.45	566.7690	713.6325	589.0994	-0.9523	0.0025	738.8570	-0.9950	0.0029	2	Forced thru RT data, generic fit.
58	51	58.46	528.8465	661.2305	549.6828	-0.8886	0.0024	684.6028	-0.9219	0.0027	2	Forced thru RT data, generic fit.
58	52	58.47	550.2210	680.5365	571.8995	-0.9245	0.0025	704.5912	-0.9489	0.0027	2	Forced thru RT data, generic fit.
58	53	58.48	553.6685	683.2945	575.4828	-0.9303	0.0025	707.4467	-0.9527	0.0027	2	Forced thru RT data, generic fit.
58	54	58.49	566.0795	695.7055	588.3828	-0.9512	0.0025	720.2964	-0.9700	0.0028	2	Forced thru RT data, generic fit.
58	55	58.50	516.4355	646.7510	536.7828	-0.8678	0.0023	669.6115	-0.9017	0.0026	2	Forced thru RT data, generic fit.
58	56	58.51	538.4995	668.1255	559.7161	-0.9048	0.0024	691.7415	-0.9316	0.0027	4	Forced thru RT data, generic fit, DATA AVAILABLE
58	57	58.52	563.3215	690.8790	585.5161	-0.9465	0.0025	715.2993	-0.9633	0.0028	4	Forced thru RT data, generic fit, DATA AVAILABLE
59	58	59.3	541.9470	679.1575	563.2994	-0.9106	0.0024	703.1635	-0.9469	0.0027	2	Forced thru RT data, generic fit.
59	59	59.53	667.4360	779.1350	693.7327	-1.1215	0.0030	806.6748	-1.0863	0.0031	2	Forced thru RT data, generic fit.
60	60	60.3	492.3030	614.3445	511.6995	-0.8272	0.0022	636.0595	-0.8566	0.0025	2	Forced thru RT data, generic fit.
60	61	60.54	602.6230	698.4635	626.3661	-1.0126	0.0027	723.1519	-0.9739	0.0028	2	Forced thru RT data, generic fit.
60	62	60.55	537.8100	632.2715	558.9995	-0.9037	0.0024	654.6202	-0.8816	0.0025	2	Forced thru RT data, generic fit.
60	63	60.56	621.9290	670.1940	646.4327	-1.0450	0.0028	693.8831	-0.9344	0.0027	3	Generic RT data, generic fit.

Mat ID	Irrad ID	Name	RT YS	RT UTS	YS, C0	YS, C1	YS, C2	UTS, C0	UTS, C1	UTS, C2	#	Yield Data Quality
#	#	#	MPa	MPa	# (MPa, °C)	# (MPa, °C)	# (MPa, °C)	# (MPa, °C)	# (MPa, °C)	# (MPa, °C)	#	#
61	361.3	455.7595	583.3170	473.7162	-0.7658	0.0020	603.9353	-0.8133	0.0023	2	Forced thru RT data, generic fit.	
61	5761.57	482.6500	620.5500	501.6662	-0.8110	0.0022	642.4844	-0.8652	0.0025	2	Forced thru RT data, generic fit.	
62	362.3	481.2710	604.0020	500.2329	-0.8087	0.0022	625.3515	-0.8421	0.0024	2	Forced thru RT data, generic fit.	
62	5862.58	668.1255	749.4865	694.4493	-1.1226	0.0030	775.9783	-1.0450	0.0030	2	Forced thru RT data, generic fit.	
62	5962.59	641.9245	734.3175	667.2160	-1.0786	0.0029	760.2732	-1.0238	0.0029	2	Forced thru RT data, generic fit.	
62	6062.60	657.0935	743.9705	682.9827	-1.1041	0.0029	770.2674	-1.0373	0.0030	2	Forced thru RT data, generic fit.	
62	6162.61	650.1985	741.2125	675.8160	-1.0925	0.0029	767.4119	-1.0335	0.0030	2	Forced thru RT data, generic fit.	
62	6262.62	658.4725	750.8655	684.4160	-1.1064	0.0030	777.4061	-1.0469	0.0030	2	Forced thru RT data, generic fit.	
62	6362.63	684.6735	766.7240	711.6493	-1.1504	0.0031	793.8251	-1.0690	0.0031	2	Forced thru RT data, generic fit.	
62	6462.64	592.2805	699.1530	615.6161	-0.9952	0.0027	723.8657	-0.9748	0.0028	2	Forced thru RT data, generic fit.	
62	6562.65	623.9975	726.0435	648.5827	-1.0485	0.0028	751.7067	-1.0123	0.0029	2	Forced thru RT data, generic fit.	
62	6662.66	659.1620	746.7285	685.1327	-1.1076	0.0030	773.1229	-1.0411	0.0030	3	Generic RT data, generic fit	
63	363.3	548.8420	637.7875	570.4661	-0.9222	0.0025	660.3312	-0.8893	0.0026	2	Forced thru RT data, generic fit.	
63	6763.67	586.0750	668.8150	609.1661	-0.9848	0.0026	692.4554	-0.9325	0.0027	2	Forced thru RT data, generic fit.	
64	364.3	564.0110	659.1620	586.2328	-0.9477	0.0025	682.4612	-0.9191	0.0026	2	Forced thru RT data, generic fit.	
64	6864.68	726.0435	799.1305	754.6493	-1.2199	0.0033	827.3771	-1.1142	0.0032	2	Forced thru RT data, generic fit.	
64	6964.69	686.0525	770.8610	713.0826	-1.1528	0.0031	798.1084	-1.0748	0.0031	2	Forced thru RT data, generic fit.	
64	7064.70	708.8060	784.6510	736.7326	-1.1910	0.0032	812.3858	-1.0940	0.0031	2	Forced thru RT data, generic fit.	
64	7164.71	666.7465	740.5230	693.0160	-1.1203	0.0030	766.6980	-1.0325	0.0030	3	Generic RT data, generic fit	
65	365.3	479.8920	592.2805	498.7995	-0.8063	0.0022	613.2157	-0.8258	0.0024	4	Forced thru RT data, generic fit, DATA AVAILABLE	
65	7265.72	517.1250	620.5500	537.4995	-0.8689	0.0023	642.4844	-0.8652	0.0025	3	Generic RT data, generic fit	
66	366.3	482.6500	664.6780	501.6662	-0.8110	0.0022	688.1722	-0.9267	0.0027	4	Forced thru RT data, generic fit, DATA AVAILABLE	
67	367.3	478.5130	619.8605	497.3662	-0.8040	0.0021	641.7705	-0.8643	0.0025	4	Forced thru RT data, generic fit, DATA AVAILABLE	
68	368.3	427.4900	565.3900	444.3329	-0.7183	0.0019	585.3747	-0.7883	0.0023	5	Guess, Should Revise	
68	7368.73	510.2300	634.3400	530.3328	-0.8573	0.0023	656.7618	-0.8844	0.0025	5	Guess, Should Revise	
69	369.3	482.6500	#VALUE!	501.6662	-0.8110	0.0022				5	Guess, Should Revise	
69	7469.74	689.5000	#VALUE!	716.6660	-1.1585	0.0031				5	Guess, Should Revise	
70	370.3	482.6500	#VALUE!	501.6662	-0.8110	0.0022				5	Guess, Should Revise	
70	7570.75	689.5000	#VALUE!	716.6660	-1.1585	0.0031				5	Guess, Should Revise	
71	371.3	482.6500	#VALUE!	501.6662	-0.8110	0.0022				5	Guess, Should Revise	
71	7671.76	689.5000	#VALUE!	716.6660	-1.1585	0.0031				5	Guess, Should Revise	
72	372.3	482.6500	#VALUE!	501.6662	-0.8110	0.0022				3	Generic RT data, generic fit	
72	7772.77	689.5000	#VALUE!	716.6660	-1.1585	0.0031				5	Guess, Should Revise	
73	373.3	344.7500	551.6000	358.3330	-0.5793	0.0015	571.0972	-0.7691	0.0022	3	Generic RT data, generic fit	
73	7873.78	448.1750	#VALUE!	465.8329	-0.7531	0.0020				3	Generic RT data, generic fit	
74	374.3	579.1800	675.7100	601.9994	-0.9732	0.0026	699.5941	-0.9421	0.0027	2	Forced thru RT data, generic fit.	
74	7974.79	772.2400	820.5050	802.6659	-1.2976	0.0035	849.5071	-1.1440	0.0033	2	Forced thru RT data, generic fit.	
75	375.3	432.3165	721.9065	449.3496	-0.7264	0.0019	747.4235	-1.0065	0.0029	2	Forced thru RT data, generic fit.	

Mat ID	Irrad ID	Name	RT YS	RT UTS	YS, C0	YS, C1	YS, C2	UTS, C0	UTS, C1	UTS, C2	#	Yield Data Quality
#	#	#	MPa	MPa	# (MPa, °C)	# (MPa, °C)	# (MPa, °C)	# (MPa, °C)	# (MPa, °C)	# (MPa, °C)	#	#
75	8075.80		792.9250	852.2220	824.1659	-1.3323	0.0036	882.3452	-1.1882	0.0034	2	Forced thru RT data, generic fit.
76	376.3		528.1570	641.2350	548.9661	-0.8874	0.0024	663.9005	-0.8941	0.0026	2	Forced thru RT data, generic fit.
76	8076.80		726.0435	779.1350	754.6493	-1.2199	0.0033	806.6748	-1.0863	0.0031	2	Forced thru RT data, generic fit.
77	377.3		575.7325	677.7785	598.4161	-0.9674	0.0026	701.7357	-0.9450	0.0027	2	Forced thru RT data, generic fit.
77	8077.80		772.2400	820.5050	802.6659	-1.2976	0.0035	849.5071	-1.1440	0.0033	2	Forced thru RT data, generic fit.
78	378.3		477.8235	608.8285	496.6495	-0.8029	0.0021	630.3486	-0.8489	0.0024	2	Forced thru RT data, generic fit.
78	8178.81		552.9790	662.6095	574.7661	-0.9292	0.0025	686.0305	-0.9239	0.0027	2	Forced thru RT data, generic fit.
78	8278.82		571.5955	673.6415	594.1161	-0.9604	0.0026	697.4525	-0.9392	0.0027	2	Forced thru RT data, generic fit.
79	379.3		496.4400	579.8695	515.9995	-0.8342	0.0022	600.3659	-0.8085	0.0023	2	Forced thru RT data, generic fit.
79	8479.84		603.3125	707.4270	627.0827	-1.0137	0.0027	732.4322	-0.9863	0.0028	2	Forced thru RT data, generic fit.
80	380.3		547.4630	633.6505	569.0328	-0.9199	0.0025	656.0480	-0.8835	0.0025	2	Forced thru RT data, generic fit.
80	8380.83		662.6095	715.7010	688.7160	-1.1134	0.0030	740.9987	-0.9979	0.0029	2	Forced thru RT data, generic fit.
81	381.3		486.0975	630.2030	505.2495	-0.8168	0.0022	652.4786	-0.8787	0.0025	2	Forced thru RT data, generic fit.
81	8581.85		531.6045	659.8515	552.5495	-0.8932	0.0024	683.1750	-0.9200	0.0026	4	Forced thru RT data, generic fit, DATA AVAILABLE
81	8681.86		588.8330	697.0845	612.0328	-0.9894	0.0026	721.7241	-0.9719	0.0028	4	Forced thru RT data, generic fit, DATA AVAILABLE
82	382.3		408.1840	567.4585	424.2663	-0.6859	0.0018	587.5163	-0.7912	0.0023	2	Forced thru RT data, generic fit.
82	8782.87		598.4860	726.7330	622.0661	-1.0056	0.0027	752.4206	-1.0133	0.0029	2	Forced thru RT data, generic fit.
83	383.3		601.2440	701.2215	624.9327	-1.0103	0.0027	726.0073	-0.9777	0.0028	2	Forced thru RT data, generic fit.
84	384.3		575.7325	686.0525	598.4161	-0.9674	0.0026	710.3022	-0.9565	0.0027	2	Forced thru RT data, generic fit.
85	385.3		601.9335	701.9110	625.6494	-1.0114	0.0027	726.7212	-0.9787	0.0028	2	Forced thru RT data, generic fit.
86	386.3		530.2255	657.7830	551.1161	-0.8909	0.0024	681.0335	-0.9171	0.0026	2	Forced thru RT data, generic fit.
87	387.3		512.2985	717.0800	532.4828	-0.8608	0.0023	742.4264	-0.9998	0.0029	2	Forced thru RT data, generic fit.
88	388.3		399.9100	550.9105	415.6663	-0.6720	0.0018	570.3834	-0.7681	0.0022	2	Forced thru RT data, generic fit.
89	389.3		479.2025	601.9335	498.0829	-0.8052	0.0021	623.2099	-0.8393	0.0024	2	Forced thru RT data, generic fit.
90	390.3		539.1890	626.0660	560.4328	-0.9060	0.0024	648.1954	-0.8729	0.0025	4	Forced thru RT data, generic fit, DATA AVAILABLE
91	391.3		453.6910	605.3810	471.5662	-0.7623	0.0020	626.7792	-0.8441	0.0024	4	Forced thru RT data, generic fit, DATA AVAILABLE
92	392.3		3219.9650	#VALUE!	3346.8301	-5.4104	0.0144				4	Forced thru RT data, generic fit, DATA AVAILABLE
93	393.3		3219.9650	#VALUE!	3346.8301	-5.4104	0.0144				2	Forced thru RT data, generic fit.
94	394.3		299.2430	575.0430	311.0330	-0.5028	0.0013	595.3689	-0.8018	0.0023	2	Forced thru RT data, generic fit.
95	395.3		489.5450	620.5500	508.8328	-0.8226	0.0022	642.4844	-0.8652	0.0025	2	Forced thru RT data, generic fit.
96	396.3		299.9325	513.6775	311.7497	-0.5040	0.0013	531.8343	-0.7162	0.0021	2	Forced thru RT data, generic fit.
97	397.3		675.7100	830.8475	702.3327	-1.1354	0.0030	860.2152	-1.1584	0.0033	2	Forced thru RT data, generic fit.
98	398.3		375.7775	524.0200	390.5830	-0.6314	0.0017	542.5424	-0.7306	0.0021	2	Forced thru RT data, generic fit.
99	399.3		403.3575	623.9975	419.2496	-0.6777	0.0018	646.0537	-0.8700	0.0025	4	Forced thru RT data, generic fit, DATA AVAILABLE
100	3100.3		359.9190	530.9150	374.0996	-0.6048	0.0016	549.6811	-0.7402	0.0021	4	Forced thru RT data, generic fit, DATA AVAILABLE
101	3101.3		268.9050	434.3850	279.4997	-0.4518	0.0012	449.7391	-0.6057	0.0017	4	Forced thru RT data, generic fit, DATA AVAILABLE

Mat ID	Irrad ID	Name	RT YS	RT UTS	YS, C0	YS, C1	YS, C2	UTS, C0	UTS, C1	UTS, C2	#	Yield Data Quality
#	#	#	MPa	MPa	# (MPa, °C)	# (MPa, °C)	# (MPa, °C)	# (MPa, °C)	# (MPa, °C)	# (MPa, °C)	#	#
102	31	102.3	386.1200	606.7600	401.3329	-0.6488	0.0017	628.2069	-0.8460	0.0024	4	Forced thru RT data, generic fit, DATA AVAILABLE
103	31	103.3	579.1800	682.6050	601.9994	-0.9732	0.0026	706.7328	-0.9517	0.0027	4	Forced thru RT data, generic fit, DATA AVAILABLE
104	31	104.3	813.6100	889.4550	845.6658	-1.3671	0.0036	920.8943	-1.2401	0.0036	4	Forced thru RT data, generic fit, DATA AVAILABLE
105	31	105.3	944.6150	985.9850	981.8324	-1.5872	0.0042	1020.8363	-1.3747	0.0040	4	Forced thru RT data, generic fit, DATA AVAILABLE
106	31	106.3	1241.1000	1303.1550	1289.9988	-2.0854	0.0056	1349.2172	-1.8170	0.0052	4	Forced thru RT data, generic fit, DATA AVAILABLE
107	31	107.3	1696.1700	1778.9100	1762.9983	-2.8500	0.0076	1841.7886	-2.4803	0.0071	4	Forced thru RT data, generic fit, DATA AVAILABLE
108	31	108.3	213.7450	#VALUE!	222.1665	-0.3591	0.0010				4	Forced thru RT data, generic fit, DATA AVAILABLE
109	31	109.3	689.5000	#VALUE!	716.6660	-1.1585	0.0031				4	Forced thru RT data, generic fit, DATA AVAILABLE
110	31	110.3	613.6550	#VALUE!	637.8327	-1.0311	0.0027				4	Forced thru RT data, generic fit, DATA AVAILABLE
111	31	111.3	1516.9000	#VALUE!	1576.6651	-2.5488	0.0068				2	Forced thru RT data, generic fit.
112	31	112.3	1599.6400	#VALUE!	1662.6651	-2.6878	0.0072				2	Forced thru RT data, generic fit.
113	31	113.3	517.1250	648.1300	537.4995	-0.8689	0.0023	671.0392	-0.9037	0.0026	2	Forced thru RT data, generic fit.
114	31	114.3	534.3625	#VALUE!	555.4161	-0.8979	0.0024				2	Forced thru RT data, generic fit.
114	9011	114.90	755.0025	#VALUE!	784.7492	-1.2686	0.0034				4	Forced thru RT data, generic fit, DATA AVAILABLE
115	31	115.3	306.8275	496.4400	318.9164	-0.5156	0.0014	513.9875	-0.6922	0.0020	2	Forced thru RT data, generic fit.
116	31	116.3	606.7600	706.7375	630.6661	-1.0195	0.0027	731.7183	-0.9854	0.0028	2	Forced thru RT data, generic fit.
117	31	117.3	464.0335	615.7235	482.3162	-0.7797	0.0021	637.4873	-0.8585	0.0025	4	Forced thru RT data, generic fit, DATA AVAILABLE
118	31	118.3	497.8190	630.8925	517.4328	-0.8365	0.0022	653.1925	-0.8796	0.0025	4	Forced thru RT data, generic fit, DATA AVAILABLE
119	31	119.3	434.3850	582.6275	451.4996	-0.7299	0.0019	603.2214	-0.8123	0.0023	4	Forced thru RT data, generic fit, DATA AVAILABLE
119	9111	119.91	513.6775	655.0250	533.9161	-0.8631	0.0023	678.1780	-0.9133	0.0026	4	Forced thru RT data, generic fit, DATA AVAILABLE
120	31	120.3	461.9650	592.9700	480.1662	-0.7762	0.0021	613.9295	-0.8268	0.0024	3	Generic RT data, generic fit.
120	9212	120.92	572.2850	686.0525	594.8328	-0.9616	0.0026	710.3022	-0.9565	0.0027	3	Generic RT data, generic fit.
121	31	121.3	337.8550	489.5450	351.1663	-0.5677	0.0015	506.8488	-0.6826	0.0020	3	Generic RT data, generic fit.
122	31	122.3	420.5950	599.8650	437.1662	-0.7067	0.0019	621.0682	-0.8364	0.0024	2	Forced thru RT data, generic fit.
123	31	123.3	448.1750	599.8650	465.8329	-0.7531	0.0020	621.0682	-0.8364	0.0024	2	Forced thru RT data, generic fit.
124	31	124.3	524.0200	655.0250	544.6661	-0.8805	0.0023	678.1780	-0.9133	0.0026	2	Forced thru RT data, generic fit.
125	31	125.3	455.0700	#VALUE!	472.9995	-0.7646	0.0020				2	Forced thru RT data, generic fit.
125	9312	125.93	696.3950	#VALUE!	723.8326	-1.1701	0.0031				2	Forced thru RT data, generic fit.
126	31	126.3	486.0975	#VALUE!	505.2495	-0.8168	0.0022				0	0
126	9412	126.94	592.9700	#VALUE!	616.3327	-0.9963	0.0027				0	0

## Appendix E - All Dataset Information

Dataset ID	Dataset	N	r	T <sub>0</sub>	ri.ni	εT <sub>0</sub>	Step 2	Step 3	Step 3 Significant	MAX Step <sub>1,2,3</sub>	SINTAP T <sub>0</sub> Final
#	#	#	#	°C	#	°C	°C	°C	#	°C	°C
1	1,3,14,,0.5,1	7	7	-54.00	0.96	7.60	-48.67	-67.64	N	-48.67	-43.37755805
2	1,3,14,,0.5,0	4	4	-4.06	0.62	9.00	-16.33	-7.31	N	-4.06	2.937169636
3	1,3,17,,0.5,1	1	1	17.46	0.13	20.10	-20.41	10.10	N	17.46	31.45789643
4	1,3,17,,0.5,0	4	1	-19.88	0.17	18.00	-53.73	-2.91	Y	-2.91	11.09328757
5	1,3,19,,0.5,1	1	1	-49.09	0.17	18.00	-83.89	-55.29	N	-49.09	-35.09453346
6	2,3,14,,0.5,1	9	5	-21.83	0.71	8.41	-26.31	-36.27	N	-21.83	-15.5663808
7	2,3,14,,0.5,0	5	5	26.45	0.73	8.41	7.88	1.81	N	26.45	32.71383174
8	2,3,17,,0.5,0	5	4	18.26	0.67	9.00	5.08	0.13	N	18.26	25.2637496
9	2,3,20,,0.5,1	1	1	-14.29	0.17	18.00	-45.37	-20.22	N	-14.29	-0.291960679
10	3,3,1,,0.5,1	9	0	-75.70	0.00	#VALUE!	-75.70	#NUM!	#NUM!	#NUM!	#NUM!
11	3,3,2,,0.5,1	4	3	-55.14	0.41	10.85	-62.65	-60.66	N	-55.14	-47.05872349
12	4,3,1,RW,0.5,1	11	0	-48.95	0.00	#VALUE!	-48.95	#NUM!	#NUM!	#NUM!	#NUM!
13	4,3,2,RW,0.5,1	2	2	-71.60	0.29	13.29	-70.88	-64.04	N	-64.04	-54.14202411
14	5,3,1,,0.5,1	5	0	-57.78	0.00	#VALUE!	-57.78	#NUM!	#NUM!	#NUM!	#NUM!
15	5,3,2,,0.5,1	1	1	-113.46	0.14	18.80	-147.59	-120.14	N	-113.46	-99.46388678
16	6,3,7,,0.5,1	4	0	-33.60	0.00	#VALUE!	-33.60	#NUM!	#NUM!	#NUM!	#NUM!
17	6,3,17,,0.5,1	3	3	-50.66	0.48	10.39	-59.32	-63.93	N	-50.66	-42.57976938
18	6,3,20,,0.5,1	1	1	-57.20	0.17	18.00	-93.87	-63.04	N	-57.20	-43.19721367
19	7,3,1,,0.5,1	7	0	-67.26	0.00	#VALUE!	-67.26	#NUM!	#NUM!	#NUM!	#NUM!
20	7,3,2,,0.5,1	3	3	-118.69	0.43	10.85	-174.92	-136.12	N	-118.69	-110.6080773
21	8,3,7,RW,0.5,1	17	0	-18.49	0.00	#VALUE!	-18.49	#NUM!	#NUM!	#NUM!	#NUM!
22	9,3,7,,0.5,1	2	0	-36.61	0.00	#VALUE!	-36.61	#NUM!	#NUM!	#NUM!	#NUM!
23	9,3,17,,0.5,1	5	5	-81.53	0.81	8.05	-87.89	-100.28	N	-81.53	-75.26445198
24	9,3,19,,0.5,1	1	1	-48.95	0.17	18.00	-84.78	-54.89	N	-48.95	-34.95440919
25	10,3,1,RW,0.5,1	28	0	-9.03	0.00	#VALUE!	-9.03	#NUM!	#NUM!	#NUM!	#NUM!
26	10,3,2,RW,0.5,1	12	12	-25.49	1.71	5.43	-38.37	-40.24	N	-25.49	-21.44873336
27	10,3,7,,0.5,1	22	15	-22.63	2.19	4.65	-25.84	-36.39	N	-22.63	-19.02012106
28	10,3,7,RW,0.5,1	13	1	-22.87	0.13	20.10	-62.82	4.19	Y	4.19	18.18506349
29	10,3,12,,0.5,1	3	0	-28.01	0.00	#VALUE!	-28.01	#NUM!	#NUM!	#NUM!	#NUM!
30	10,3,14,RW,0.5,1	3	2	-23.15	0.29	13.29	-72.46	-39.27	N	-23.15	-13.25509591
31	10,3,14,W-R,0.5,0	21	4	22.70	0.60	9.40	9.31	19.11	N	22.70	29.70076227
32	10,3,17,RW,0.5,1	4	4	-17.25	0.17	9.00	-18.80	-14.89	N	-14.89	-7.887481781
33	10,3,17,W-R,0.5,1	3	3	-26.85	0.50	10.39	-33.94	-33.32	N	-26.85	-18.76718669
34	10,3,17,W-R,0.5,0	20	20	-11.14	3.26	4.02	-9.02	-24.55	N	-9.02	-5.889403817
35	10,3,19,RW,0.5,1	5	5	-22.39	0.83	8.05	-28.65	-38.39	N	-22.39	-16.13298395
36	10,3,20,W-R,0.5,0	5	3	-6.74	0.50	10.39	-56.28	-24.23	N	-6.74	1.346430245
37	10,3,21,RW,0.5,1	4	2	-44.91	0.33	12.73	-88.22	-58.27	N	-44.91	-35.00578057
38	10,3,35,RW,0.5,1	1	0	-51.81	0.00	#VALUE!	-51.81	#NUM!	#NUM!	#NUM!	#NUM!
39	10,6,7,,0.5,1	28	21	53.58	3.48	3.93	59.61	44.40	N	59.61	62.6699891
40	11,3,1,,0.5,1	2	0	-30.81	0.00	#VALUE!	-30.81	#NUM!	#NUM!	#NUM!	#NUM!
41	11,3,7,RW,0.5,1	9	0	-0.31	0.00	#VALUE!	-0.31	#NUM!	#NUM!	#NUM!	#NUM!
42	11,3,8,,0.5,1	8	5	-31.80	0.79	8.05	-37.74	-47.76	N	-31.80	-25.53679113
43	11,3,45,,0.5,1	3	3	-29.61	0.48	10.39	-38.67	-41.19	N	-29.61	-21.53009723
44	11,88,1,,0.5,1	2	0	25.51	0.00	#VALUE!	25.51	#NUM!	#NUM!	#NUM!	#NUM!
45	11,88,8,,0.5,1	4	3	52.36	0.45	10.85	41.46	37.20	N	52.36	60.4415504
46	11,88,45,,0.5,1	3	3	33.35	0.48	10.39	26.04	26.84	N	33.35	41.43423167
47	11,89,1,,0.5,1	3	0	42.96	0.00	#VALUE!	42.96	#NUM!	#NUM!	#NUM!	#NUM!
48	11,89,8,,0.5,1	6	3	85.00	0.45	10.85	31.71	94.74	Y	94.74	102.8255638

Dataset ID	Dataset	N	r	T <sub>0</sub>	ri.ni	εT <sub>0</sub>	Step 2	Step 3	Step 3 Significant	MAX Step <sub>1, 2, 3</sub>	SINTAP T <sub>0</sub> Final
#	#	#	#	°C	#	°C	°C	°C	#	°C	°C
49	11,89,45,,0.5,1	3	3	58.48	0.48	10.39	56.81	51.02	N	58.48	66.55999876
50	12,3,7,,0.5,1	31	23	-56.69	3.65	3.75	-52.08	-45.87	N	-45.87	-42.95215517
51	12,3,14,,0.5,1	20	15	-61.63	2.40	4.65	-61.37	-62.78	N	-61.37	-57.75497923
52	12,3,17,,0.5,1	16	6	-59.61	1.00	7.35	-59.61	-46.48	Y	-46.48	-40.76012011
53	12,3,19,,0.5,1	3	0	-49.60	0.00	#VALUE!	-49.60	#NUM!	#NUM!	#NUM!	#NUM!
54	12,3,20,,0.5,1	4	0	-70.70	0.00	#VALUE!	-70.70	#NUM!	#NUM!	#NUM!	#NUM!
55	12,4,7,,0.5,1	37	12	21.31	1.88	5.20	24.39	33.19	Y	33.19	37.23124693
56	12,4,14,,0.5,1	23	6	26.57	0.98	7.35	17.59	41.66	Y	41.66	47.37406815
57	12,4,17,,0.5,1	14	8	29.18	1.33	6.36	27.81	25.28	N	29.18	34.12993138
58	13,3,7,,0.5,1	35	30	-61.07	4.58	3.29	-61.89	-89.42	N	-61.07	-58.51204543
59	13,3,14,,0.5,1	20	15	-61.92	2.40	4.65	-60.50	-75.29	N	-60.50	-56.88511593
60	13,3,17,,0.5,1	16	10	-61.54	1.67	5.69	-59.95	-71.70	N	-59.95	-55.52465834
61	13,3,19,,0.5,1	2	0	-59.36	0.00	#VALUE!	-59.36	#NUM!	#NUM!	#NUM!	#NUM!
62	13,3,20,,0.5,1	4	0	-68.31	0.00	#VALUE!	-68.31	#NUM!	#NUM!	#NUM!	#NUM!
63	13,5,7,,0.5,1	32	23	43.10	3.31	3.75	40.24	41.50	N	43.10	46.01594954
64	13,5,14,,0.5,1	23	5	28.52	0.83	8.05	32.99	59.76	Y	59.76	66.02115255
65	13,5,17,,0.5,1	11	8	34.13	1.33	6.36	29.37	20.32	N	34.13	39.08114328
66	14,3,7,,0.5,1	155	105	-103.66	17.50	1.76	-103.18	-84.21	Y	-84.21	-82.84690858
67	15,3,3,T-S,0.5,1	35	30	-95.94	3.50	3.29	-95.94	-74.14	Y	-74.14	-71.58296783
68	15,3,4,T-S,0.5,1	29	15	-100.62	2.00	4.65	-99.73	-91.27	Y	-91.27	-87.655936
69	15,3,8,T-S,0.5,1	29	10	-86.87	1.67	5.69	-91.09	-74.28	Y	-74.28	-69.8538568
70	15,3,9,T-S,0.5,1	30	8	-109.51	1.33	6.36	-110.32	-84.57	Y	-84.57	-79.616452
71	15,3,10,T-S,0.5,1	34	10	-106.08	1.67	5.69	-105.56	-96.98	Y	-96.98	-92.55027539
72	15,3,23,T-S,0.5,1	44	28	-106.98	1.17	#VALUE!	-107.15	-44.06	Y	-44.06	-41.41607753
73	15,3,27,T-S,0.5,1	70	18	-107.08	2.50	4.24	-104.26	-95.93	Y	-95.93	-92.62964894
74	15,3,30,T-S,0.5,1	61	3	-100.00	0.50	10.39	-88.70	-74.56	Y	-74.56	-66.47436631
75	15,3,32,T-S,0.5,1	30	0	-104.96	0.00	#VALUE!	-104.96	#NUM!	#NUM!	#NUM!	#NUM!
76	15,3,34,T-S,0.5,1	12	0	-104.78	0.00	#VALUE!	-104.78	#NUM!	#NUM!	#NUM!	#NUM!
77	16,3,7,C-R,0.5,1	15	10	-8.61	1.67	5.69	-3.75	5.20	Y	5.20	9.626550787
78	16,3,14,C-R,0.5,1	9	9	-30.89	1.50	6.00	-21.52	4.00	Y	4.00	8.662510735
79	16,3,17,C-R,0.5,1	5	5	0.67	0.71	8.41	-2.94	-3.70	N	0.67	6.92760073
80	17,3,5,,0.5,1	38	20	-79.80	3.33	4.02	-79.67	0.64	Y	0.64	3.769520846
81	17,3,7,,0.5,1	51	26	-82.35	4.33	3.53	-74.09	-22.53	Y	-22.53	-19.7804358
82	17,3,14,,0.5,1	26	12	-86.72	2.00	5.20	-86.72	-81.16	N	-81.16	-77.11945521
83	17,3,17,,0.5,1	6	6	-84.74	1.00	7.35	-80.76	-79.63	N	-79.63	-73.90958523
84	19,3,5,,0.5,1	12	12	-62.39	1.33	5.20	-65.69	-56.91	N	-56.91	-52.86892788
85	19,3,7,,0.5,1	31	26	-52.96	3.94	3.53	-49.50	-57.91	N	-49.50	-46.75086084
86	19,3,14,,0.5,1	12	10	-58.01	1.67	5.69	-68.06	-80.58	N	-58.01	-53.58111866
87	19,3,17,,0.5,1	2	2	-46.92	0.33	12.73	-49.91	-54.11	N	-46.92	-37.02394057
88	19,12,5,,0.5,1	11	11	28.96	1.83	5.43	35.51	24.57	N	35.51	39.7357278
89	19,12,7,,0.5,1	21	11	33.96	1.83	5.43	33.62	48.41	Y	48.41	52.63240617
90	19,12,23,,0.5,1	18	18	33.56	2.81	4.43	40.29	32.39	N	40.29	43.58913248
91	19,13,23,,0.5,1	7	7	2.49	0.00	7.11	18.52	13.94	N	18.52	23.80741251
92	20,3,5,,0.5,1	8	8	-40.57	1.17	6.65	-34.43	-26.00	Y	-26.00	-21.05090373
93	20,3,7,,0.5,1	25	19	-34.45	3.02	4.13	-34.80	-40.25	N	-34.45	-31.24107225
94	20,14,5,,0.5,1	6	6	68.66	1.00	7.35	59.26	47.19	N	68.66	74.37452077
95	20,14,12,,0.5,1	13	13	59.76	2.00	4.99	60.25	57.24	N	60.25	64.13203034
96	20,14,23,,0.5,1	9	9	45.86	1.29	6.27	30.50	25.38	N	45.86	50.52782969
97	22,3,7,,0.5,1	10	7	-90.00	1.08	6.80	-87.31	-65.05	Y	-65.05	-59.76150457
98	22,7,7,,0.5,1	15	15	-80.00	1.64	4.65	-75.59	-74.03	N	-74.03	-70.41342747

Dataset ID	Dataset	N	r	T <sub>0</sub>	ri.ni	εT <sub>0</sub>	Step 2	Step 3	Step 3 Significant	MAX Step <sub>1,2,3</sub>	SINTAP T <sub>0</sub> Final
#	#	#	#	°C	#	°C	°C	°C	#	°C	°C
99	23,3,7,,0.5,1	21	17	-12.99	2.63	4.37	-13.36	-38.77	N	-12.99	-9.592876641
100	23,8,7,,0.5,1	16	12	21.10	1.98	5.20	27.99	2.45	N	27.99	32.02991264
101	24,3,7,,0.5,1	10	6	-62.20	1.00	7.35	-62.20	-42.92	Y	-42.92	-37.1997364
102	24,9,7,,0.5,1	16	11	-38.20	1.79	5.43	-43.93	-24.19	Y	-24.19	-19.96658536
103	25,3,7,,0.5,1	7	4	-40.00	0.67	9.00	-40.40	-37.48	N	-37.48	-30.47663718
104	25,10,7,,0.5,1	15	10	-15.04	1.55	5.69	-25.36	6.81	Y	6.81	11.23301807
105	25,10,12,,0.5,1	1	1	0.71	0.17	18.00	-36.65	-3.38	N	0.71	14.71
106	26,3,5,,0.5,1	70	63	-42.47	8.37	2.27	-41.49	-49.77	N	-41.49	-39.72754165
107	26,3,6,,0.5,1	13	13	-24.66	2.17	4.99	-30.83	-46.73	N	-24.66	-20.77316691
108	26,3,7,,0.5,1	44	36	-42.64	5.81	3.00	-42.76	-71.67	N	-42.64	-40.31154488
109	26,3,11,,0.5,1	12	12	-35.46	2.00	5.20	-49.00	-56.78	N	-35.46	-31.41486662
110	26,3,14,,0.5,1	4	4	-46.32	0.67	9.00	-47.42	-53.01	N	-46.32	-39.31685055
111	26,3,15,,0.5,1	6	6	-46.96	1.00	7.35	-48.56	-63.03	N	-46.96	-41.24090786
112	26,3,17,,0.5,1	3	2	-43.83	0.31	12.73	-88.65	-57.34	N	-43.83	-33.92831798
113	26,3,18,,0.5,1	1	1	-13.69	0.17	18.00	-44.74	-19.65	N	-13.69	0.31217662
114	27,3,23,,0.5,1	34	22	-100.17	1.67	#VALUE!	-99.68	-79.98	Y	-79.98	-76.99455894
115	27,3,31,,0.5,1	69	8	-100.33	1.33	6.36	-100.06	-96.22	N	-96.22	-91.27293754
116	27,3,33,,0.5,1	16	0	-103.60	0.00	#VALUE!	-103.60	#NUM!	#NUM!	#NUM!	#NUM!
117	28,3,5,,0.5,1	55	55	-82.92	8.33	2.43	-77.66	-81.18	N	-77.66	-75.76765438
118	28,3,6,,0.5,1	8	8	-70.20	1.33	6.36	-68.11	-68.98	N	-68.11	-63.16358573
119	28,3,7,,0.5,1	28	23	-79.46	3.74	3.75	-79.46	-53.08	Y	-53.08	-50.15905634
120	28,3,11,,0.5,1	8	8	-79.55	1.33	6.36	-98.50	-92.37	N	-79.55	-74.60350603
121	28,3,14,,0.5,1	4	4	-93.54	0.67	9.00	-95.39	-107.05	N	-93.54	-86.53732118
122	28,3,15,,0.5,1	4	4	-88.89	0.67	9.00	-91.22	-100.78	N	-88.89	-81.89036103
123	28,3,16,,0.5,1	11	9	-91.47	1.50	6.00	-84.78	-91.30	N	-84.78	-80.11180573
124	28,3,17,,0.5,1	6	5	-88.40	0.83	8.05	-102.55	-81.30	N	-81.30	-75.04088046
125	29,3,24,,0.5,1	60	49	-57.94	2.62	#VALUE!	-50.86	-70.83	N	-50.86	-48.86422614
126	29,3,25,,0.5,1	58	48	-53.03	5.00	2.71	-48.77	-60.62	N	-48.77	-46.74922384
127	29,3,26,,0.5,1	4	4	-70.34	0.50	10.05	-59.95	-53.53	N	-53.53	-46.52601086
128	29,3,28,,0.5,1	28	22	-48.43	3.52	3.84	-63.23	-71.14	N	-48.43	-45.44642894
129	29,3,29,,0.5,1	26	23	-33.24	3.50	3.75	-40.35	-63.54	N	-33.24	-30.32522793
130	30,3,7,,0.5,1	7	7	-112.14	1.17	6.80	-106.75	-101.54	N	-101.54	-96.24448578
131	30,3,22,,0.5,1	7	7	-119.69	1.17	6.80	-121.36	-80.32	Y	-80.32	-75.02928052
132	30,3,23,,0.5,1	32	32	-129.93	4.24	3.32	-128.72	-133.90	N	-128.72	-126.2455357
133	31,3,7,,0.5,1	6	0	-118.28	0.00	#VALUE!	-118.28	#NUM!	#NUM!	#NUM!	#NUM!
134	31,3,22,,0.5,1	7	7	-128.10	1.00	7.11	-117.38	-110.73	N	-110.73	-105.4413151
135	31,3,23,,0.5,1	6	6	-115.70	0.86	7.68	-115.70	-127.06	N	-115.70	-109.9855446
136	32,3,23,,0.5,1	7	7	-104.79	1.00	7.11	-114.67	-113.28	N	-104.79	-99.50091199
137	32,18,22,,0.5,1	10	9	107.85	1.33	6.27	122.16	122.08	N	122.16	126.8224657
138	33,3,23,,0.5,1	6	6	-90.61	0.86	7.68	-98.24	-94.59	N	-90.61	-84.89149172
139	34,3,7,,0.5,1	9	9	-78.51	1.29	6.27	-81.91	-73.21	N	-73.21	-68.53834606
140	34,3,23,,0.5,1	10	10	-94.16	1.50	5.69	-92.26	-108.17	N	-92.26	-87.83525052
141	34,17,5,,0.5,1	4	4	-45.19	0.57	9.40	-58.69	-59.71	N	-45.19	-38.18947483
142	34,17,22,,0.5,1	6	6	-42.10	0.86	7.68	-29.10	-37.64	N	-29.10	-23.38949931
143	35,3,23,,0.5,1	9	9	-94.55	1.29	6.27	-95.50	-102.12	N	-94.55	-89.88775251
144	36,3,23,,0.5,1	7	7	-123.97	1.00	6.80	-127.08	-140.46	N	-123.97	-118.6795437
145	37,3,23,,0.5,1	9	9	-132.97	1.17	6.27	-134.30	-133.92	N	-132.97	-128.3027882
146	38,3,23,,0.5,1	6	6	-73.39	0.75	8.21	-70.80	-90.11	N	-70.80	-65.08258978
147	39,3,23,,0.5,1	8	8	-64.92	1.14	6.65	-71.35	-81.75	N	-64.92	-59.97252801
148	40,3,23,,0.5,1	8	8	-91.70	1.14	6.65	-105.30	-105.59	N	-91.70	-86.7506755



Dataset ID	Dataset	N	r	T <sub>0</sub>	ri.ni	εT <sub>0</sub>	Step 2	Step 3	Step 3 Significant	MAX Step <sub>1,2,3</sub>	SINTAP T <sub>0</sub> Final
#	#	#	#	°C	#	°C	°C	°C	#	°C	°C
149	41,3,23,,0.5,1	10	10	-120.78	1.50	5.95	-97.22	-107.73	N	-97.22	-92.79175597
150	42,3,23,,0.5,1	7	7	-78.29	0.88	7.60	-89.37	-96.92	N	-78.29	-73.00179601
151	43,3,23,,0.5,1	8	8	-95.25	1.14	6.65	-96.20	-106.73	N	-95.25	-90.30223266
152	44,3,23,,0.5,1	7	7	-138.80	0.67	7.60	-131.29	-121.37	Y	-121.37	-116.0779349
153	45,3,23,,0.5,1	9	9	-93.60	1.29	6.27	-98.20	-114.70	N	-93.60	-88.9364504
154	46,3,1,,0.5,1	6	6	-88.64	1.00	7.35	-79.93	-75.55	N	-75.55	-69.83341604
155	46,3,7,,0.5,1	6	6	-77.87	1.00	7.35	-72.23	-73.97	N	-72.23	-66.50953252
156	46,3,22,,0.5,1	8	8	-94.03	1.14	6.65	-89.62	-75.01	Y	-75.01	-70.05928593
157	46,3,23,,0.5,1	11	11	-105.03	1.29	6.06	-106.08	-112.61	N	-105.03	-100.8095023
158	46,15,1,,0.5,1	4	4	42.87	0.67	9.00	30.52	31.95	N	42.87	49.87044502
159	46,15,22,,0.5,1	9	9	47.59	1.29	6.27	44.11	29.46	N	47.59	52.25794441
160	47,3,5,,0.5,1	7	7	-88.51	1.00	7.11	-92.31	-86.23	N	-86.23	-80.93919713
161	47,3,22,,0.5,1	7	7	-102.66	1.00	7.11	-103.67	-108.96	N	-102.66	-97.37211515
162	47,3,23,,0.5,1	8	8	-99.56	1.14	6.65	-99.08	-114.37	N	-99.08	-94.1280732
163	47,16,1,,0.5,1	2	2	91.62	0.29	13.29	90.70	88.19	N	91.62	101.5191089
164	47,16,22,,0.5,1	12	12	60.78	1.71	5.43	61.92	57.12	N	61.92	65.96381647
165	49,3,7,,0.5,1	6	5	-52.13	0.79	8.05	-52.13	-42.62	Y	-42.62	-36.35562248
166	49,19,36,,0.5,1	4	3	20.71	0.46	10.39	29.73	79.40	Y	79.40	87.47939381
167	50,3,5,,0.5,1	12	10	-59.76	1.58	5.69	-69.99	-76.51	N	-59.76	-55.33709404
168	50,20,5,,0.5,1	7	6	-13.46	0.93	7.35	-22.24	-26.54	N	-13.46	-7.741913014
169	50,21,5,,0.5,1	6	6	-35.98	0.77	7.35	-30.54	-42.23	N	-30.54	-24.82893594
170	50,22,5,,0.5,1	5	4	-58.88	0.64	9.00	-49.01	-55.16	N	-49.01	-42.0130292
171	50,23,5,,0.5,1	8	6	-32.54	0.93	7.35	-41.83	-49.38	N	-32.54	-26.8285226
172	50,24,5,,0.5,1	5	4	5.06	0.60	9.00	11.42	2.99	N	11.42	18.41803207
173	51,3,7,,0.5,1	6	5	-32.57	0.77	8.05	-40.54	-49.44	N	-32.57	-26.30616128
174	51,25,7,,0.5,1	4	4	26.35	0.64	9.00	23.70	13.94	N	26.35	33.35055543
175	51,26,36,,0.5,1	5	5	45.75	0.79	8.05	41.81	47.54	N	47.54	53.798342
176	51,27,36,,0.5,1	4	4	49.16	0.67	9.00	36.52	34.69	N	49.16	56.16457131
177	52,3,7,,0.5,1	10	5	-43.00	0.83	8.05	-49.18	#NUM!	#NUM!	#NUM!	#NUM!
178	52,28,36,,0.5,1	5	5	63.23	0.83	8.05	79.39	110.36	Y	110.36	116.6171819
179	53,3,5,,0.5,1	10	8	-9.34	1.04	6.65	-11.30	-19.32	N	-9.34	-4.389764317
180	53,3,7,,0.5,1	4	3	-19.65	0.48	10.39	-25.74	-21.72	N	-19.65	-11.56471334
181	53,3,12,,0.5,1	4	3	-10.46	0.48	10.39	-57.20	-28.90	N	-10.46	-2.378802008
182	53,29,5,,0.5,1	4	3	52.70	0.46	10.39	55.99	67.09	Y	67.09	75.17598253
183	53,29,7,,0.5,1	3	2	66.02	0.31	12.73	65.36	63.28	N	66.02	75.91692109
184	53,30,5,,0.5,1	5	3	94.30	0.29	10.85	88.95	100.76	N	100.76	108.8468309
185	53,30,7,,0.5,1	3	2	81.74	0.31	12.73	86.27	90.09	N	90.09	99.98628578
186	53,31,5,,0.5,1	4	2	78.32	0.31	12.73	37.00	103.00	Y	103.00	112.9044003
187	53,31,7,,0.5,1	3	2	50.00	0.33	12.73	47.85	69.19	Y	69.19	79.08790983
188	53,32,5,,0.5,1	6	4	50.27	0.64	9.00	-6.56	57.06	N	57.06	64.05676129
189	53,32,7,,0.5,1	3	3	35.78	0.46	10.39	30.20	42.80	N	42.80	50.88576546
190	53,33,5,,0.5,1	6	4	36.07	0.63	9.00	33.65	31.76	N	36.07	43.07168465
191	53,33,7,,0.5,1	3	2	39.03	0.33	12.73	38.64	37.53	N	39.03	48.9326718
192	54,3,5,,0.5,1	15	12	-23.46	1.60	5.20	-31.11	33.35	Y	33.35	37.38897521
193	54,34,5,,0.5,1	12	8	60.57	1.24	6.36	59.57	99.35	Y	99.35	104.3035414
194	55,3,5,,0.5,1	14	11	-28.20	1.43	5.43	-32.57	-31.83	N	-28.20	-23.9779114
195	55,35,5,,0.5,1	12	8	122.54	1.27	6.36	115.84	122.47	N	122.54	127.4854168
196	56,3,5,,0.5,1	15	9	-12.78	1.41	6.00	-21.07	-24.75	N	-12.78	-8.112238896
197	56,36,5,,0.5,1	12	8	143.40	1.18	6.65	129.20	124.68	N	143.40	148.3452774
198	57,3,5,,0.5,1	9	7	-65.54	0.77	6.80	-65.54	-84.30	N	-65.54	-60.25341947

Dataset ID	Dataset	N	r	T <sub>0</sub>	ri.ni	εT <sub>0</sub>	Step 2	Step 3	Step 3 Significant	MAX Step <sub>1,2,3</sub>	SINTAP T <sub>0</sub> Final
#	#	#	#	°C	#	°C	°C	°C	#	°C	°C
199	57,37,5,,0.5,1	9	6	18.86	0.93	7.35	26.96	40.60	Y	40.60	46.31412574
200	57,38,5,,0.5,1	10	6	-35.83	0.93	7.35	-30.10	-3.43	Y	-3.43	2.286859019
201	58,3,5,,0.5,1	22	19	-47.94	2.65	4.13	-47.24	-21.58	Y	-21.58	-18.36560872
202	58,3,7,L-T,0.5,1	3	3	-34.01	0.46	10.39	-41.95	-37.64	N	-34.01	-25.92788312
203	58,3,7,T-L,0.5,1	5	4	-34.12	0.60	9.00	-37.88	-51.47	N	-34.12	-27.12449571
204	58,3,12,,0.5,1	3	3	-33.93	0.46	10.39	-41.87	-37.64	N	-33.93	-25.84507725
205	58,3,37,,0.5,1	1	1	-32.23	0.17	18.00	-62.78	-37.65	N	-32.23	-18.23457764
206	58,39,36,T-L,0.5,1	2	0	110.10	0.00	#VALUE!	110.10	#NUM!	#NUM!	#NUM!	#NUM!
207	58,40,36,L-T,0.5,1	4	4	61.79	0.62	9.00	47.70	47.85	N	61.79	68.78513305
208	58,41,5,,0.5,1	10	6	56.70	0.95	7.35	55.01	66.68	Y	66.68	72.39845056
209	58,41,7,,0.5,1	4	3	58.36	0.48	10.39	49.12	43.44	N	58.36	66.43900979
210	58,42,5,,0.5,1	7	5	78.06	0.72	8.41	60.66	83.00	N	83.00	89.26283141
211	58,42,7,,0.5,1	3	2	84.90	0.29	13.29	41.03	96.41	Y	96.41	106.3070192
212	58,43,5,,0.5,1	8	5	60.08	0.76	8.41	55.96	96.85	Y	96.85	103.1114925
213	58,43,7,,0.5,1	5	4	51.01	0.64	9.00	37.35	36.44	N	51.01	58.00722248
214	58,44,5,,0.5,1	9	6	43.58	0.91	7.35	42.54	31.09	N	43.58	49.29664016
215	58,44,7,,0.5,1	5	4	48.73	0.60	9.40	45.97	39.56	N	48.73	55.72740237
216	58,45,5,,0.5,1	10	8	28.77	1.27	6.36	23.72	11.77	N	28.77	33.71849962
217	58,45,7,,0.5,1	5	3	33.87	0.33	10.39	-18.39	32.50	N	33.87	41.95622779
218	58,46,37,,0.5,1	8	6	32.77	0.95	7.35	23.51	15.32	N	32.77	38.48359457
219	58,47,5,,0.5,1	8	7	26.29	1.10	6.80	29.75	36.37	N	36.37	41.66517821
220	58,48,5,,0.5,1	7	4	55.57	0.60	9.40	-4.02	145.01	Y	145.01	152.0051741
221	58,49,5,,0.5,1	7	5	44.73	0.77	8.05	49.14	42.34	N	49.14	55.40288782
222	58,50,5,,0.5,1	8	6	8.43	0.98	7.35	7.72	6.74	N	8.43	14.1473448
223	58,51,5,,0.5,1	7	6	28.49	0.87	7.35	22.17	135.70	Y	135.70	141.4204123
224	58,51,37,,0.5,1	1	1	20.65	0.17	18.00	-15.20	16.23	N	20.65	34.65414328
225	58,52,5,,0.5,1	6	4	70.88	0.54	9.40	56.92	55.23	N	70.88	77.88348633
226	59,3,5,,0.5,1	15	12	-7.32	1.91	5.20	-5.58	-12.54	N	-5.58	-1.536880317
227	59,53,5,,0.5,1	11	7	85.04	1.08	6.80	76.81	85.45	N	85.45	90.74083209
228	60,3,7,,0.5,1	5	5	-54.71	0.79	8.05	-52.86	-67.68	N	-52.86	-46.60081084
229	60,54,36,,0.5,1	6	5	58.58	0.79	8.05	68.13	84.09	Y	84.09	90.3542777
230	60,55,36,,0.5,1	4	4	-6.23	0.60	9.00	-6.23	-1.38	N	-1.38	5.621832508
231	60,56,36,,0.5,1	5	4	69.47	0.60	9.00	89.62	88.54	N	89.62	96.6177464
232	61,3,7,,0.5,1	6	5	-53.83	0.77	8.05	-56.08	-41.37	Y	-41.37	-35.11073416
233	61,57,36,,0.5,1	5	4	36.47	0.64	9.00	40.10	40.93	N	40.93	47.92913314
234	62,3,5,,0.5,1	9	6	-33.07	0.91	7.35	-39.31	-39.11	N	-33.07	-27.35806455
235	62,58,5,,0.5,1	7	5	82.90	0.76	8.05	83.80	98.98	Y	98.98	105.2368202
236	62,59,5,,0.5,1	8	4	67.35	0.60	9.40	53.50	51.28	N	67.35	74.34906604
237	62,60,5,,0.5,1	6	4	29.91	0.62	9.00	32.42	61.09	Y	61.09	68.08934406
238	62,61,5,,0.5,1	8	5	94.55	0.72	8.41	77.14	73.90	N	94.55	100.8146463
239	62,62,5,,0.5,1	7	4	89.22	0.58	9.40	97.67	83.95	N	97.67	104.6687717
240	62,63,5,,0.5,1	7	5	84.81	0.72	8.05	95.27	105.38	Y	105.38	111.64101
241	62,64,5,,0.5,1	9	6	35.55	0.89	7.35	56.20	40.29	N	56.20	61.91872366
242	62,65,5,,0.5,1	8	5	70.91	0.72	8.41	64.70	67.62	N	70.91	77.16768174
243	62,66,5,,0.5,1	8	4	90.74	0.56	9.40	83.70	126.00	Y	126.00	132.9964494
244	63,3,7,,0.5,1	5	4	-77.82	0.64	9.00	-88.64	-57.11	Y	-57.11	-50.10540278
245	63,67,36,,0.5,1	7	7	14.91	0.95	6.80	14.38	6.57	N	14.91	20.19696074
246	64,3,5,,0.5,1	7	6	-75.96	0.64	7.68	-75.74	-36.33	Y	-36.33	-30.61888874
247	64,68,5,,0.5,1	8	5	44.64	0.79	8.05	45.09	32.26	N	45.09	51.34670152
248	64,69,5,,0.5,1	8	6	23.31	0.95	7.35	23.31	26.04	N	26.04	31.75456921

Dataset ID	Dataset	N	r	T <sub>0</sub>	ri.ni	εT <sub>0</sub>	Step 2	Step 3	Step 3 Significant	MAX Step <sub>1,2,3</sub>	SINTAP T <sub>0</sub> Final
#	#	#	#	°C	#	°C	°C	°C	#	°C	°C
249	64,70,5,,0.5,1	6	5	11.86	0.79	8.05	9.65	21.71	Y	21.71	27.97494304
250	64,71,5,,0.5,1	7	5	13.32	0.81	8.05	-3.31	-4.91	N	13.32	19.57889876
251	65,3,7,,0.5,1	8	4	-66.90	0.64	9.00	-79.58	63.95	Y	63.95	70.95314193
252	65,72,36,,0.5,1	4	3	17.81	0.48	10.39	21.67	6.72	N	21.67	29.75782983
253	66,3,5,,0.5,1	6	6	7.83	1.00	7.35	10.77	-2.62	N	10.77	16.48830293
254	66,3,7,,0.5,1	6	6	8.55	1.00	7.35	-0.19	-11.71	N	8.55	14.26089971
255	66,3,12,,0.5,1	47	47	17.05	6.65	2.74	13.33	-24.66	N	17.05	19.09510567
256	66,3,23,,0.5,1	13	10	-5.08	1.00	6.36	-9.82	55.00	Y	55.00	59.42284232
257	66,3,37,,0.5,1	45	45	11.81	6.83	2.68	10.22	-4.17	N	11.81	13.89337664
258	66,3,38,,0.5,1	11	11	0.00	1.79	5.43	-11.26	-20.11	N	0.00	4.221158824
259	66,3,39,,0.5,1	3	3	0.71	0.50	10.39	-7.99	-12.40	N	0.71	8.792903769
260	66,3,40,,0.5,1	33	30	-8.75	3.26	3.43	-12.04	7.49	Y	7.49	10.04908435
261	67,3,5,,0.5,1	24	24	-93.80	3.83	3.67	-91.78	-108.46	N	-91.78	-88.92346757
262	67,3,23,,0.5,1	22	22	-97.71	2.50	4.01	-103.17	-81.36	Y	-81.36	-78.37541299
263	67,3,23,L-T,0.5,1	16	16	-115.42	2.33	4.50	-118.37	-82.86	Y	-82.86	-79.36438864
264	67,3,23,S-T,0.5,1	6	6	-116.90	0.83	7.68	-120.45	-126.02	N	-116.90	-111.1856619
265	67,3,23,T-L,0.5,1	12	12	-115.15	1.33	5.43	-116.43	-116.39	N	-115.15	-111.1066255
266	67,3,41,,0.5,1	17	17	-100.53	1.83	4.56	-98.36	-110.49	N	-98.36	-94.96676904
267	67,3,41,L-T,0.5,1	2	2	-137.02	0.17	13.29	-130.30	-125.22	N	-125.22	-115.3248159
268	67,3,41,S-T,0.5,1	2	2	-128.89	0.33	12.73	-132.87	-138.40	N	-128.89	-118.9951485
269	67,3,41,T-L,0.5,1	2	2	-117.70	0.33	12.73	-160.37	-129.53	N	-117.70	-107.8008493
270	68,3,9,L-T,0.5,1	4	2	-96.58	0.33	12.73	-97.54	-99.48	N	-96.58	-86.67874637
271	68,3,40,L-T,0.5,1	18	16	-110.10	1.33	4.70	-117.54	-112.16	N	-110.10	-106.5956124
272	68,3,42,L-T,0.5,1	19	8	-114.10	1.17	6.36	-108.34	-69.29	Y	-69.29	-64.34520761
273	68,3,43,L-T,0.5,1	4	0	-95.49	0.00	#VALUE!	-95.49	#NUM!	#NUM!	#NUM!	#NUM!
274	68,73,40,L-T,0.5,1	22	22	-22.90	2.95	3.84	-13.55	13.18	Y	13.18	16.16467121
275	68,73,42,L-T,0.5,1	26	26	-5.28	3.71	3.53	-3.65	9.99	Y	9.99	12.73656813
276	69,3,7,,0.5,1	6	3	-101.22	0.33	10.39	-94.64	-46.76	Y	-46.76	-38.68100491
277	69,3,7,,0.5,0	7	4	-45.38	0.67	9.00	-45.38	-26.09	Y	-26.09	-19.09041684
278	69,3,14,,0.5,1	6	2	-111.19	0.29	12.73	-102.60	-53.97	Y	-53.97	-44.07344711
279	69,3,14,,0.5,0	7	4	-55.14	0.63	9.00	-43.39	-52.77	N	-43.39	-36.38841124
280	69,3,20,,0.5,1	3	1	-100.89	0.17	18.00	-131.31	-70.18	Y	-70.18	-56.17833882
281	69,3,44,,0.5,1	10	6	-70.53	0.79	7.35	-71.23	-51.65	Y	-51.65	-45.93688368
282	69,3,44,,0.5,0	9	6	-25.04	0.81	7.35	-26.54	-26.44	N	-25.04	-19.31972776
283	69,74,44,,0.5,1	11	8	-39.22	1.29	6.36	-29.36	-36.71	N	-29.36	-24.40730897
284	69,74,44,,0.5,0	12	9	-12.30	1.35	6.00	-7.47	10.26	Y	10.26	14.92827604
285	70,3,7,,0.5,1	7	2	-82.40	0.31	12.73	-123.27	-25.05	Y	-25.05	-15.14641909
286	70,3,7,,0.5,0	7	4	-39.74	0.64	9.00	-40.13	15.92	Y	15.92	22.91716888
287	70,3,14,,0.5,1	7	2	-75.28	0.14	12.73	-71.59	-21.85	Y	-21.85	-11.94628115
288	70,3,14,,0.5,0	6	0	-131.22	0.00	#VALUE!	-131.22	#NUM!	#NUM!	#NUM!	#NUM!
289	70,3,44,,0.5,1	12	5	-67.79	0.79	8.05	-72.14	58.35	Y	58.35	64.61387036
290	70,3,44,,0.5,0	12	8	-35.01	1.12	6.36	-38.23	-10.82	Y	-10.82	-5.867196168
291	70,75,44,,0.5,1	10	7	81.97	1.12	6.80	85.11	95.47	Y	95.47	100.763463
292	70,75,44,,0.5,0	11	7	102.51	1.12	6.80	106.47	110.38	N	110.38	115.6759257
293	71,3,7,,0.5,1	7	4	-59.48	0.63	9.00	-62.74	-38.27	Y	-38.27	-31.26627376
294	71,3,7,,0.5,0	6	3	-33.66	0.48	10.39	-40.04	-13.65	Y	-13.65	-5.563872047
295	71,3,14,,0.5,1	7	4	-60.09	0.63	9.00	-72.63	95.21	Y	95.21	102.2132534
296	71,3,14,,0.5,0	6	3	-42.57	0.48	10.39	-45.05	-40.68	N	-40.68	-32.59838752
297	71,3,20,,0.5,1	3	1	-89.26	0.17	18.00	-128.78	-71.39	Y	-71.39	-57.39019348
298	71,3,44,,0.5,1	10	4	-45.34	0.67	9.00	-41.21	92.08	Y	92.08	99.08463275

Dataset ID	Dataset	N	r	T <sub>0</sub>	ri.ni	εT <sub>0</sub>	Step 2	Step 3	Step 3 Significant	MAX Step <sub>1,2,3</sub>	SINTAP T <sub>0</sub> Final
#	#	#	#	°C	#	°C	°C	°C	#	°C	°C
299	71,3,44,,0.5,0	9	6	-18.08	0.63	8.21	-20.73	-29.82	N	-18.08	-12.36540089
300	71,76,44,,0.5,1	13	8	19.25	1.20	6.36	12.15	28.07	Y	28.07	33.02046427
301	71,76,44,,0.5,0	12	8	47.46	1.20	6.36	46.13	49.13	N	49.13	54.07632049
302	72,3,7,,0.5,1	6	2	-48.97	0.33	12.73	-52.47	#NUM!	#NUM!	#NUM!	#NUM!
303	72,3,7,,0.5,0	5	4	-12.84	0.64	9.00	-14.07	-23.61	N	-12.84	-5.843217454
304	72,3,14,,0.5,1	7	3	-48.99	0.50	10.39	-57.02	-33.19	Y	-33.19	-25.10435859
305	72,3,14,,0.5,0	6	3	-26.13	0.48	10.39	-16.93	-30.02	N	-16.93	-8.850805008
306	72,3,44,,0.5,1	11	7	-36.72	0.50	7.11	-40.74	-15.66	Y	-15.66	-10.36394706
307	72,3,44,,0.5,0	11	8	-10.93	0.92	6.65	-14.26	-27.09	N	-10.93	-5.979801487
308	72,77,44,,0.5,1	10	5	111.96	0.42	8.41	108.12	#NUM!	#NUM!	#NUM!	#NUM!
309	72,77,44,,0.5,0	11	5	173.90	0.79	8.05	175.66	177.93	N	177.93	184.189846
310	73,3,37,,0.5,1	7	6	-91.91	0.75	7.35	-88.62	-87.12	N	-87.12	-81.39994502
311	73,78,37,,0.5,1	6	5	-23.55	0.60	8.41	-38.97	-29.97	N	-23.55	-17.2863373
312	74,3,37,,0.5,1	11	10	-131.91	1.37	5.69	-130.70	-125.27	N	-125.27	-120.8406636
313	74,79,37,,0.5,1	12	8	-100.48	1.29	6.36	-105.36	-101.36	N	-100.48	-95.52646399
314	75,3,40,,0.5,1	11	10	-155.71	1.20	5.95	-148.20	-161.06	N	-148.20	-143.7680355
315	75,80,40,,0.5,1	7	6	-87.07	0.98	7.35	-60.71	-68.32	N	-60.71	-54.99041761
316	76,3,40,,0.5,1	11	9	-151.19	1.23	6.00	-152.70	-144.14	N	-144.14	-139.4745495
317	76,80,40,,0.5,1	11	7	-109.65	1.14	6.80	-109.65	-72.59	Y	-72.59	-67.30212001
318	77,3,40,,0.5,1	11	9	-149.11	1.20	6.00	-152.45	-150.76	N	-149.11	-144.4405358
319	77,80,40,,0.5,1	9	6	-118.56	0.76	7.68	-113.84	-97.55	Y	-97.55	-91.83490363
320	78,3,23,,0.5,1	9	8	-70.01	0.62	#VALUE!	-75.19	-78.58	N	-70.01	-65.05718821
321	78,81,23,,0.5,1	7	7	-31.99	0.62	#VALUE!	-36.34	-41.65	N	-31.99	-26.69694016
322	78,82,23,,0.5,1	9	9	-13.49	0.87	#VALUE!	-16.02	-15.55	N	-13.49	-8.823537243
323	79,3,23,,0.5,1	4	4	-93.74	0.33	#VALUE!	-94.68	-105.87	N	-93.74	-86.74279894
324	79,84,23,,0.5,1	6	6	-77.09	0.62	#VALUE!	-76.32	-84.44	N	-76.32	-70.60655457
325	80,3,23,,0.5,1	8	8	-61.23	0.79	7.11	-61.23	-61.75	N	-61.23	-56.28213507
326	80,83,23,,0.5,1	8	7	-8.36	1.12	6.80	-6.22	-16.26	N	-6.22	-0.924796982
327	81,3,23,,0.5,1	9	9	-60.68	0.62	#VALUE!	-67.62	-49.37	Y	-49.37	-44.69870068
328	81,85,23,,0.5,1	8	8	-38.40	0.62	#VALUE!	-24.55	-32.19	N	-24.55	-19.59529215
329	81,86,23,,0.5,1	9	9	-11.05	1.20	6.27	-6.46	42.12	Y	42.12	46.78540952
330	82,3,40,,0.5,1	20	20	-42.66	3.00	4.02	-47.03	-54.85	N	-42.66	-39.53388091
331	82,87,40,,0.5,1	14	14	71.09	2.00	5.02	79.03	78.68	N	79.03	82.77043793
332	91,3,5,,0.5,1	32	32	-45.66	4.83	3.18	-40.96	-47.97	N	-40.96	-38.48785915
333	91,3,7,,0.5,1	7	0	-59.05	0.00	#VALUE!	-59.05	#NUM!	#NUM!	#NUM!	#NUM!
334	91,3,12,T-L,0.5,1	18	12	-55.93	2.00	5.20	-64.57	-83.58	N	-55.93	-51.88632589
335	91,3,17,L-T,0.5,0	11	4	-27.42	0.67	9.00	-38.52	-36.52	N	-27.42	-20.42181551
336	91,3,23,,0.5,1	7	7	-75.40	0.83	7.11	-70.91	-39.35	Y	-39.35	-34.06035171
337	91,3,38,L-T,0.5,0	8	8	-8.14	1.33	6.36	-12.82	-17.27	N	-8.14	-3.186571019
338	91,3,75,,0.5,1	16	16	-46.11	1.63	#VALUE!	-22.05	-14.98	N	-14.98	-11.48419565
339	92,3,3,,0.5,1	208	136	-90.00	21.36	1.54	-81.02	8.92	Y	8.92	10.11796134
340	92,3,3,Ductile,0.5,1	51	0	-140.91	0.00	#VALUE!	-140.91	#NUM!	#NUM!	#NUM!	#NUM!
341	92,3,8,,0.5,1	183	100	-88.54	16.67	1.80	-86.65	-62.92	Y	-62.92	-61.51780193
342	92,3,8,Ductile,0.5,1	42	0	-113.15	0.00	#VALUE!	-113.15	#NUM!	#NUM!	#NUM!	#NUM!
343	92,3,45,,0.5,1	167	36	-92.80	6.00	3.00	-92.16	-73.39	Y	-73.39	-71.06095902
344	92,3,45,Ductile,0.5,1	21	0	-119.62	0.00	#VALUE!	-119.62	#NUM!	#NUM!	#NUM!	#NUM!
345	92,3,46,,0.5,1	58	15	-93.84	2.50	4.65	-95.53	-89.54	N	-89.54	-85.92480379
346	92,3,46,Ductile,0.5,1	3	0	-137.74	0.00	#VALUE!	-137.74	#NUM!	#NUM!	#NUM!	#NUM!
347	92,3,55,,0.5,1	20	0	-99.05	0.00	#VALUE!	-99.05	#NUM!	#NUM!	#NUM!	#NUM!
348	93,3,3,,0.5,1	11	11	-106.35	1.83	5.43	-88.35	-83.74	N	-83.74	-79.51702735

Dataset ID	Dataset	N	r	T <sub>0</sub>	ri.ni	εT <sub>0</sub>	Step 2	Step 3	Step 3 Significant	MAX Step <sub>1, 2, 3</sub>	SINTAP T <sub>0</sub> Final
#	#	#	#	°C	#	°C	°C	°C	#	°C	°C
349	93,3,3,Ductile,0.5,1	1	0	-129.49	0.00	#VALUE!	-129.49	#NUM!	#NUM!	#NUM!	#NUM!
350	93,3,45,,0.5,1	24	24	-109.56	0.00	3.67	-106.29	-99.22	N	-99.22	-96.36120666
351	94,3,23,,0.5,1	38	32	-17.10	3.57	3.55	-16.42	27.50	Y	27.50	29.97024992
352	94,3,23,L-S,0.5,1	19	13	-20.80	1.57	5.21	-20.61	56.88	Y	56.88	60.76225256
353	94,3,23,L-S,0.5,0	77	41	55.74	4.58	3.14	83.89	88.44	N	88.44	90.62221272
354	94,3,78,,0.5,1	24	12	-12.68	1.71	5.43	-13.24	8.50	Y	8.50	12.54026109
355	95,3,7,,0.5,1	9	8	-112.49	1.29	6.36	-112.49	-119.81	N	-112.49	-107.5370739
356	95,3,7,,0.5,0	31	18	-23.65	2.80	4.24	53.33	58.92	N	58.92	62.2185071
357	96,3,8,L-T,0.5,1	5	4	-32.22	0.60	9.00	-23.37	-23.68	N	-23.37	-16.36733195
358	96,3,8,L-T,0.5,0	5	4	50.05	0.60	9.40	48.46	34.99	N	50.05	57.04759209
359	97,3,8,C-R,0.5,1	5	3	-134.80	0.48	10.39	-189.89	-135.50	N	-134.80	-126.7147787
360	97,3,8,C-R,0.5,0	5	4	-87.22	0.64	9.00	-100.60	-92.70	N	-87.22	-80.22261235
361	97,3,47,C-R,0.5,1	2	2	-122.79	0.33	12.73	-165.11	-135.88	N	-122.79	-112.8903297
362	97,3,48,C-R,0.5,1	1	0	-119.53	0.00	#VALUE!	-119.53	#NUM!	#NUM!	#NUM!	#NUM!
363	98,3,8,,0.5,1	7	5	-19.33	0.79	8.05	-35.38	-36.99	N	-19.33	-13.06748389
364	98,3,8,,0.5,0	7	4	28.77	0.60	9.40	14.60	11.25	N	28.77	35.76972273
365	98,3,46,,0.5,1	6	6	-23.85	0.98	7.35	-43.29	-45.22	N	-23.85	-18.13709534
366	99,3,8,L-T,0.5,1	2	2	-126.07	0.33	12.73	-119.89	-112.93	N	-112.93	-103.0336256
367	99,3,8,L-T,0.5,0	5	5	-81.43	0.81	8.05	-83.53	-68.88	Y	-68.88	-62.62054569
368	99,3,46,L-T,0.5,1	7	7	-120.51	0.96	6.80	-117.92	-127.79	N	-117.92	-112.6317681
369	100,3,8,T-L,0.5,1	4	3	-112.51	0.43	10.85	-113.52	-81.13	Y	-81.13	-73.04779167
370	100,3,8,T-L,0.5,0	7	6	-60.28	0.79	7.35	-62.81	-76.26	N	-60.28	-54.56552393
371	101,3,49,,0.5,0	15	0	51.65	0.00	#VALUE!	51.65	#NUM!	#NUM!	#NUM!	#NUM!
372	101,3,49,,0.5,1	6	0	-49.69	0.00	#VALUE!	-49.69	#NUM!	#NUM!	#NUM!	#NUM!
373	102,3,49,,0.5,0	21	4	11.57	0.60	9.40	0.12	#NUM!	#NUM!	#NUM!	#NUM!
374	102,3,49,,0.5,1	9	0	-16.15	0.00	#VALUE!	-16.15	#NUM!	#NUM!	#NUM!	#NUM!
375	103,3,49,,0.5,0	12	4	-64.62	0.52	10.05	-56.31	#NUM!	#NUM!	#NUM!	#NUM!
376	103,3,49,,0.5,1	2	0	332.20	0.00	#VALUE!	332.20	#NUM!	#NUM!	#NUM!	#NUM!
377	104,3,49,,0.5,0	23	13	-27.67	1.83	5.21	-22.26	-26.68	N	-22.26	-18.37670902
378	104,3,49,,0.5,1	21	10	-56.53	1.36	5.95	-74.45	-79.99	N	-56.53	-52.10739924
379	105,3,49,,0.5,0	7	5	-112.97	0.77	8.05	-117.03	-116.43	N	-112.97	-106.7058322
380	105,3,49,,0.5,1	6	4	-141.80	0.64	9.00	-153.30	-128.51	Y	-128.51	-121.5081284
381	107,3,49,,0.5,1	17	5	-30.24	0.74	8.05	-31.29	-1.46	Y	-1.46	4.797533926
382	113,3,45,,0.5,0	44	44	-56.11	6.98	2.71	-55.05	-55.49	N	-55.05	-52.94399677
383	114,3,23,T-L,0.5,0	12	9	35.26	0.79	#VALUE!	39.14	53.16	Y	53.16	57.82731173
384	114,90,23,T-L,0.5,0	13	11	149.44	1.01	#VALUE!	156.79	172.79	Y	172.79	177.0158274
385	115,3,50,L-T,0.5,0	80	42	-62.85	5.70	2.78	-37.33	#NUM!	#NUM!	#NUM!	#NUM!
386	116,3,8,,0.5,0	49	37	-75.96	5.79	2.96	-61.83	14.69	Y	14.69	16.99111313
387	116,3,27,,0.5,1	45	38	-113.07	5.93	2.92	-109.48	-53.23	Y	-53.23	-50.95758998
388	118,3,46,,0.5,0	22	22	-54.86	3.33	3.84	-53.41	-58.53	N	-53.41	-50.42749735
389	119,3,45,,0.5,1	7	7	-8.64	1.14	6.80	-6.57	-18.39	N	-6.57	-1.277742357
390	119,91,8,,0.5,1	5	4	45.43	0.60	9.00	41.55	27.97	N	45.43	52.4269489
391	120,3,45,,0.5,1	6	5	-34.37	0.81	8.05	-37.83	-42.19	N	-34.37	-28.10691467
392	120,92,45,,0.5,1	5	5	7.40	0.64	8.05	5.62	-14.63	N	7.40	13.65849034
393	121,3,45,,0.5,0	9	7	-49.54	0.93	7.11	-38.03	-36.50	N	-36.50	-31.20498849
394	121,3,45,,0.5,1	7	6	-110.51	0.93	7.35	-100.37	-10.12	Y	-10.12	-4.400848666
395	121,3,51,,0.5,0	44	8	12.67	0.97	6.65	26.32	#NUM!	#NUM!	#NUM!	#NUM!
396	121,3,51,,0.5,1	9	1	-71.27	0.14	18.80	-103.29	#NUM!	#NUM!	#NUM!	#NUM!
397	122,3,51,,0.5,0	48	2	12.23	0.25	14.21	8.44	#NUM!	#NUM!	#NUM!	#NUM!
398	122,3,51,,0.5,1	9	2	-52.97	0.29	13.29	-102.20	#NUM!	#NUM!	#NUM!	#NUM!

Dataset ID	Dataset	N	r	T <sub>0</sub>	ri.ni	εT <sub>0</sub>	Step 2	Step 3	Step 3 Significant	MAX Step <sub>1,2,3</sub>	SINTAP T <sub>0</sub> Final
#	#	#	#	°C	#	°C	°C	°C	#	°C	°C
399	123,3,51,,0.5,0	26	13	-57.92	1.90	5.21	-50.86	#NUM!	#NUM!	#NUM!	#NUM!
400	123,3,51,,0.5,1	10	7	-118.77	1.04	7.11	-119.13	-55.02	Y	-55.02	-49.7289311
401	124,3,8,,0.5,0	43	30	-79.89	4.77	3.29	-69.36	-68.00	N	-68.00	-65.44378126
402	124,3,45,,0.5,0	8	6	-61.85	0.98	7.35	-57.63	-74.77	N	-57.63	-51.91300802
403	124,3,47,,0.5,0	5	4	-50.00	0.50	9.00	-51.29	-53.96	N	-50.00	-43
404	125,3,9,,0.5,1	24	24	-66.22	2.00	3.67	-70.08	-86.80	N	-66.22	-63.36034842
405	125,3,40,,0.5,1	32	32	-81.19	5.10	3.18	-76.02	-92.99	N	-76.02	-73.54883838
406	125,93,40,,0.5,1	8	8	72.47	1.14	6.65	101.10	90.07	N	101.10	106.0543415
407	126,3,9,,0.5,1	24	24	-97.22	4.00	3.67	-98.75	-101.37	N	-97.22	-94.35996747
408	126,3,40,,0.5,1	10	10	-119.19	1.50	5.69	-110.51	-93.15	Y	-93.15	-88.71796409
409	126,94,40,,0.1,1	7	7	-23.87	1.00	7.11	-23.87	11.08	Y	11.08	16.3754002
410	127,3,12,LT,0.5,1								N	0.00	#DIV/0!
411	128,3,12,LT,0.5,1								N	0.00	#DIV/0!
412	129,3,12,TL,0.5,1								N	0.00	#DIV/0!
413	130,3,12,TL,0.5,1								N	0.00	#DIV/0!
414	131,3,52,TL,0.5,1								N	0.00	#DIV/0!
415	133,3,54,TL,0.5,1								N	0.00	#DIV/0!
416	134,3,54,TL,0.5,1								N	0.00	#DIV/0!
417	135,3,54,TL,0.5,1								N	0.00	#DIV/0!
418	136,3,37,TL,0.5,1								N	0.00	#DIV/0!
419	137,3,37,TL,0.5,1								N	0.00	#DIV/0!
420	138,3,37,TL,0.5,1								N	0.00	#DIV/0!
421	139,3,37,TL,0.5,1								N	0.00	#DIV/0!
422	140,3,37,TL,0.5,1								N	0.00	#DIV/0!
423	141,3,12,TL,0.5,1								N	0.00	#DIV/0!
424	142,3,12,TL,0.5,1								N	0.00	#DIV/0!
425	143,3,12,TL,0.5,1								N	0.00	#DIV/0!
426	144,3,12,TL,0.5,1								N	0.00	#DIV/0!
427	145,3,12,TL,0.5,1								N	0.00	#DIV/0!
428	147,3,12,,0.5,1								N	0.00	#DIV/0!
429	147,3,12,,0.8,1								N	0.00	#DIV/0!
430	149,3,23,,0.5,1								N	0.00	#DIV/0!
431	149,3,37,,0.5,1								N	0.00	#DIV/0!
432	149,96,22,,0.5,1								N	0.00	#DIV/0!
433	150,3,37,,0.5,1								N	0.00	#DIV/0!
434	150,97,22,,0.5,1								N	0.00	#DIV/0!
435	151,3,23,,0.5,1								N	0.00	#DIV/0!
436	151,3,37,,0.5,1								N	0.00	#DIV/0!
437	151,98,22,,0.5,1								N	0.00	#DIV/0!
438	152,3,23,,0.5,1								N	0.00	#DIV/0!
439	152,3,37,,0.5,1								N	0.00	#DIV/0!
440	153,3,23,,0.5,1								N	0.00	#DIV/0!
441	153,3,37,,0.5,1								N	0.00	#DIV/0!
442	154,3,12,,0.5,1								N	0.00	#DIV/0!
443	154,3,22,,0.5,1								N	0.00	#DIV/0!
444	154,101,22,,0.5,1								N	0.00	#DIV/0!
445	154,102,5,,0.5,1								N	0.00	#DIV/0!
446	155,3,12,,0.5,1								N	0.00	#DIV/0!
447	156,3,23,,0.5,1								N	0.00	#DIV/0!
448	156,99,23,,0.5,1								N	0.00	#DIV/0!

Dataset ID	Dataset	N	r	T <sub>0</sub>	ri.ni	εT <sub>0</sub>	Step 2	Step 3	Step 3 Significant	MAX Step <sub>1, 2, 3</sub>	SINTAP T <sub>0</sub> Final
#	#	#	#	°C	#	°C	°C	°C	#	°C	°C
449	157,100,23,,0.5,1								N	0.00	#DIV/0!
450	158,103,23,,0.5,1										
451	159,104,5,,0.5,1										
452	160,105,5,,0.5,1										
453	161,3,12,,0.5,1										
454	161,3,37,,0.5,1										
455	161,3,40,L-S,0.5,1										
456	161,3,54,,0.5,1										
457	161,3,54,L-S,0.5,1										
458	161,3,56,L-S,0.5,1										
459	161,3,57,L-S,0.5,1										
460	161,3,58,L-S,0.5,1										
461	161,3,59,L-S,0.5,1										
462	161,3,60,L-S,0.5,1										
463	161,3,61,L-S,0.5,1										
464	161,3,62,L-S,0.5,1										
465	161,3,63,L-S,0.5,1										
466	161,3,64,L-S,0.5,1										
467	161,3,65,L-S,0.5,1										
468	161,3,66,L-S,0.5,1										
469	161,3,67,L-S,0.5,1										
470	161,3,68,L-S,0.5,1										
471	161,3,69,L-S,0.5,1										
472	161,3,70,L-S,0.5,1										
473	161,3,71,,0.5,1										
474	161,3,71,,0.7,1										
475	161,3,71,,0.8,1										
476	161,3,72,,0.5,1										
477	161,3,73,,0.5,1										
478	161,3,74,,0.5,1										
479	161,3,75,,0.5,1										
480	161,3,76,,0.5,1										
481	161,3,77,,0.5,1										
482	162,3,9,,0.5,1										
483	162,3,9,Ductile,0.5,1										
484	163,3,80,0,0.5,1	12	12	-94.85	1.93	5.20	-98.53	-87.95			
485	164,3,23,0,0.5,1	12	12	-76.87	1.57	5.43	-69.48	-57.31			

## Appendix F - Valid Dataset Information

Dataset ID	Dataset	N	r	T0	ri.Ni	εT0	Step 2	Step 3	Step 3 Significant	MAX Step1, 2, 3	SINTAP T0 Final
#	#	#	#	°C	#	°C	°C	°C	#	°C	°C
26	10,3,2,RW,0.5,1	12	12	-25.49	1.71	5.43	-38.37	-40.24	N	-25.49	-21.44873336
27	10,3,7,,0.5,1	22	15	-22.63	2.19	4.65	-25.84	-36.39	N	-22.63	-19.02012106
39	10,6,7,,0.5,1	28	21	53.58	3.48	3.93	59.61	44.40	N	59.61	62.6699891
50	12,3,7,,0.5,1	31	23	-56.69	3.65	3.75	-52.08	-45.87	N	-45.87	-42.95215517
51	12,3,14,,0.5,1	20	15	-61.63	2.40	4.65	-61.37	-62.78	N	-61.37	-57.75497923
52	12,3,17,,0.5,1	16	6	-59.61	1.00	7.35	-59.61	-46.48	Y	-46.48	-40.76012011
55	12,4,7,,0.5,1	37	12	21.31	1.88	5.20	24.39	33.19	Y	33.19	37.23124693
57	12,4,17,,0.5,1	14	8	29.18	1.33	6.36	27.81	25.28	N	29.18	34.12993138
58	13,3,7,,0.5,1	35	30	-61.07	4.58	3.29	-61.89	-89.42	N	-61.07	-58.51204543
59	13,3,14,,0.5,1	20	15	-61.92	2.40	4.65	-60.50	-75.29	N	-60.50	-56.88511593
60	13,3,17,,0.5,1	16	10	-61.54	1.67	5.69	-59.95	-71.70	N	-59.95	-55.52465834
63	13,5,7,,0.5,1	32	23	43.10	3.31	3.75	40.24	41.50	N	43.10	46.01594954
65	13,5,17,,0.5,1	11	8	34.13	1.33	6.36	29.37	20.32	N	34.13	39.08114328
66	14,3,7,,0.5,1	155	105	-103.66	17.50	1.76	-103.18	-84.21	Y	-84.21	-82.84690858
67	15,3,3,T-S,0.5,1	35	30	-95.94	3.50	3.29	-95.94	-74.14	Y	-74.14	-71.58296783
68	15,3,4,T-S,0.5,1	29	15	-100.62	2.00	4.65	-99.73	-91.27	Y	-91.27	-87.655936
69	15,3,8,T-S,0.5,1	29	10	-86.87	1.67	5.69	-91.09	-74.28	Y	-74.28	-69.8538568
70	15,3,9,T-S,0.5,1	30	8	-109.51	1.33	6.36	-110.32	-84.57	Y	-84.57	-79.616452
71	15,3,10,T-S,0.5,1	34	10	-106.08	1.67	5.69	-105.56	-96.98	Y	-96.98	-92.55027539
72	15,3,23,T-S,0.5,1	44	28	-106.98	1.17	#VALUE!	-107.15	-44.06	Y	-44.06	-41.41607753
73	15,3,27,T-S,0.5,1	70	18	-107.08	2.50	4.24	-104.26	-95.93	Y	-95.93	-92.62964894
77	16,3,7,C-R,0.5,1	15	10	-8.61	1.67	5.69	-3.75	5.20	Y	5.20	9.626550787
78	16,3,14,C-R,0.5,1	9	9	-30.89	1.50	6.00	-21.52	4.00	Y	4.00	8.662510735
80	17,3,5,,0.5,1	38	20	-79.80	3.33	4.02	-79.67	0.64	Y	0.64	3.769520846
81	17,3,7,,0.5,1	51	26	-82.35	4.33	3.53	-74.09	-22.53	Y	-22.53	-19.7804358
82	17,3,14,,0.5,1	26	12	-86.72	2.00	5.20	-86.72	-81.16	N	-81.16	-77.11945521
83	17,3,17,,0.5,1	6	6	-84.74	1.00	7.35	-80.76	-79.63	N	-79.63	-73.90958523
84	19,3,5,,0.5,1	12	12	-62.39	1.33	5.20	-65.69	-56.91	N	-56.91	-52.86892788
85	19,3,7,,0.5,1	31	26	-52.96	3.94	3.53	-49.50	-57.91	N	-49.50	-46.75086084
86	19,3,14,,0.5,1	12	10	-58.01	1.67	5.69	-68.06	-80.58	N	-58.01	-53.58111866
88	19,12,5,,0.5,1	11	11	28.96	1.83	5.43	35.51	24.57	N	35.51	39.7357278
89	19,12,7,,0.5,1	21	11	33.96	1.83	5.43	33.62	48.41	Y	48.41	52.63240617
90	19,12,23,,0.5,1	18	18	33.56	2.81	4.43	40.29	32.39	N	40.29	43.58913248
92	20,3,5,,0.5,1	8	8	-40.57	1.17	6.65	-34.43	-26.00	Y	-26.00	-21.05090373
93	20,3,7,,0.5,1	25	19	-34.45	3.02	4.13	-34.80	-40.25	N	-34.45	-31.24107225
94	20,14,5,,0.5,1	6	6	68.66	1.00	7.35	59.26	47.19	N	68.66	74.37452077
95	20,14,12,,0.5,1	13	13	59.76	2.00	4.99	60.25	57.24	N	60.25	64.13203034
96	20,14,23,,0.5,1	9	9	45.86	1.29	6.27	30.50	25.38	N	45.86	50.52782969
97	22,3,7,,0.5,1	10	7	-90.00	1.08	6.80	-87.31	-65.05	Y	-65.05	-59.76150457
98	22,7,7,,0.5,1	15	15	-80.00	1.64	4.65	-75.59	-74.03	N	-74.03	-70.41342747
99	23,3,7,,0.5,1	21	17	-12.99	2.63	4.37	-13.36	-38.77	N	-12.99	-9.592876641
100	23,8,7,,0.5,1	16	12	21.10	1.98	5.20	27.99	2.45	N	27.99	32.02991264
101	24,3,7,,0.5,1	10	6	-62.20	1.00	7.35	-62.20	-42.92	Y	-42.92	-37.1997364
102	24,9,7,,0.5,1	16	11	-38.20	1.79	5.43	-43.93	-24.19	Y	-24.19	-19.96658536
104	25,10,7,,0.5,1	15	10	-15.04	1.55	5.69	-25.36	6.81	Y	6.81	11.23301807
106	26,3,5,,0.5,1	70	63	-42.47	8.37	2.27	-41.49	-49.77	N	-41.49	-39.72754165
107	26,3,6,,0.5,1	13	13	-24.66	2.17	4.99	-30.83	-46.73	N	-24.66	-20.77316691



Dataset ID	Dataset	N	r	T0	ri.Ni	eT0	Step 2	Step 3	Step 3 Significant	MAX Step1, 2, 3	SINTAP T0 Final
#	#	#	#	°C	#	°C	°C	°C	#	°C	°C
108	26,3,7,,0,5,1	44	36	-42.64	5.81	3.00	-42.76	-71.67	N	-42.64	-40.31154488
109	26,3,11,,0,5,1	12	12	-35.46	2.00	5.20	-49.00	-56.78	N	-35.46	-31.41486662
111	26,3,15,,0,5,1	6	6	-46.96	1.00	7.35	-48.56	-63.03	N	-46.96	-41.24090786
114	27,3,23,,0,5,1	34	22	-100.17	1.67	#VALUE!	-99.68	-79.98	Y	-79.98	-76.99455894
115	27,3,31,,0,5,1	69	8	-100.33	1.33	6.36	-100.06	-96.22	N	-96.22	-91.27293754
117	28,3,5,,0,5,1	55	55	-82.92	8.33	2.43	-77.66	-81.18	N	-77.66	-75.76765438
118	28,3,6,,0,5,1	8	8	-70.20	1.33	6.36	-68.11	-68.98	N	-68.11	-63.16358573
119	28,3,7,,0,5,1	28	23	-79.46	3.74	3.75	-79.46	-53.08	Y	-53.08	-50.15905634
120	28,3,11,,0,5,1	8	8	-79.55	1.33	6.36	-98.50	-92.37	N	-79.55	-74.60350603
123	28,3,16,,0,5,1	11	9	-91.47	1.50	6.00	-84.78	-91.30	N	-84.78	-80.11180573
125	29,3,24,,0,5,1	60	49	-57.94	2.62	#VALUE!	-50.86	-70.83	N	-50.86	-48.86422614
126	29,3,25,,0,5,1	58	48	-53.03	5.00	2.71	-48.77	-60.62	N	-48.77	-46.74922384
128	29,3,28,,0,5,1	28	22	-48.43	3.52	3.84	-63.23	-71.14	N	-48.43	-45.44642894
129	29,3,29,,0,5,1	26	23	-33.24	3.50	3.75	-40.35	-63.54	N	-33.24	-30.32522793
130	30,3,7,,0,5,1	7	7	-112.14	1.17	6.80	-106.75	-101.54	N	-101.54	-96.24448578
131	30,3,22,,0,5,1	7	7	-119.69	1.17	6.80	-121.36	-80.32	Y	-80.32	-75.02928052
132	30,3,23,,0,5,1	32	32	-129.93	4.24	3.32	-128.72	-133.90	N	-128.72	-126.2455357
134	31,3,22,,0,5,1	7	7	-128.10	1.00	7.11	-117.38	-110.73	N	-110.73	-105.4413151
136	32,3,23,,0,5,1	7	7	-104.79	1.00	7.11	-114.67	-113.28	N	-104.79	-99.50091199
137	32,18,22,,0,5,1	10	9	107.85	1.33	6.27	122.16	122.08	N	122.16	126.8224657
139	34,3,7,,0,5,1	9	9	-78.51	1.29	6.27	-81.91	-73.21	N	-73.21	-68.53834606
140	34,3,23,,0,5,1	10	10	-94.16	1.50	5.69	-92.26	-108.17	N	-92.26	-87.83525052
143	35,3,23,,0,5,1	9	9	-94.55	1.29	6.27	-95.50	-102.12	N	-94.55	-89.88775251
144	36,3,23,,0,5,1	7	7	-123.97	1.00	6.80	-127.08	-140.46	N	-123.97	-118.6795437
145	37,3,23,,0,5,1	9	9	-132.97	1.17	6.27	-134.30	-133.92	N	-132.97	-128.3027882
147	39,3,23,,0,5,1	8	8	-64.92	1.14	6.65	-71.35	-81.75	N	-64.92	-59.97252801
148	40,3,23,,0,5,1	8	8	-91.70	1.14	6.65	-105.30	-105.59	N	-91.70	-86.7506755
149	41,3,23,,0,5,1	10	10	-120.78	1.50	5.95	-97.22	-107.73	N	-97.22	-92.79175597
151	43,3,23,,0,5,1	8	8	-95.25	1.14	6.65	-96.20	-106.73	N	-95.25	-90.30223266
153	45,3,23,,0,5,1	9	9	-93.60	1.29	6.27	-98.20	-114.70	N	-93.60	-88.9364504
154	46,3,1,,0,5,1	6	6	-88.64	1.00	7.35	-79.93	-75.55	N	-75.55	-69.83341604
155	46,3,7,,0,5,1	6	6	-77.87	1.00	7.35	-72.23	-73.97	N	-72.23	-66.50953252
156	46,3,22,,0,5,1	8	8	-94.03	1.14	6.65	-89.62	-75.01	Y	-75.01	-70.05928593
157	46,3,23,,0,5,1	11	11	-105.03	1.29	6.06	-106.08	-112.61	N	-105.03	-100.8095023
159	46,15,22,,0,5,1	9	9	47.59	1.29	6.27	44.11	29.46	N	47.59	52.25794441
160	47,3,5,,0,5,1	7	7	-88.51	1.00	7.11	-92.31	-86.23	N	-86.23	-80.93919713
161	47,3,22,,0,5,1	7	7	-102.66	1.00	7.11	-103.67	-108.96	N	-102.66	-97.37211515
162	47,3,23,,0,5,1	8	8	-99.56	1.14	6.65	-99.08	-114.37	N	-99.08	-94.1280732
164	47,16,22,,0,5,1	12	12	60.78	1.71	5.43	61.92	57.12	N	61.92	65.96381647
167	50,3,5,,0,5,1	12	10	-59.76	1.58	5.69	-69.99	-76.51	N	-59.76	-55.33709404
179	53,3,5,,0,5,1	10	8	-9.34	1.04	6.65	-11.30	-19.32	N	-9.34	-4.389764317
192	54,3,5,,0,5,1	15	12	-23.46	1.60	5.20	-31.11	33.35	Y	33.35	37.38897521
193	54,34,5,,0,5,1	12	8	60.57	1.24	6.36	59.57	99.35	Y	99.35	104.3035414
194	55,3,5,,0,5,1	14	11	-28.20	1.43	5.43	-32.57	-31.83	N	-28.20	-23.9779114
195	55,35,5,,0,5,1	12	8	122.54	1.27	6.36	115.84	122.47	N	122.54	127.4854168
196	56,3,5,,0,5,1	15	9	-12.78	1.41	6.00	-21.07	-24.75	N	-12.78	-8.112238896
197	56,36,5,,0,5,1	12	8	143.40	1.18	6.65	129.20	124.68	N	143.40	148.3452774
201	58,3,5,,0,5,1	22	19	-47.94	2.65	4.13	-47.24	-21.58	Y	-21.58	-18.36560872
216	58,45,5,,0,5,1	10	8	28.77	1.27	6.36	23.72	11.77	N	28.77	33.71849962
219	58,47,5,,0,5,1	8	7	26.29	1.10	6.80	29.75	36.37	N	36.37	41.66517821

Dataset ID	Dataset	N	r	T0	ri.Ni	εT0	Step 2	Step 3	Step 3 Significant	MAX Step1, 2, 3	SINTAP T0 Final
#	#	#	#	°C	#	°C	°C	°C	#	°C	°C
226	59,3,5,,0,5,1	15	12	-7.32	1.91	5.20	-5.58	-12.54	N	-5.58	-1.536880317
227	59,53,5,,0,5,1	11	7	85.04	1.08	6.80	76.81	85.45	N	85.45	90.74083209
253	66,3,5,,0,5,1	6	6	7.83	1.00	7.35	10.77	-2.62	N	10.77	16.48830293
254	66,3,7,,0,5,1	6	6	8.55	1.00	7.35	-0.19	-11.71	N	8.55	14.26089971
255	66,3,12,,0,5,1	47	47	17.05	6.65	2.74	13.33	-24.66	N	17.05	19.09510567
256	66,3,23,,0,5,1	13	10	-5.08	1.00	6.36	-9.82	55.00	Y	55.00	59.42284232
257	66,3,37,,0,5,1	45	45	11.81	6.83	2.68	10.22	-4.17	N	11.81	13.89337664
258	66,3,38,,0,5,1	11	11	0.00	1.79	5.43	-11.26	-20.11	N	0.00	4.221158824
260	66,3,40,,0,5,1	33	30	-8.75	3.26	3.43	-12.04	7.49	Y	7.49	10.04908435
261	67,3,5,,0,5,1	24	24	-93.80	3.83	3.67	-91.78	-108.46	N	-91.78	-88.92346757
262	67,3,23,,0,5,1	22	22	-97.71	2.50	4.01	-103.17	-81.36	Y	-81.36	-78.37541299
263	67,3,23,L-T,0,5,1	16	16	-115.42	2.33	4.50	-118.37	-82.86	Y	-82.86	-79.36438864
265	67,3,23,T-L,0,5,1	12	12	-115.15	1.33	5.43	-116.43	-116.39	N	-115.15	-111.1066255
266	67,3,41,,0,5,1	17	17	-100.53	1.83	4.56	-98.36	-110.49	N	-98.36	-94.96676904
271	68,3,40,L-T,0,5,1	18	16	-110.10	1.33	4.70	-117.54	-112.16	N	-110.10	-106.5956124
272	68,3,42,L-T,0,5,1	19	8	-114.10	1.17	6.36	-108.34	-69.29	Y	-69.29	-64.34520761
274	68,73,40,L-T,0,5,1	22	22	-22.90	2.95	3.84	-13.55	13.18	Y	13.18	16.16467121
275	68,73,42,L-T,0,5,1	26	26	-5.28	3.71	3.53	-3.65	9.99	Y	9.99	12.73656813
283	69,74,44,,0,5,1	11	8	-39.22	1.29	6.36	-29.36	-36.71	N	-29.36	-24.40730897
291	70,75,44,,0,5,1	10	7	81.97	1.12	6.80	85.11	95.47	Y	95.47	100.763463
300	71,76,44,,0,5,1	13	8	19.25	1.20	6.36	12.15	28.07	Y	28.07	33.02046427
312	74,3,37,,0,5,1	11	10	-131.91	1.37	5.69	-130.70	-125.27	N	-125.27	-120.8406636
313	74,79,37,,0,5,1	12	8	-100.48	1.29	6.36	-105.36	-101.36	N	-100.48	-95.52646399
314	75,3,40,,0,5,1	11	10	-155.71	1.20	5.95	-148.20	-161.06	N	-148.20	-143.7680355
316	76,3,40,,0,5,1	11	9	-151.19	1.23	6.00	-152.70	-144.14	N	-144.14	-139.4745495
317	76,80,40,,0,5,1	11	7	-109.65	1.14	6.80	-109.65	-72.59	Y	-72.59	-67.30212001
318	77,3,40,,0,5,1	11	9	-149.11	1.20	6.00	-152.45	-150.76	N	-149.11	-144.4405358
326	80,83,23,,0,5,1	8	7	-8.36	1.12	6.80	-6.22	-16.26	N	-6.22	-0.924796982
329	81,86,23,,0,5,1	9	9	-11.05	1.20	6.27	-6.46	42.12	Y	42.12	46.78540952
330	82,3,40,,0,5,1	20	20	-42.66	3.00	4.02	-47.03	-54.85	N	-42.66	-39.53388091
331	82,87,40,,0,5,1	14	14	71.09	2.00	5.02	79.03	78.68	N	79.03	82.77043793
332	91,3,5,,0,5,1	32	32	-45.66	4.83	3.18	-40.96	-47.97	N	-40.96	-38.48785915
334	91,3,12,T-L,0,5,1	18	12	-55.93	2.00	5.20	-64.57	-83.58	N	-55.93	-51.88632589
338	91,3,75,,0,5,1	16	16	-46.11	1.63	#VALUE!	-22.05	-14.98	N	-14.98	-11.48419565
339	92,3,3,,0,5,1	208	136	-90.00	21.36	1.54	-81.02	8.92	Y	8.92	10.11796134
341	92,3,8,,0,5,1	183	100	-88.54	16.67	1.80	-86.65	-62.92	Y	-62.92	-61.51780193
343	92,3,45,,0,5,1	167	36	-92.80	6.00	3.00	-92.16	-73.39	Y	-73.39	-71.06095902
345	92,3,46,,0,5,1	58	15	-93.84	2.50	4.65	-95.53	-89.54	N	-89.54	-85.92480379
348	93,3,3,,0,5,1	11	11	-106.35	1.83	5.43	-88.35	-83.74	N	-83.74	-79.51702735
351	94,3,23,,0,5,1	38	32	-17.10	3.57	3.55	-16.42	27.50	Y	27.50	29.97024992
352	94,3,23,L-S,0,5,1	19	13	-20.80	1.57	5.21	-20.61	56.88	Y	56.88	60.76225256
354	94,3,78,,0,5,1	24	12	-12.68	1.71	5.43	-13.24	8.50	Y	8.50	12.54026109
355	95,3,7,,0,5,1	9	8	-112.49	1.29	6.36	-112.49	-119.81	N	-112.49	-107.5370739
378	104,3,49,,0,5,1	21	10	-56.53	1.36	5.95	-74.45	-79.99	N	-56.53	-52.10739924
387	116,3,27,,0,5,1	45	38	-113.07	5.93	2.92	-109.48	-53.23	Y	-53.23	-50.95758998
389	119,3,45,,0,5,1	7	7	-8.64	1.14	6.80	-6.57	-18.39	N	-6.57	-1.277742357
400	123,3,51,,0,5,1	10	7	-118.77	1.04	7.11	-119.13	-55.02	Y	-55.02	-49.7289311

Dataset ID	Dataset	N	r	T0	ri.Ni	εT0	Step 2	Step 3	Step 3 Significant	MAX Step1, 2, 3	SINTAP T0 Final
#	#	#	#	°C	#	°C	°C	°C	#	°C	°C
404	125,3,9,,0.5,1	24	24	-66.22	2.00	3.67	-70.08	-86.80	N	-66.22	-63.36034842
405	125,3,40,,0.5,1	32	32	-81.19	5.10	3.18	-76.02	-92.99	N	-76.02	-73.54883838
406	125,93,40,,0.5,1	8	8	72.47	1.14	6.65	101.10	90.07	N	101.10	106.0543415
407	126,3,9,,0.5,1	24	24	-97.22	4.00	3.67	-98.75	-101.37	N	-97.22	-94.35996747
408	126,3,40,,0.5,1	10	10	-119.19	1.50	5.69	-110.51	-93.15	Y	-93.15	-88.71796409
409	126,94,40,,0.1,1	7	7	-23.87	1.00	7.11	-23.87	11.08	Y	11.08	16.3754002
484	163,3,80,0,0.5,1	12	12	-94.85	1.93	5.20	-98.53	-87.95	N	-87.95	-83.90425253
485	164,3,23,0,0.5,1	12	12	-76.87	1.57	5.43	-69.48	-57.31	Y	-57.31	-53.26472382

## Appendix G - Visual Basic Macro Used to Calculate SINTAP Step 1,2 and 3 Values of $T_0$ and Error on $T_0$

```
Private Sub CalcT0Button_Click()

Application.ScreenUpdating = False

L = 3

For N = 4 To 10000

If Worksheets("Toughness").Range("F" & N) = "" Then GoTo 100

L = L + 1

' Clear previous values from "T0 Calc" spreadsheet

Worksheets("T0 Calc").Range("A4:F10000").Clear
Worksheets("T0 Calc").Range("G5:AH10000").Clear
Worksheets("T0 Calc").Range("AJ4:BR10000").Clear

' Copy data from "Toughness" to "T0 Calc"

CopyDataFrom = Worksheets("Toughness").Range("F" & N)
CopyDataTo = "A4"

Worksheets("Toughness").Range(CopyDataFrom).Copy
Worksheets("T0 Calc").Range(CopyDataTo).PasteSpecial _
    Paste:=xlPasteValues, Operation:=xlPasteSpecialOperationNone, _
    SkipBlanks:=False, Transpose:=False

' Populate 1st T0 calculation table

FirstRow2 = 4
LastRow2 = Worksheets("T0 Calc").Range("A3") + 3
If FirstRow2 = LastRow2 Then GoTo 1
Worksheets("T0 Calc").Range("G4:AC4").AutoFill _
    Destination:=Worksheets("T0 Calc").Range("G4:AC" & LastRow2), Type:=xlFillCopy
1

' Use GoalSeek to calculate T0

Worksheets("T0 Calc").Range("AH" & FirstRow2) = 0

For i = 1 To 10

T0Old = Worksheets("T0 Calc").Range("AH" & FirstRow2)

With Worksheets("T0 Calc")
.Range("T" & FirstRow2).Formula = "=D" & FirstRow2 & "-AH$" & FirstRow2
If FirstRow2 = LastRow2 Then GoTo 2
.Range("T" & FirstRow2).AutoFill _
    Destination:=Worksheets("T0 Calc").Range("T" & FirstRow2 & ":T" & LastRow2)
2
.Range("AE" & FirstRow2).Formula = "=SUM(AB" & FirstRow2 & ":AB" & LastRow2 & ")"
.Range("AF" & FirstRow2).Formula = "=SUM(AC" & FirstRow2 & ":AC" & LastRow2 & ")"

Check1 = Worksheets("T0 Calc").Range("L3")
If Check1 = True Then GoTo 100

.Range("AG" & FirstRow2).GoalSeek _
    Goal:=0, _
    ChangingCell:=Worksheets("T0 Calc").Range("AH" & FirstRow2)
End With

CopyCalcDataFrom1 = "A" & FirstRow2 & ":AH" & LastRow2
CopyCalcDataTo1 = "A" & LastRow2 + 2

Worksheets("T0 Calc").Range(CopyCalcDataFrom1).Copy
```

```

Worksheets("T0 Calc").Range(CopyCalcDataTo1).PasteSpecial _
    Paste:=xlPasteAll, Operation:=xlPasteSpecialOperationNone, _
    SkipBlanks:=False, Transpose:=False

NumberInSet = LastRow2 - FirstRow2
FirstRow2 = LastRow2 + 2
LastRow2 = FirstRow2 + NumberInSet

Worksheets("T0 Calc").Range("U" & FirstRow2).Formula = _
    = "IF(AND(T" & FirstRow2 & "<=50,T" & FirstRow2 & ">=-50),1,0)"
If FirstRow2 = LastRow2 Then GoTo 3
Worksheets("T0 Calc").Range("U" & FirstRow2).AutoFill _
    Destination:=Worksheets("T0 Calc").Range("U" & FirstRow2 & ":U" & LastRow2), _
    Type:=xlFillCopy
3

T0New = Worksheets("T0 Calc").Range("AH" & FirstRow2)

If Round(T0Old, 3) = Round(T0New, 3) Then GoTo 200

Next i

200 ' Calculate if T0 valid to E1921-05

Worksheets("T0 Calc").Range("AJ" & FirstRow2).Formula = _
    =IF(AND(ROUND(T" & FirstRow2 & ",0)>-14,ROUND(T" & FirstRow2 & ",0)<50,Q" & FirstRow2 & "=1,U" &
    FirstRow2 & "=1),1,0)"
Worksheets("T0 Calc").Range("AK" & FirstRow2).Formula = _
    =IF(AND(ROUND(T" & FirstRow2 & ",0)>-36,ROUND(T" & FirstRow2 & ",0)<-14,Q" & FirstRow2 & "=1,U" &
    FirstRow2 & "=1),1,0)"
Worksheets("T0 Calc").Range("AL" & FirstRow2).Formula = _
    =IF(AND(ROUND(T" & FirstRow2 & ",0)>-50,ROUND(T" & FirstRow2 & ",0)<-35,Q" & FirstRow2 & "=1,U" &
    FirstRow2 & "=1),1,0)"
Worksheets("T0 Calc").Range("AM" & FirstRow2).Formula = _
    =(AJ" & FirstRow2 & "/6)+(AK" & FirstRow2 & "/7)+(AL" & FirstRow2 & "/8)"
If FirstRow2 = LastRow2 Then GoTo 4
Worksheets("T0 Calc").Range("AJ" & FirstRow2 & ":AM" & FirstRow2).AutoFill _
    Destination:=Worksheets("T0 Calc").Range("AJ" & FirstRow2 & ":AM" & LastRow2)
4
Worksheets("T0 Calc").Range("AM" & LastRow2 + 1).Formula = _
    =SUM(AM" & FirstRow2 & ":AM" & LastRow2 & ")

' Calculate error on T0

With Worksheets("T0 Calc")
.Range("AO" & FirstRow2).Formula = _
    =IF(AND(Q" & FirstRow2 & "=1,U" & FirstRow2 & "=1),30+(70*EXP(0.019*T" & FirstRow2 & ")),0)"
If FirstRow2 = LastRow2 Then GoTo 5
.Range("AO" & FirstRow2).AutoFill _
    Destination:=Worksheets("T0 Calc").Range("AO" & FirstRow2 & ":AO" & LastRow2)
5
.Range("U" & LastRow2 + 1).Formula = _
    =SUM(U" & FirstRow2 & ":U" & LastRow2 & ")
.Range("AP" & FirstRow2).Formula = _
    =SUM(AO" & FirstRow2 & ":AO" & LastRow2 & ")/U" & LastRow2 + 1
.Range("AQ" & FirstRow2).Formula = _
    =BETA(ROUND(AP" & FirstRow2 & ",0))"
.Range("AR" & FirstRow2).Formula = _
    =AQ" & FirstRow2 & "/SQRT(U" & LastRow2 + 1 & ")

End With

' SINTAP Step 3

With Worksheets("T0 Calc")

.Range("AT" & FirstRow2).Formula = _
    =D" & FirstRow2 & "-(LN((((I" & FirstRow2 & "-Const & Equ!C$4)*((U$" & LastRow2 + 1 & "/LN(2))^0.25)-
    11)/77))/0.019)"
If FirstRow2 = LastRow2 Then GoTo 6
.Range("AT" & FirstRow2).AutoFill _

```

```

        Destination:=Worksheets("T0 Calc").Range("AT" & FirstRow2 & ":AT" & LastRow2), _
        Type:=xlFillCopy
6
.Range("AU" & FirstRow2).Formula = _
    "=MAX(AT" & FirstRow2 & ":AT" & LastRow2 & ")"
End With

' Transfer T0, ni.ri, error T0, Step 3 results to "Datasets"

With Worksheets("Datasets")

.Range("J" & L) = Worksheets("T0 Calc").Range("AH" & FirstRow2)
.Range("H" & L) = NumberInSet + 1
.Range("K" & L) = Worksheets("T0 Calc").Range("AM" & LastRow2 + 1)
.Range("I" & L) = Worksheets("T0 Calc").Range("U" & LastRow2 + 1)
.Range("L" & L) = Worksheets("T0 Calc").Range("AR" & FirstRow2)
.Range("N" & L) = Worksheets("T0 Calc").Range("AU" & FirstRow2)

End With

'Calculate Step 2 using Goalseek

T0Old = Worksheets("T0 Calc").Range("AH" & FirstRow2)

With Worksheets("T0 Calc")
.Range("AW" & FirstRow2).Value = _
    Worksheets("T0 Calc").Range("AH" & FirstRow2)
.Range("AX" & FirstRow2).Formula = _
    "=D" & FirstRow2
.Range("AY" & FirstRow2).Formula = _
    "=AX" & FirstRow2 & "-AW$" & FirstRow2
.Range("AZ" & FirstRow2).Formula = _
    "=I" & FirstRow2
.Range("BA" & FirstRow2).Formula = _
    "=30+(70*EXP(0.019*AY" & FirstRow2 & "))"
.Range("BB" & FirstRow2).Formula = _
    "=MIN(AZ" & FirstRow2 & ",BA" & FirstRow2 & ")"
.Range("BC" & FirstRow2).Formula = _
    "=IF(AZ" & FirstRow2 & "<BA" & FirstRow2 & ",1,0)"
.Range("BD" & FirstRow2).Formula = _
    "=U" & FirstRow2
.Range("BF" & FirstRow2).Formula = _
    "=AX" & FirstRow2 & "-BR$" & FirstRow2
.Range("BG" & FirstRow2).Formula = _
    "=EXP(0.019*BF" & FirstRow2 & ")"
.Range("BH" & FirstRow2).Formula = _
    "=BC" & FirstRow2 & "*BG" & FirstRow2
.Range("BI" & FirstRow2).Formula = _
    "=11+(77*BG" & FirstRow2 & ")"
.Range("BJ" & FirstRow2).Formula = _
    "=(BB" & FirstRow2 & "-Const & Equ!C$4)^4)*BG" & FirstRow2
.Range("BK" & FirstRow2).Formula = _
    "=BI" & FirstRow2 & "^5"
.Range("BL" & FirstRow2).Formula = _
    "=BD" & FirstRow2 & "*(BH" & FirstRow2 & "/BI" & FirstRow2 & ")"
.Range("BM" & FirstRow2).Formula = _
    "=BD" & FirstRow2 & "*(BJ" & FirstRow2 & "/BK" & FirstRow2 & ")"
If FirstRow2 = LastRow2 Then GoTo 7
.Range("AX" & FirstRow2 & ":BM" & FirstRow2).AutoFill _
    Destination:=Worksheets("T0 Calc").Range("AX" & FirstRow2 & ":BM" & LastRow2), _
    Type:=xlFillCopy
7

.Range("AX" & FirstRow2 & ":AX" & LastRow2).Copy
.Range("AX" & FirstRow2 & ":AX" & LastRow2).PasteSpecial _
    Paste:=xlPasteValues, Operation:=xlPasteSpecialOperationNone, _
    SkipBlanks:=False, Transpose:=False

.Range("AZ" & FirstRow2 & ":AZ" & LastRow2).Copy
.Range("AZ" & FirstRow2 & ":AZ" & LastRow2).PasteSpecial _
    Paste:=xlPasteValues, Operation:=xlPasteSpecialOperationNone, _

```

```

SkipBlanks:=False, Transpose:=False

.Range("BD" & FirstRow2 & ":BD" & LastRow2).Copy
.Range("BD" & FirstRow2 & ":BD" & LastRow2).PasteSpecial _
    Paste:=xlPasteValues, Operation:=xlPasteSpecialOperationNone, _
    SkipBlanks:=False, Transpose:=False

.Range("BO" & FirstRow2).Formula = _
    "=SUM(BL" & FirstRow2 & ":BL" & LastRow2 & ")"
.Range("BP" & FirstRow2).Formula = _
    "=SUM(BM" & FirstRow2 & ":BM" & LastRow2 & ")"
.Range("BQ" & FirstRow2).Formula = _
    "=BO" & FirstRow2 & "-BP" & FirstRow2
.Range("BR" & FirstRow2).Value = _
    Worksheets("T0 Calc").Range("AW" & FirstRow2)

End With

For i = 1 To 30

With Worksheets("T0 Calc")

T0Old = Worksheets("T0 Calc").Range("BR" & FirstRow2)

.Range("BQ" & FirstRow2).GoalSeek _
    Goal:=0, _
    ChangingCell:=Worksheets("T0 Calc").Range("BR" & FirstRow2)

T0New = Worksheets("T0 Calc").Range("BR" & FirstRow2)

If Round(T0Old, 3) = Round(T0New, 3) Then GoTo 300
If T0New < T0Old Then GoTo 300

.Range("AW" & FirstRow2 & ":BR" & LastRow2).Copy
.Range("AW" & LastRow2 + 2).PasteSpecial _
    Paste:=xlPasteAll, Operation:=xlPasteSpecialOperationNone, _
    SkipBlanks:=False, Transpose:=False

.Range("AW" & LastRow2 + 2).Value = _
    Worksheets("T0 Calc").Range("BR" & FirstRow2)

FirstRow2 = LastRow2 + 2
LastRow2 = FirstRow2 + NumberInSet

.Range("AY" & FirstRow2).Formula = _
    "=AX" & FirstRow2 & "-AW$" & FirstRow2
If FirstRow2 = LastRow2 Then GoTo 8
.Range("AY" & FirstRow2).AutoFill _
    Destination:=Worksheets("T0 Calc").Range("AY" & FirstRow2 & ":AY" & LastRow2), _
    Type:=xlFillCopy
8

.Range("BF" & FirstRow2).Formula = _
    "=AX" & FirstRow2 & "-BR$" & FirstRow2
If FirstRow2 = LastRow2 Then GoTo 9
.Range("BF" & FirstRow2).AutoFill _
    Destination:=Worksheets("T0 Calc").Range("BF" & FirstRow2 & ":BF" & LastRow2), _
    Type:=xlFillCopy
9

End With

Next i

300 "Transfer Step 2 Result to "Datasets"

Worksheets("Datasets").Range("M" & L) = Worksheets("T0 Calc").Range("BR" & FirstRow2)
Worksheets("Datasets").Range("S2") = L

Application.ScreenUpdating = True
Application.ScreenUpdating = False

```

```
100 Next N
```

```
Application.ScreenUpdating = True
```

```
End Sub
```



## Appendix H - Visual Basic Macro Used to Automatically Generate Plots of Valid Data

```
Private Sub ChartButton_1_Click()
    Charts.Add
    ActiveChart.ChartType = xlXYScatter

    L = 1

    For i = 4 To 1000

        If Worksheets("Chart Ref").Range("E" & i) = 0 Then GoTo 10

        SeriesName = Worksheets("Chart Ref").Range("A" & i)
        FirstRow = Worksheets("Chart Ref").Range("B" & i)
        LastRow = Worksheets("Chart Ref").Range("C" & i)

        ActiveChart.SeriesCollection.NewSeries
        ActiveChart.SeriesCollection(L).XValues = "=KjData!R" & FirstRow & "C8:R" & LastRow & "C8"
        ActiveChart.SeriesCollection(L).Values = "=KjData!R" & FirstRow & "C9:R" & LastRow & "C9"
        ActiveChart.SeriesCollection(L).Name = SeriesName

        L = L + 1
    Next i

    ActiveChart.Location Where:=xlLocationAsNewSheet
    With ActiveChart
        .HasTitle = False
        .Axes(xlCategory, xlPrimary).HasTitle = True
        .Axes(xlCategory, xlPrimary).AxisTitle.Characters.Text = "T - T0 [°C]"
        .Axes(xlValue, xlPrimary).HasTitle = True
        .Axes(xlValue, xlPrimary).AxisTitle.Characters.Text = "KJ25mm"
    End With
    With ActiveChart.Axes(xlCategory)
        .HasMajorGridlines = True
        .HasMinorGridlines = False
    End With
    With ActiveChart.Axes(xlValue)
        .HasMajorGridlines = True
        .HasMinorGridlines = False
    End With
    ActiveChart.ApplyDataLabels Type:=xlDataLabelsShowNone, LegendKey:=False
    Sheets("Chart2").Select
    Sheets("Chart2").Move After:=Sheets(6)
End Sub
```

## **Appendix I - Output of Visual Basic macro in Appendix G**

Appendix I is located on the pull out sheet opposite.

1	2	3	4	5	6	7	8	9	10	11	12	13	14	15	16	17	18
Mat ID	Irrad ID	Geom ID	Temp	a/W	$K_{J_{min}}^{0.5}$	Thickness	$K_{J_{25mm}}$	b	$\sigma_y$	E	Spec Type	$\nu$	$K_{J_{limit}}$	$\delta$	$K_{J_{el}}$	$T-T_0$	$\delta Temp$
#	#	#	°C	mm/mm	MPam <sup>0.5</sup>	mm	MPam <sup>0.5</sup>	m	MPa	MPa	#	mm/mm	MPam <sup>0.5</sup>	#	MPam <sup>0.5</sup>	°C	#
164	3	23	-80	0.5382	175.26	10.01	143.50	4.62E-03	6.43E+02	2.12E+05	SE(B)	0.3	1.25E+02	0	1.25E+02	-3.13	1
164	3	23	-110	0.5458	62.57	10.01	53.86	4.55E-03	6.83E+02	2.13E+05	SE(B)	0.3	1.28E+02	1	5.39E+01	-33.13	1
164	3	23	-85	0.5224	66.13	10.01	56.69	4.78E-03	6.49E+02	2.12E+05	SE(B)	0.3	1.28E+02	1	5.67E+01	-8.13	1
164	3	23	-100	0.5356	105.77	10.01	88.23	4.65E-03	6.69E+02	2.13E+05	SE(B)	0.3	1.28E+02	1	8.82E+01	-23.13	1
164	3	23	-85	0.5231	91.20	10.01	76.64	4.77E-03	6.49E+02	2.12E+05	SE(B)	0.3	1.27E+02	1	7.66E+01	-8.13	1
164	3	23	-90	0.5152	122.68	10.01	101.67	4.85E-03	6.56E+02	2.12E+05	SE(B)	0.3	1.29E+02	1	1.02E+02	-13.13	1
164	3	23	-70	0.5205	125.21	10.01	103.69	4.80E-03	6.30E+02	2.11E+05	SE(B)	0.3	1.26E+02	1	1.04E+02	6.87	1
164	3	23	-95	0.5543	73.26	10.01	62.37	4.46E-03	6.62E+02	2.13E+05	SE(B)	0.3	1.25E+02	1	6.24E+01	-18.13	1
164	3	23	-90	0.5288	88.21	10.01	74.26	4.72E-03	6.56E+02	2.12E+05	SE(B)	0.3	1.27E+02	1	7.43E+01	-13.13	1
164	3	23	-100	0.5779	47.87	10.01	42.17	4.22E-03	6.69E+02	2.13E+05	SE(B)	0.3	1.22E+02	1	4.22E+01	-23.13	1
164	3	23	-75	0.5212	190.29	10.01	155.45	4.79E-03	6.36E+02	2.11E+05	SE(B)	0.3	1.26E+02	0	1.26E+02	1.87	1
164	3	23	-60	0.5096	148.64	10.01	122.32	4.91E-03	6.18E+02	2.11E+05	SE(B)	0.3	1.26E+02	1	1.22E+02	16.87	1

164	3	23	-80	0.5382	175.26	10.01	143.50	4.62E-03	6.43E+02	2.12E+05	SE(B)	0.3	1.25E+02	0	1.25E+02	-3.13	1
164	3	23	-110	0.5458	62.57	10.01	53.86	4.55E-03	6.83E+02	2.13E+05	SE(B)	0.3	1.28E+02	1	5.39E+01	-33.13	1
164	3	23	-85	0.5224	66.13	10.01	56.69	4.78E-03	6.49E+02	2.12E+05	SE(B)	0.3	1.28E+02	1	5.67E+01	-8.13	1
164	3	23	-100	0.5356	105.77	10.01	88.23	4.65E-03	6.69E+02	2.13E+05	SE(B)	0.3	1.28E+02	1	8.82E+01	-23.13	1
164	3	23	-85	0.5231	91.20	10.01	76.64	4.77E-03	6.49E+02	2.12E+05	SE(B)	0.3	1.27E+02	1	7.66E+01	-8.13	1
164	3	23	-90	0.5152	122.68	10.01	101.67	4.85E-03	6.56E+02	2.12E+05	SE(B)	0.3	1.29E+02	1	1.02E+02	-13.13	1
164	3	23	-70	0.5205	125.21	10.01	103.69	4.80E-03	6.30E+02	2.11E+05	SE(B)	0.3	1.26E+02	1	1.04E+02	6.87	1
164	3	23	-95	0.5543	73.26	10.01	62.37	4.46E-03	6.62E+02	2.13E+05	SE(B)	0.3	1.25E+02	1	6.24E+01	-18.13	1
164	3	23	-90	0.5288	88.21	10.01	74.26	4.72E-03	6.56E+02	2.12E+05	SE(B)	0.3	1.27E+02	1	7.43E+01	-13.13	1
164	3	23	-100	0.5779	47.87	10.01	42.17	4.22E-03	6.69E+02	2.13E+05	SE(B)	0.3	1.22E+02	1	4.22E+01	-23.13	1
164	3	23	-75	0.5212	190.29	10.01	155.45	4.79E-03	6.36E+02	2.11E+05	SE(B)	0.3	1.26E+02	0	1.26E+02	1.87	1
164	3	23	-60	0.5096	148.64	10.01	122.32	4.91E-03	6.18E+02	2.11E+05	SE(B)	0.3	1.26E+02	1	1.22E+02	16.87	1

164	3	23	-80	0.5382	175.26	10.01	143.50	4.62E-03	6.43E+02	2.12E+05	SE(B)	0.3	1.25E+02	0	1.25E+02	-3.13	1
164	3	23	-110	0.5458	62.57	10.01	53.86	4.55E-03	6.83E+02	2.13E+05	SE(B)	0.3	1.28E+02	1	5.39E+01	-33.13	1
164	3	23	-85	0.5224	66.13	10.01	56.69	4.78E-03	6.49E+02	2.12E+05	SE(B)	0.3	1.28E+02	1	5.67E+01	-8.13	1
164	3	23	-100	0.5356	105.77	10.01	88.23	4.65E-03	6.69E+02	2.13E+05	SE(B)	0.3	1.28E+02	1	8.82E+01	-23.13	1
164	3	23	-85	0.5231	91.20	10.01	76.64	4.77E-03	6.49E+02	2.12E+05	SE(B)	0.3	1.27E+02	1	7.66E+01	-8.13	1
164	3	23	-90	0.5152	122.68	10.01	101.67	4.85E-03	6.56E+02	2.12E+05	SE(B)	0.3	1.29E+02	1	1.02E+02	-13.13	1
164	3	23	-70	0.5205	125.21	10.01	103.69	4.80E-03	6.30E+02	2.11E+05	SE(B)	0.3	1.26E+02	1	1.04E+02	6.87	1
164	3	23	-95	0.5543	73.26	10.01	62.37	4.46E-03	6.62E+02	2.13E+05	SE(B)	0.3	1.25E+02	1	6.24E+01	-18.13	1
164	3	23	-90	0.5288	88.21	10.01	74.26	4.72E-03	6.56E+02	2.12E+05	SE(B)	0.3	1.27E+02	1	7.43E+01	-13.13	1
164	3	23	-100	0.5779	47.87	10.01	42.17	4.22E-03	6.69E+02	2.13E+05	SE(B)	0.3	1.22E+02	1	4.22E+01	-23.13	1
164	3	23	-75	0.5212	190.29	10.01	155.45	4.79E-03	6.36E+02	2.11E+05	SE(B)	0.3	1.26E+02	0	1.26E+02	1.87	1
164	3	23	-60	0.5096	148.64	10.01	122.32	4.91E-03	6.18E+02	2.11E+05	SE(B)	0.3	1.26E+02	1	1.22E+02	16.87	1

Copy from database	Copy from Calc 1
Look up from geometry spreadsheet	Validity check -50 < Col 17 < 50
Calc Equation 2	Copy from Calc 2
Calc Equation 3	Validity check on dataset calc, Equation 7
Look up from strength spreadsheet	Calculate error on T0, calc Equation 8, 9 and 10
Calc Equation 4	Calculate SINTAP Step 3, calc Equation 11
Constant	Copy from Calc 3
Calc Equation 5	Calc Equation 6
Validity check Col 8 < Col 14	Calc Equation 8
Minimum Col 8, Col 14	Minimum Col 43, Col 44
Calc Equation 6	Validity check Col 43 < Col 44
Validity check set to 1	Copy from Calc 7
Maximum likelihood estimator	

19	20	21	22	23	24	25
$Q = \text{Exp}(0.019(T-T_0))$	$A = d \cdot Q$	$B = 11 + (77 \cdot Q)$	$C = (K_{30} - K_{\text{min}})^2 \cdot Q$	$D = B^5$	A/B	C/D
#	#	#	#	#	#	#

26	27	28	29
$\Sigma A/B$	$\Sigma C/D$	$\Sigma A/B - \Sigma C/D$	$T_0$
#	#	#	°C

30	31	32	33
50 to -14	-15 to -35	-36 to -50	$r_f \cdot N_f$
#	#	#	#

34	35	36	37
$K_{\text{Jmed}}$	$K_{\text{JFormed}}$	$\beta$	$\sigma$
MPam <sup>0.5</sup>	MPam <sup>0.5</sup>	°C	°C

9.42E-01	0.00E+00	8.36E+01	1.14E+08	4.07E+09	0.00E+00	2.79E-02
5.33E-01	5.33E-01	5.20E+01	7.00E+05	3.81E+08	1.02E-02	1.84E-03
8.57E-01	8.57E-01	7.70E+01	1.55E+06	2.70E+09	1.11E-02	5.74E-04
6.44E-01	6.44E-01	6.06E+01	1.40E+07	8.18E+08	1.06E-02	1.71E-02
8.57E-01	8.57E-01	7.70E+01	8.82E+06	2.70E+09	1.11E-02	3.26E-03
7.79E-01	7.79E-01	7.10E+01	3.47E+07	1.80E+09	1.10E-02	1.92E-02
1.14E+00	1.14E+00	9.87E+01	5.59E+07	9.38E+09	1.15E-02	5.96E-03
7.09E-01	7.09E-01	6.56E+01	2.28E+06	1.21E+09	1.08E-02	1.89E-03
7.79E-01	7.79E-01	7.10E+01	6.75E+06	1.80E+09	1.10E-02	3.74E-03
6.44E-01	6.44E-01	6.06E+01	1.56E+05	8.18E+08	1.06E-02	1.90E-04
1.04E+00	0.00E+00	9.08E+01	1.32E+08	6.17E+09	0.00E+00	2.15E-02
1.38E+00	1.38E+00	1.17E+02	1.51E+08	2.20E+10	1.18E-02	6.86E-03

1.10E-01	1.10E-01	-1.82E-04	-76.87
Calc 1			

9.42E-01	0.00E+00	8.36E+01	1.14E+08	4.07E+09	0.00E+00	2.79E-02
5.33E-01	5.33E-01	5.20E+01	7.00E+05	3.81E+08	1.02E-02	1.84E-03
8.57E-01	8.57E-01	7.70E+01	1.55E+06	2.70E+09	1.11E-02	5.74E-04
6.44E-01	6.44E-01	6.06E+01	1.40E+07	8.18E+08	1.06E-02	1.71E-02
8.57E-01	8.57E-01	7.70E+01	8.82E+06	2.70E+09	1.11E-02	3.26E-03
7.79E-01	7.79E-01	7.10E+01	3.47E+07	1.80E+09	1.10E-02	1.92E-02
1.14E+00	1.14E+00	9.87E+01	5.59E+07	9.38E+09	1.15E-02	5.96E-03
7.09E-01	7.09E-01	6.56E+01	2.28E+06	1.21E+09	1.08E-02	1.89E-03
7.79E-01	7.79E-01	7.10E+01	6.75E+06	1.80E+09	1.10E-02	3.74E-03
6.44E-01	6.44E-01	6.06E+01	1.56E+05	8.18E+08	1.06E-02	1.90E-04
1.04E+00	0.00E+00	9.08E+01	1.32E+08	6.17E+09	0.00E+00	2.15E-02
1.38E+00	1.38E+00	1.17E+02	1.51E+08	2.20E+10	1.18E-02	6.86E-03

1.10E-01	1.10E-01	-1.82E-04	-76.87
Calc 2			

9.42E-01	0.00E+00	8.36E+01	1.14E+08	4.07E+09	0.00E+00	2.79E-02
5.33E-01	5.33E-01	5.20E+01	7.00E+05	3.81E+08	1.02E-02	1.84E-03
8.57E-01	8.57E-01	7.70E+01	1.55E+06	2.70E+09	1.11E-02	5.74E-04
6.44E-01	6.44E-01	6.06E+01	1.40E+07	8.18E+08	1.06E-02	1.71E-02
8.57E-01	8.57E-01	7.70E+01	8.82E+06	2.70E+09	1.11E-02	3.26E-03
7.79E-01	7.79E-01	7.10E+01	3.47E+07	1.80E+09	1.10E-02	1.92E-02
1.14E+00	1.14E+00	9.87E+01	5.59E+07	9.38E+09	1.15E-02	5.96E-03
7.09E-01	7.09E-01	6.56E+01	2.28E+06	1.21E+09	1.08E-02	1.89E-03
7.79E-01	7.79E-01	7.10E+01	6.75E+06	1.80E+09	1.10E-02	3.74E-03
6.44E-01	6.44E-01	6.06E+01	1.56E+05	8.18E+08	1.06E-02	1.90E-04
1.04E+00	0.00E+00	9.08E+01	1.32E+08	6.17E+09	0.00E+00	2.15E-02
1.38E+00	1.38E+00	1.17E+02	1.51E+08	2.20E+10	1.18E-02	6.86E-03

1.10E-01	1.10E-01	-1.82E-04	-76.87
Calc 3			

Calc 4

0	0	0	0.00E+00
0	1	0	1.43E-01
1	0	0	1.67E-01
0	1	0	1.43E-01
1	0	0	1.67E-01
1	0	0	1.67E-01
1	0	0	1.67E-01
0	1	0	1.43E-01
1	0	0	1.67E-01
0	1	0	1.43E-01
0	0	0	0.00E+00
1	0	0	1.67E-01
			1.57E+00

0.00E+00	7.35E+01	18.8	5.43
6.73E+01			
9.00E+01			
7.51E+01			
9.00E+01			
8.45E+01			
1.10E+02			
7.96E+01			
8.45E+01			
7.51E+01			
0.00E+00			
1.26E+02			

Calc 5

38	39
Step 3 TOI	Max TOI
°C	°C

40	41	42	43	44	45	46	47
OldT <sub>o</sub>	Temp	T - OldT <sub>o</sub>	K <sub>ac25mm</sub>	K <sub>cond</sub>	K <sub>rel</sub>	Step 2 δ	δTemp
°C	°C	°C	MPam <sup>0.5</sup>	MPam <sup>0.5</sup>	MPam <sup>0.5</sup>	#	#

48	49	50	51	52	53	54	55
T-T <sub>o</sub>	Q = Exp(0.019(T-T <sub>o</sub> ))	A = d.Q	B = 11 + (77.Q)	C = (K <sub>rel</sub> - K <sub>min</sub> ) <sup>2</sup> .Q	D = B <sup>2</sup>	A/B	C/D
°C	#	#	#	#	#	#	#

56	57	58	59
ΣA/B	ΣC/D	ΣA/B - ΣC/D	T <sub>o</sub>
#	#	#	°C

Calc 6

-140.03	-57.31
-95.15	
-75.13	
-126.82	
-101.09	
-127.03	
-108.40	
-93.91	
-103.58	
-57.31	
-140.11	
-109.63	

-76.87	-80	-3.13	1.44E+02	9.60E+01	9.60E+01	0	1	-10.52	8.19E-01	0.00E+00	7.40E+01	2.73E+07	2.23E+09	0.00E+00	1.22E-02	8.63E-02	8.62E-02	3.29E-05	-69.48
	-110	-33.13	5.39E+01	6.73E+01	5.39E+01	1	1	-40.52	4.63E-01	4.63E-01	4.67E+01	6.09E+05	2.21E+08	9.92E-03	2.75E-03				
	-85	-8.13	5.67E+01	9.00E+01	5.67E+01	1	1	-15.52	7.45E-01	7.45E-01	6.83E+01	1.35E+06	1.49E+09	1.09E-02	9.06E-04				
	-100	-23.13	8.82E+01	7.51E+01	7.51E+01	0	1	-30.52	5.60E-01	0.00E+00	5.41E+01	5.16E+06	4.64E+08	0.00E+00	1.11E-02				
	-85	-8.13	7.66E+01	9.00E+01	7.66E+01	1	1	-15.52	7.45E-01	7.45E-01	6.83E+01	7.66E+06	1.49E+09	1.09E-02	5.14E-03				
	-90	-13.13	1.02E+02	8.45E+01	8.45E+01	0	1	-20.52	6.77E-01	0.00E+00	6.31E+01	1.17E+07	1.00E+09	0.00E+00	1.17E-02				
	-70	6.87	1.04E+02	1.10E+02	1.04E+02	1	1	-0.52	9.90E-01	9.90E-01	8.72E+01	4.86E+07	5.05E+09	1.13E-02	9.61E-03				
	-95	-18.13	6.24E+01	7.96E+01	6.24E+01	1	1	-25.52	6.16E-01	6.16E-01	5.84E+01	1.98E+06	6.80E+08	1.05E-02	2.92E-03				
	-90	-13.13	7.43E+01	8.45E+01	7.43E+01	1	1	-20.52	6.77E-01	6.77E-01	6.31E+01	5.87E+06	1.00E+09	1.07E-02	5.85E-03				
	-100	-23.13	4.22E+01	7.51E+01	4.22E+01	1	1	-30.52	5.60E-01	5.60E-01	5.41E+01	1.35E+05	4.64E+08	1.03E-02	2.91E-04				
	-75	1.87	1.55E+02	1.03E+02	1.03E+02	0	1	-5.52	9.00E-01	0.00E+00	8.03E+01	4.18E+07	3.34E+09	0.00E+00	1.25E-02				
	-60	16.87	1.22E+02	1.26E+02	1.22E+02	1	1	9.48	1.20E+00	1.20E+00	1.03E+02	1.31E+08	1.17E+10	0.00E+00	1.12E-02				

Calc 7

-69.48	-80	-10.52	1.44E+02	8.73E+01	8.73E+01	0	1	-10.52	8.19E-01	0.00E+00	7.40E+01	1.68E+07	2.23E+09	0.00E+00	7.55E-03	6.33E-02	6.31E-02	1.96E-04	-69.48
	-110	-40.52	5.39E+01	6.24E+01	5.39E+01	1	1	-40.52	4.63E-01	4.63E-01	4.67E+01	6.09E+05	2.21E+08	9.92E-03	2.75E-03				
	-85	-15.52	5.67E+01	8.21E+01	5.67E+01	1	1	-15.52	7.45E-01	7.45E-01	6.83E+01	1.35E+06	1.49E+09	1.09E-02	9.06E-04				
	-100	-30.52	8.82E+01	6.92E+01	6.92E+01	0	1	-30.52	5.60E-01	0.00E+00	5.41E+01	3.28E+06	4.64E+08	0.00E+00	7.07E-03				
	-85	-15.52	7.66E+01	8.21E+01	7.66E+01	1	1	-15.52	7.45E-01	7.45E-01	6.83E+01	7.66E+06	1.49E+09	1.09E-02	5.14E-03				
	-90	-20.52	1.02E+02	7.74E+01	7.74E+01	0	1	-20.52	6.77E-01	0.00E+00	6.31E+01	7.35E+06	1.00E+09	0.00E+00	7.32E-03				
	-70	-0.52	1.04E+02	9.93E+01	9.93E+01	0	1	-0.52	9.90E-01	0.00E+00	8.72E+01	3.92E+07	5.05E+09	0.00E+00	7.75E-03				
	-95	-25.52	6.24E+01	7.31E+01	6.24E+01	1	1	-25.52	6.16E-01	6.16E-01	5.84E+01	1.98E+06	6.80E+08	1.05E-02	2.92E-03				
	-90	-20.52	7.43E+01	7.74E+01	7.43E+01	1	1	-20.52	6.77E-01	6.77E-01	6.31E+01	5.87E+06	1.00E+09	1.07E-02	5.85E-03				
	-100	-30.52	4.22E+01	6.92E+01	4.22E+01	1	1	-30.52	5.60E-01	5.60E-01	5.41E+01	1.35E+05	4.64E+08	1.03E-02	2.91E-04				
	-75	-5.52	1.55E+02	9.30E+01	9.30E+01	0	1	-5.52	9.00E-01	0.00E+00	8.03E+01	2.56E+07	3.34E+09	0.00E+00	7.66E-03				
	-60	9.48	1.22E+02	1.14E+02	1.14E+02	0	1	9.48	1.20E+00	0.00E+00	1.03E+02	9.27E+07	1.17E+10	0.00E+00	7.92E-03				

Calc 8



*Appendix C*

**Process Modelling of Low Alloy  
Steel**

## **RDN18472 Process Modelling of Low Alloy Steel Summary**

Process modelling can be broadly defined as understanding the effects of the chosen route of manufacture on the suitability of a component for service. For low alloy steel (LAS) heavy section forgings the suitability of a component is defined by the mechanical properties of the material from which it is constructed. The mechanical properties of all materials, including LAS, are controlled by the microstructure of the material. The effect of processing route on the microstructure and resultant mechanical properties is currently not fully quantitatively understood for heavy section forgings.

The manufacturing route is defined via collective prior experience of heavy section forging manufacture; however, this approach is qualitative and can result in technical surprises when dealing with non-standard components and complex geometries. Traditionally, the manufacturing route was designed to achieve tensile and impact properties as defined by the relevant standard for mechanical performance. The suitability of heavy section forgings for nuclear applications is primarily defined by fracture toughness and tensile properties. This generates a number of concerns for the procurement of such components

The fracture toughness properties of LAS are governed by the extremes of microstructure dependent distributions, i.e. a cleavage failure is most likely to be initiated by the largest grains and the largest secondary particles. The tensile properties are controlled by the average microstructure of the material and as such good tensile properties do not always equate to good fracture toughness.

In order to establish the mechanical properties throughout a forging it must be destructively tested. The cost of a single nuclear grade heavy section forging makes this prohibitive and as such prolonged or trepanned material is used to define the properties used for safety assessment. All though this material is believed to be representative the possibility exists that the material may not behave as expected in regions which simply cannot be accessed without destroying the component.

Process modelling has become widely used in industries where the production rates are low or the cost of individual components is so high as to be prohibitive for evolutionary developments to the manufacturing processes to be undertaken. Process modelling offers the ability to establish the resultant mechanical properties



indirectly, via empirical relationships to known processing parameters, or directly via microstructure assessment, utilising thermodynamic modelling and transformation kinetics. This can be performed throughout the component establishing estimates of mechanical properties in regions that cannot be tested routinely.

Simple forming and microstructure models have been developed in previous programmes which have shown good correlation between predicted microstructural features and transition toughness measurements. Information gathered from these assessments has also been of use in defining the poor toughness performance of some forgings.



*Appendix D*

**NPCT Process Modelling Phase 2  
Detailed Plan**

## **RDN18651 NPCT Process Modelling Phase 2 Plan Summary**

This document partially fulfils a deliverable item for the NPCT A2.2.4.6 Process Modelling of Ferritic Steels – Phase 1 work stream. Included in this report is a detailed three year plan for the work to be conducted which was bid for funding under NPCT A2.2.4.6 – Phase 2 with the intent funding would commence in Q2 2009. A second report, RDN18272, fulfils the other criteria of a feasibility study on process modelling of large primary components as set out in the work instruction document.

The intention of the programme is to produce validated models which make high fidelity predictions of the mechanical properties of a heavy section low alloy steel forging solely from knowledge of the manufacturing route utilised. This work will concentrate on the material used for civil pressure vessel forgings, ASME A508 Grade 3 Class 1 (A508-3-1). It is believed that the strengthening mechanisms and fracture processes are similar across a wide range of low alloy steel compositions; therefore, the tools developed within in this programme will be broadly applicable to other low alloy steel materials requiring that only simple material parameters be measured as model inputs.

The following work falls broadly into three areas: observation, modelling and validation. The programme also conveniently splits into two work packages that can run largely concurrently; these are development of predictive methods and the generation of representative material for characterisation. Preliminary work is required for both work packages to provide basic material property information for use in modelling efforts and to define the materials to be manufactured for validation.

Large forgings are commonly specified on tensile and impact properties alone. The crucial properties for safety justification are tensile and transition toughness performance and at present contracting against toughness properties are considered, as a minimum, problematic. By demonstrating to forging suppliers that the required toughness properties can be achieved in forgings before production via the use of validated models it is hoped that transition toughness performance can be added to the standard specifications used for procurement of heavy section forgings.

The cost of certain primary components makes it prohibitive to experiment with manufacturing route and material selection. By producing 'virtual' components with

which to test ideas before manufacture, confidence can be increased in changing the manufacturing route or material to produce consistently tough high quality forgings.

A Gantt chart is included to define the time-scales required for each part of programme and how these activities are linked to form a cohesive programme of work.



*Appendix E*

**NPCT Toughness Strategy –  
Technical Justification**

## **RDN18732 NPCT Toughness Strategy Summary**

Providing highly accurate and validated predictions of transition toughness behaviour is key to conservative operation of the plant while allowing the maximum possible operational lifetimes to be achieved. The Start of Life properties also form the basis for through life integrity predictions when combined with irradiation shift models. Ensuring that the most accurate model is used for these predictions provides significant benefit to through life integrity by the reduction of end of life margins.

A major benefit of this work is the development of tools which can be used to support emergent work and safety assessments. By taking a proactive approach to toughness measurement and estimation, the ability to respond to problems with accurate and well understood material property information is greatly increased. Assessment of these models and methods before they are needed provides a significant level of security that the models are appropriate for the materials considered and applied correctly to a given situation.

This document contains a detailed technical justification for the work items proposed for NPCT A2.2.5.7 Fracture Micro-Mechanisms. A description of the current modelling practice is given to define areas in need of further work and assessment. This programme is intended to produce validated physical models of transition toughness properties via comparison to well established or improved empirical models of toughness data, offering large increases in demonstrable accuracy. The programme will also support the development of a number of advanced toughness estimation methods allowing best use in safety assessments of the developed physical and improved empirical models.





*Appendix F*

**The Effects of Microstructure on  
the Mechanical Properties of  
A508-3 Heavy Section Forgings**

# The effects of microstructure on the mechanical properties of A508-3 heavy section forgings

by Daniel Cogswell

## Introduction

Production of good quality nuclear grade forgings is a time-consuming and costly process. Only a handful of facilities exist worldwide with the capability to manufacture heavy section forgings, resulting in extended lead times as nuclear new build goes through the current resurgence. It is important that these forgings are right first time for a number of reasons: the cost of re-manufacture could be prohibitive and the resulting delay to a build programme could easily become years. Despite a large base of experience of producing heavy section forgings, the consistency of transition toughness (as measured by elastic-plastic fracture mechanics testing) can be lacking.

A comparative programme was undertaken to analyse two sets of forgings - one set procured in the 1980s - Batch A - and the other in 1990s - Batch B. Each set was from a different manufacturer utilising different production routes, but manufactured to the same specification and final design, the current ASME SA508 Grade 3 Class 1 (A508-3-1) [1] specification at the time of manufacture, plus several additional requirements on properties and chemistry, specified for both orders. Where practical, the Batch B forgings were a repeat of those ordered for Batch A.

Both suppliers used standard production techniques to produce the ingot and the basic form. Differences were limited to heat treatment time and the final forging operations. Different philosophies were adopted to produce a near net shape component for quality heat treatment; Batch A were forged much closer to net shape, whereas Batch B achieved net shape by substantial machining. This has resulted in a difference in the forging ratio of the prolongation material used for

acceptance testing and later assessment with the Batch B forgings receiving less work.

The expectation was for similar or better mechanical properties in the later Batch B forgings due to evolutionary improvements in chemistry control and manufacturing processes. In reality some properties did show improvement; however the transition toughness was poorer than expected. Therefore, a wide-ranging assessment of the controlling parameters for brittle fracture in forgings manufactured to this specification was conducted to gain a better understanding of these differences, which is the substance of this paper.

The lower toughness poses no threat to plant integrity, as the toughness is sufficient for safe operation. However, future high-integrity safety cases may require yet lower plant failure probabilities, which could call for increased toughness in specific components. If the consistency of heavy section forgings, with respect to transition toughness, cannot be guaranteed using today's specifications, an increased understanding of the production methods that deliver high-toughness materials will be required to ensure the specification for any new forgings is written with sufficient accuracy and controls so as to deliver the right quality.

## Difference in Transition Toughness

In order to establish the difference in median toughness curves (see Figure 1) between the two suppliers, the data (a collation of all valid toughness data for forgings procured to the above specification from Batch A and B) was normalised by the size correction from the Master Curve (MC) concept developed by K. Wallin [2 - 5] and available as an ASTM standard [6]. Toughness values were established from specimens of various thicknesses dependent on the volume and shape of material available for testing. The MC method normalises the data to a crack front length of 25mm [6] by employing a simple proportionality to

© Rolls-Royce 2009 © Rolls-Royce plc 2009

The information in this article is the property of Rolls-Royce and may not be copied, or communicated, to a third party or used, for any purpose other than that for which it is supplied without the express written consent of Rolls-Royce plc.



the assessed volume ahead of the crack tip, allowing comparisons across multiple testing programmes.

### Comparison between Forging Suppliers

To enable a complete picture to be visible for evaluation a comparison was made between various mechanical and microstructural properties of the two batches of forgings. The comparisons included: (i) chemical composition, (ii) thermal history, (iii) inclusion study of Batch B material, (iv) tensile properties, (v) impact properties, (vi) processing route, and (vii) grain size analysis. These aspects are covered in the following sections:

#### Chemical Composition

The chemical composition of the Batch B forgings represents an improvement over Batch A with respect to the level of impurities (see Table 1). The only noted difference in the main alloying elements was an increase in the levels of chromium and silicon, by 0.07wt% and 0.03wt% respectively, from Batch A to B. Although significant in terms of a relative percentage between the two batches (40.5% difference in Cr, 16.2% difference in Si), in real terms the difference is considered negligible and has no major effect on the material properties.

The concentrations of micro-alloying elements (titanium, vanadium and niobium) were of a similar order for both batches and, as such, would be expected to have the same effect on the microstructure in both cases. The micro-alloying elements form grain boundary carbides at high temperatures, which act to pin prior austenite grain boundaries and preclude blooming of large grains.

The prior austenite structure is completely transformed during the final quench and temper quality heat treatment of low alloy steels of this type; however, the ferritic grains nucleate on the prior austenite grain boundaries and at triple points. A finer prior austenite structure will yield a finer ferritic structure; hence large prior austenite grain sizes are detrimental to the resultant mechanical properties, specifically strength and toughness. A low concentration of micro-alloying elements does not necessarily imply a large grain size for the material. If worked and heat-treated carefully, the grain size will remain small and uniform.

#### Thermal History

Comparison of the thermal histories of each batch exhibits a significant difference in the austenitising and tempering times (see Table 2). The heat treatment times, both austenitising and tempering, for the Batch A forgings were much more consistent. This was found to be due to the fact that each forging was heat-treated individually. For the Batch B production, a larger heat treatment furnace was utilised where two forgings were treated at once; however, only one quench tank was available leading to variation in treatment times. The temperature control for both suppliers was very good with limited variation around the selected heat treatment temperatures.

The quantitative effect of austenitising time has yet to be clearly understood for A508-3-1 forgings, but the effect on grain growth can be inferred qualitatively; longer austenitising times will lead to increased austenite grain growth. As both sets of

Supplier	C	Mn	P	S	Si	Cr	Ni	Mo	Cu	V	Nb	Ti	Co	Al	B	Sb	As	Sn	N <sub>2</sub>	H <sub>2</sub>
	Wt %																			ppm
Average																				
Batch A (High Toughness)	0.16	1.35	0.005	0.005	0.198	0.168	0.744	0.514	0.074	0.004	0.004	0.002	0.011	0.016		0.001	0.015	0.007		0.27
Average																				
Batch B (Low Toughness)	0.17	1.37	0.004	0.002	0.230	0.236	0.774	0.521	0.035	0.008	0.004	0.002	0.009	0.020	0.001	0.002	0.004	0.005	0.008	0.52
Difference	0.01	0.02	-0.001	-0.003	0.032	0.068	0.030	0.007	-0.039	0.004	0.000	0.000	-0.002	0.005		0.001	-0.011	-0.002		0.25
Difference %	6.3	1.5	-20.0	-60.0	16.2	40.5	4.0	1.4	-52.7	100.0	0.0	0.0	-18.2	33.3		100.0	-73.3	-28.6		92.6

Table 1: Comparison of average compositions for Batch A and Batch B forgings

Supplier	Heat Treatment <sup>a</sup>	Austenitising		Tempering		Simulated Post Weld Heat Treatment		Note a: Where a maximum (or minimum) is expressed, this is the average of the recorded maximum (or minimum) values for each individual heat treatment within a batch.
		Temp °C	Time hrs	Temp °C	Time hrs	Temp °C	Time hrs	
Batch A (High-Toughness)	Average Max.	883	10	650	10	610	10	Note b: Batch B forgings were heat treated two at a time with access to only one quench tank resulting in some forgings receiving longer treatment times.
	Average Min.	860		635				
Batch B (Low-Toughness) <sup>b</sup>	Average Max.	886	15	656	22	614	15	
	Average Min.	864	11	644	16			
Difference	Average Max.	3	5	6	7	4	5	
	Average Min.	4		9				

**Table 2: Comparison of quality heat treatment thermal histories for Batch A and Batch B forgings**

forgings contained low concentrations of micro-alloying elements, the prior-austenite grains may have bloomed to large sizes. As the quality heat treatment follows the forging processes, it is possible that grain growth, driven by internal stresses following the forging process, may be limited to particular crystal orientations such that only a small number of grains increase in size dramatically.

It can be shown, via use of the Hollomon and Jaffe tempering model [7], that the difference in tempering times is expected to have a limited effect on the resultant mechanical properties. The forgings from both suppliers were nearly in the 'completely tempered condition', therefore continued heat treatment at the same temperature past 10 hours would have a limited effect on the hardness of the material (see Figure 2).

#### Inclusion Study of 1990s Material

Inclusion initiated fracture can have a highly detrimental effect on toughness. It would be expected that comparisons between low and high inclusion content materials would yield high and low toughness values, respectively, if the mechanical behaviour of the matrices were equivalent. From experience, it is known that modern forgings (post 1980) tend to be very clean, i.e. the impurity and inclusion content (manganese sulphides, metal oxides, etc.) of the iron ore and scrap used for ingot manufacture is very low. One

possible explanation considered for the lower transition toughness of Batch B forging material was the presence of hard, angular or brittle inclusions which degrade toughness by creating micro-defects in the material, such as titanium-vanadium carbo-nitrides and metal oxides [8].

A very comprehensive inclusion study was performed on the Batch B forging material to assess the concentration of observable inclusions. It was found that only sulphides and oxides were present, and that the forging material was exceptionally clean. The Batch A material was not formally assessed for inclusion content; however, casual observations of the microstructure did not reveal evidence of any deleterious inclusions. These improvements in steel production are expected to remain in the future due to general improvements in the understanding of steel production and inclusion initiated fracture is not believed to be a major threat to plant integrity in current and future forgings.

#### Tensile Properties

The average tensile properties for the Batch A and B forgings are given in Table 3. There is a notable difference between the tensile properties of these materials, with improvements exhibited by the Batch B material in both proof stress ( $\sigma_{0.2}$ ) and tensile strength (UTS). It should be noted that Batch B specimens were taken from much closer to a quench surface due to the selection of a different

Supplier	Test Temperature	0.2% Proof Stress	UTS	Elongation	Reduction of Area
	[°C]	[MPa]	[MPa]	[%]	[%]
Batch A (High Toughness) Average Values	RT	439	580	26	60
	354	360	528	24	64
Batch B (Low Toughness) Average Values	RT	469	622	27	72
	354	411	562	24	72
Numerical Difference (Percentage Difference)	RT	30 (6.8)	42 (7.2)	1 (3.8)	12 (20)
	354	51 (14.2)	34 (6.4)	0 (0)	8 (12.5)

**Table 3: Average tensile properties for Batch A and Batch B forgings**

specimen location method: the  $2t \times t$  method was used for Batch B, whereas,  $\frac{1}{4}T \times T$  was used for Batch A. Both of these selection methods are in accordance with the requirements of the ASME Code Section II SA-508/SA-508M [1]. It is believed that the difference in tensile properties is predominantly due to a 'near surface' or 'quench rate' effect where a more efficient quench nearer the material surface is associated with generally improved tensile properties and better transition fracture toughness.

The quench effect is modelled well via the introduction of an equivalent distance (Figure 3). The equivalent distance is simply calculated as the reciprocal of the sum of the reciprocal distance of nearby quenched surfaces, i.e. for  $n$  surfaces the expression is defined as:

$$\text{Equation 1: } Z(n) = \left( \frac{1}{d_1} + \dots + \frac{1}{d_n} \right)^{-1}$$

By utilising an expression gained from fitting proof stress data against equivalent distance in a representative prolongation, it is possible to map the proof stress expected in a cross-section of a forging. An example is given (Figure 4) for a cross-section through a typical forging prolongation. The effect of three surfaces has been considered in this example and it can clearly be seen that adopting the  $t \times 2t$  method, where  $t$  is the distance from an as quenched surface to the area of significant loading (a minimum value of 20mm is permitted if the distance cannot be established), may result in significant over-estimation of bulk properties

compared to the  $\frac{1}{4}T \times T$  method, where  $T$  equals the maximum thickness of the heat-treated forging. This further highlights the difference between the two specimen selection methods stated in the ASME code for A508-3-1, and therefore significant assessment is required to produce viable data for use in comparisons

It has been demonstrated that the effect of specimen depth can have a large effect on measured mechanical properties. This effect has been quantified for Batch B forging prolongation material so that the increase in  $\sigma_{0.2}$  and UTS could be established. An increase in  $\sigma_{0.2}$  of approximately 19MPa and an increase in UTS of 21MPa can be attributed to the quench rate effect between near surface (equivalent to  $2t \times t$ ) and centre forging material (equivalent to  $\frac{1}{4}T \times T$ ).

The remaining difference in tensile properties can, at least partially, be explained by the reduced inclusion content of the Batch B material. The effect of inclusion content can only be estimated, however, a well-established knowledge of the material allows the following to be inferred. Inclusions act as sites for local deformation as opposed to general yielding; this reduces the measured bulk  $\sigma_{0.2}$  of the material by increasing the local stresses around inclusions leading to premature material flow. The effect of local stresses is exaggerated at the UTS due to void formation around inclusions, creating regions of local necking between voids. In a clean material, void nucleation will be limited, resulting in a

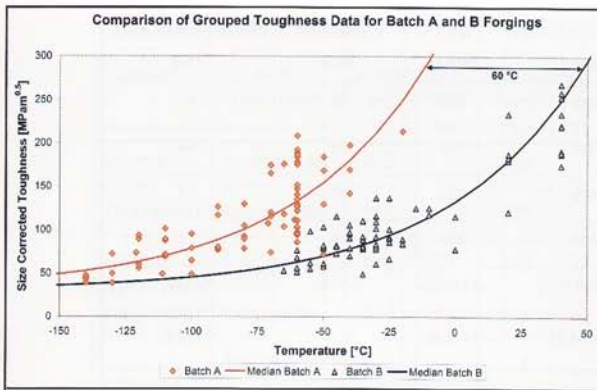


**Figure 1 - Comparison of size corrected transition toughness for Batch A and Batch B forging material**

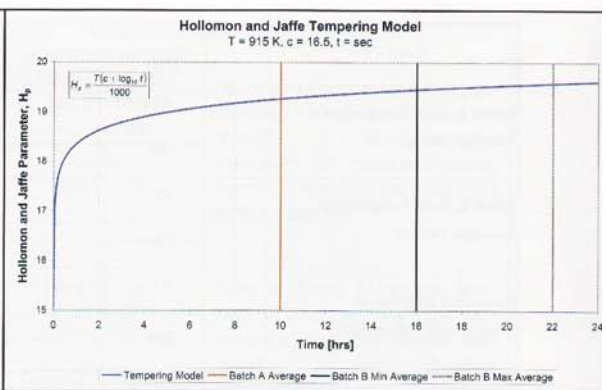


**Figure 2 - Effect of increased tempering time on Hollomon and Jaffe tempering parameter**

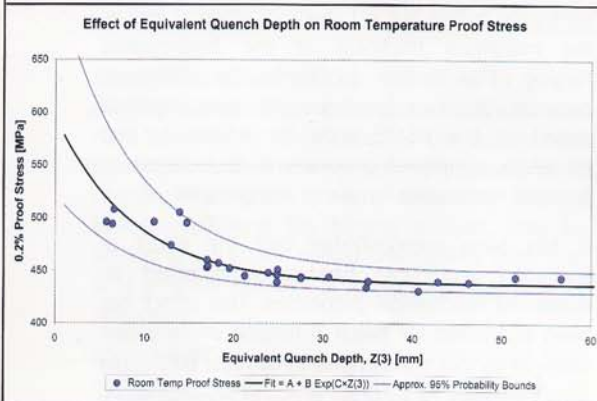


**Figure 3 - Effect of equivalent distance from quenched surface on room temperature proof stress for A508-3-1 material**

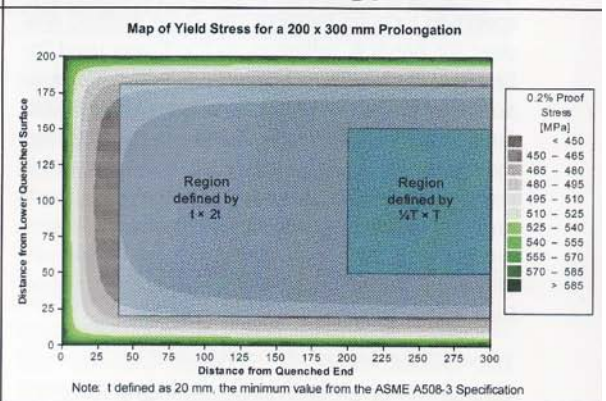


**Figure 4 - Map of proof stress for a typical forging prolongation**

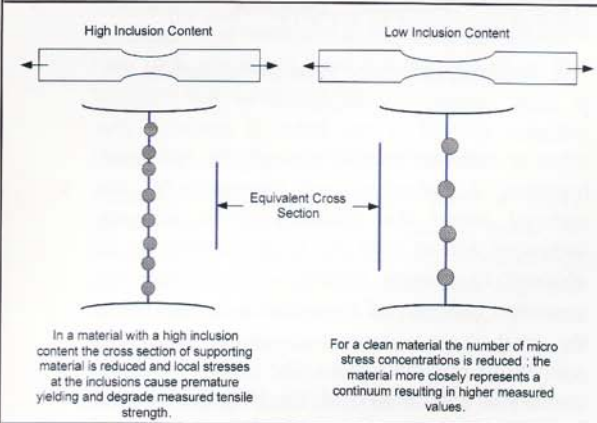


**Figure 5 - The effect of inclusion content on the tensile properties of low alloy steel**

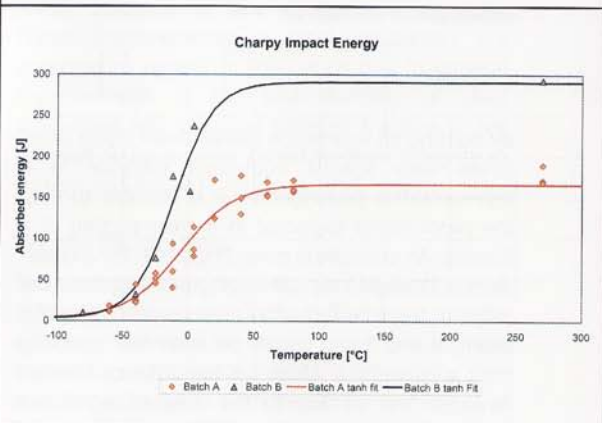


**Figure 6 - Manufacturer supplied Charpy transition data**

general necking of the material at a higher stress level. Evidence for reduced void formation in the Batch B material comes in the form of an increase in the average reduction of area percentage; 20% relative change from Batch A average at room temperature. This implies that the dominant necking region, formed during testing of the Batch B material, was able to deform to a greater extent due to an increased level of continuity in the material (see Figure 5).

### Impact Properties

Impact specimens were taken at the same sampling positions as the tensile specimens. It has been noted that clean materials exhibit a tighter impact transition and a higher upper shelf due to reduced void formation. This would be expected to result in a noticeable, albeit subtle, effect in the Batch B data when compared to Batch A. An improvement in the impact energy transition (i.e. a shift of the transition to lower temperatures and an increase in upper shelf energy) would also be expected due to the refined microstructure which was present in the Batch B samples as a result of the quench rate effect. It would appear that the refined microstructure of the quench affected material is acting in addition to the effect of reduced inclusion content, resulting in greatly improved properties (see Figure 6). This is a good example that reliance on the impact properties as a substitute for toughness measurement is not always advisable; clearly the impact transition properties from this near surface region cannot be used to estimate the transition toughness of the central regions of the forging.

### Grain Size Analysis

Production of electron backscatter diffraction (EBSD) grain maps, following suitable sample preparation, provides a very convenient method of determining the grain size of materials and was used in this study. EBSD is an electron microscope technique which assesses the crystal orientation of the material at a point or pixel [9]. By scanning a surface to build up an image of many pixels, it is possible to establish regions of similar orientation, such as a grain, creating a crystal orientation map of the surface. Comparison was made between a typical lower toughness Batch B forging and the highest toughness Batch A material available to accentuate any differences; it was found that both microstructures are ferritic in nature (tempered bainite).

Representative grain maps produced for A508-3-1 material by this method are shown in Figure 7, the colours marking areas of the same orientation. The black regions represent areas where the crystal orientation could not be determined or the grain size area was below a threshold value. These maps were used to deduce idealised grain diameters (based on hexagonal representations of the measured grain areas) and grain size distributions. A plot of the idealised grain size distribution for each material is shown in Figure 8. It can be clearly seen that the two distributions show little difference across the majority of the distribution; however, the distributions begin to diverge significantly above the 90<sup>th</sup> percentile. The results show that the largest grains in the Batch B material are approaching twice the size of their Batch A counterparts.

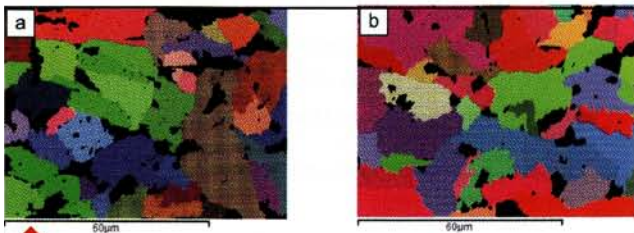
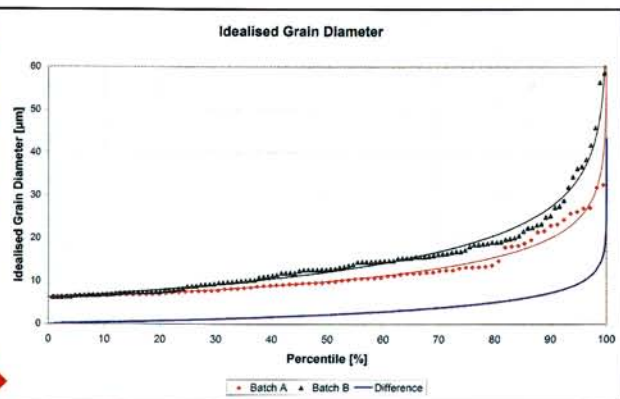


Figure 7: Typical EBSD grain maps for a) Batch A and b) Batch B material used for grain size analysis

Figure 8: Idealised grain diameter distribution comparison between Batch A & Batch B forging material





The tensile properties of low alloy steels are heavily dependent on the average grain size (Hall-Petch relationship [10]) of the material. As a small corresponding difference was observed in both the average grain size and the tensile properties, this would appear to hold true for these materials. However, toughness is dependent on finding the most potent crack initiator in the material; the presence of large grains would certainly increase the potency of any initiation event, thereby decreasing the toughness on the basis that it is mechanistically more likely for fracture to initiate from the largest grains in the microstructure, if all other parameters are equal.

### Summary and Conclusions

Metallurgical investigations were carried out to characterise the differences between two batches of A508-3-1 RPV forgings, Batch A and Batch B, with the objective of exposing the reasons for the differences in transition toughness. The following key points were established.

- The Batch B forgings represent an improvement over those from the Batch A in terms of chemistry control and inclusion content.
- Despite the differences in specimen sampling method, which can lead to large variability in comparisons if the quench effect is not taken into account, it has been demonstrated that the tensile properties of the Batch B forgings are equivalent to, or marginally improved over, Batch A.

### References

- [1] 'SA-508/SA-508M Specification for quenched and tempered vacuum-treated carbon and alloy steel forgings for pressure vessels', ASME Boiler and Pressure Vessel 1995 Edition, pgs 785 - 792.
- [2] K. Wallin, T. Saario and K. Törrönen: 'Statistical model for carbide induced brittle fracture in steel', *Metal Science*, 1984, Vol.18, pgs 13-16.
- [3] K. Wallin: 'The scatter in  $K_{IC}$ -results', *Engineering Fracture Mechanics*, 1984, Vol.19, No.6, pgs 1085-1093.
- [4] K. Wallin: 'The size effect in  $K_{IC}$  results', *Engineering Fracture Mechanics*, 1985, Vol.22, No.1, pgs 149-163.
- [5] D. McCabe, J. Merkle and K. Wallin: 'An introduction to the development and use of the Master Curve method', ASTM Manual Series, ASTM International, West Conshohocken, ISBN 0-8031-3368-5, 2005.
- [6] 'E1921-05 Standard test method for the determination of reference temperature,  $T_0$ , for ferritic steels in the transition range', ASTM International, West Conshohocken, 2005.
- [7] J.H. Hollomon and L.D. Jaffe: 'Time-temperature Relations in Tempering Steel', *Transactions of the American Institute of Mining and Metallurgical Engineers*, 1945, Vol.162, pgs 223-249.
- [8] S.G. Druce, G.P. Gibson and M. Capel: 'Microstructural Control of Cleavage Fracture in an A508 Class 3 Pressure Vessel Steel', *Fracture Mechanics: Twenty Second Symposium (Volume I)*, ASTM STP 1131, H.A. Ernst, A. Saxena and D.L McDowell (Eds), American Society for Testing and Materials, pgs 682-706, 1992.
- [9] V. Randle: 'Recent Developments in Electron Backscatter Diffraction', *Advances in Imaging and Electron Physics*, Vol.151, pg 363-416, 2008.
- [10] R.W.K. Honeycombe & H.K.D.H. Bhadeshia: 'Steels - Microstructure and Properties 2<sup>nd</sup> edition', Butterworth-Heinemann, Oxford, 2000.

- Microstructural differences are limited to the upper bounds of the grain size distributions and the inclusion content for each sample. The largest grains in the Batch B material are significantly larger in diameter than those in the Batch A material. The measured inclusion content of Batch B was found to be very low.
- The large grains, in the upper bounds of the grain size distribution, act as preferential sites for brittle fracture initiation and are believed to be a major contributing factor to the poorer transition toughness of Batch B material.

This article barely scratches the surface of a problem which has eluded a solution since large steel components were first made: how can the quality of a component, in this case toughness, be guaranteed and the properties predicted? The modelling of forging practices have improved greatly since the production of the Batch B in the 1990s, with increased use of computer modelling resulting in high toughness forgings being produced on a consistent basis.

However, it is still not possible to predict the toughness of a material solely from knowledge of the processing route used for manufacture. This work represents the first of the many steps required to produce predictions of this type and much more needs to be done to develop a full understanding of the links between processing, microstructure and mechanical properties.



*Appendix G*

**Upper Transition Model  
Assessment**

## **RRMP33915 Upper Transition Model Summary**

The modelling of transition toughness behaviour of low alloy steels in the upper transition is difficult due to the competition and interaction between brittle and ductile failure mechanisms. In the work presented, the upper transition has been characterised as the region of the transition where cleavage failure can still occur beyond the well modelled and well characterised mid-transition region. The upper transition is defined by a relative temperature of  $T-T_0 > 50^\circ\text{C}$  using the Master Curve description of transition behaviour.

Following assessment of a number of modelling approaches using statistical testing, the FRACT1ab model (developed by Rolls-Royce) as an extension to the Master Curve model, has been found to be the most applicable to the data in the upper transition region. FRACT1ab is a physically informed model taking account of ductile crack extension effects by means of a break away temperature which relates to the onset of significant ductile tearing for the material. This model was originally developed as a deterministic description of the upper transition region, i.e. the model was developed to provide a representative lower bound to experimentally measured toughness data within this region.

The FRACT1ab model does not encompass all known effects on the transition toughness of low alloy steels; at present constraint effects are not considered. However, the present work has shown that constraint correction methods require further work to include ductile tearing and, until this issue is resolved, FRACT1ab offers a more realistic representation of toughness data obtained experimentally for the upper transition than the basic Master Curve description. Continued use of this model is thus recommended as the most appropriate and applicable model for transition toughness behaviour in the upper transition with limitations to prevent possible optimistic assessments.

The FRACT1ab model was developed primarily to provide bounding toughness data for deterministic assessments. This investigation has shown that the model is suitable across the entire probability distribution for modern low inclusion content nuclear grade pressure vessel steels and as such, is also suitable for probabilistic assessments of these materials. Further work is required to establish the use of beneficial model parameters for other materials and a comprehensive set of recommendations have been included to provide an outline plan of the work required

to generate the necessary information for the use of material dependent model parameters.

The scientific merit and findings of this work have been externally reviewed by Dr Graham Wardle of Warhelle Consulting Ltd. Dr Wardle concurs with the conclusions and recommendations of this report. Both an extended commentary (Appendix 1) on the technical aspects of the report, containing recommendations for future work, and an endorsement statement (Appendix 2) are included with the report.

The findings of this work are endorsed by the relevant internal authority (Fracture Metallurgy) and the FRACT1ab model will continue to be used in current and future production of safety case arguments. Potential developments of this and alternative models do not impinge on the application and future use of FRACT1ab.

